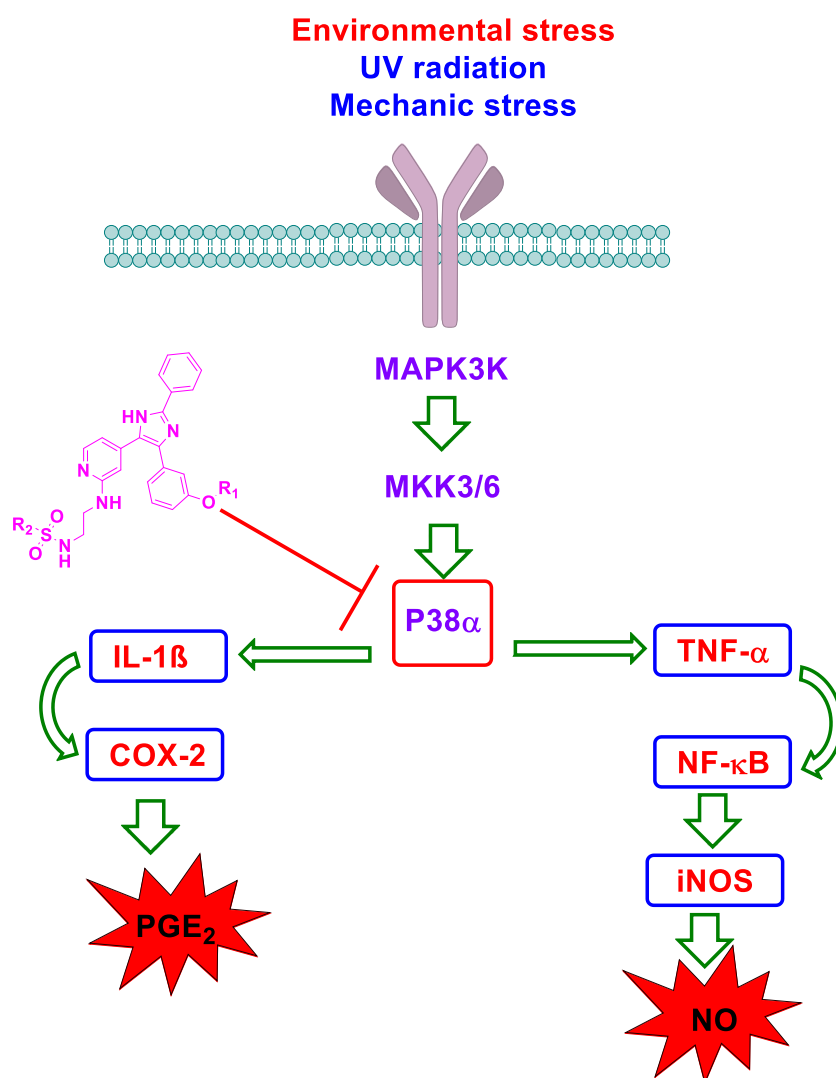


## Graphical Abstract



## Design, synthesis and anti-inflammatory activity of imidazol-5-yl pyridine derivatives as p38 $\alpha$ /mapk14 inhibitor

Eslam M. H. Ali<sup>a,b,c</sup>, Mohammed S. Abdel-Maksoud<sup>d</sup>, Hassan R.M<sup>d</sup>, Karim I. Mersal<sup>a,b</sup>, Usama M. Ammar<sup>e</sup>, Choi Se-In<sup>f</sup>, Han He-Soof<sup>f</sup>, Hee-Kwon Kim<sup>g,h</sup>, Anna Lee<sup>i</sup>, Kyung-Tae Lee<sup>f,\*</sup>, Chang-Hyun Oh<sup>a,b,\*</sup>

<sup>a</sup>*Center for Biomaterials, Korea Institute of Science & Technology (KIST School), Seoul, Seongbuk-gu, 02792, Republic of Korea.*

<sup>b</sup>*University of Science & Technology (UST), Daejeon, Yuseong-gu, 34113, Republic of Korea.*

<sup>c</sup>*Pharmaceutical Chemistry Department, Faculty of Pharmacy, Modern University for Technology and Information (MTI), Cairo, 12055, Egypt.*

<sup>d</sup>*Medicinal & Pharmaceutical Chemistry Department, Pharmaceutical and Drug Industries Research Division, National Research Centre (NRC), (ID: 60014618), P.O. 12622, Dokki, Giza, Egypt.*

<sup>e</sup>*Strathclyde Institute of Pharmacy and Biomedical Sciences, University of Strathclyde, 161 Cathedral Street, Glasgow G4 0NR, Scotland, United Kingdom.*

<sup>f</sup>*Department of Pharmaceutical Biochemistry, College of Pharmacy, Kyung Hee University, 1 Hoegi-dong, Dongdaemun-gu, Seoul 130-701, Republic of Korea*

<sup>g</sup>*Department of Nuclear Medicine, Molecular Imaging & Therapeutic Medicine Research Center, Jeonbuk National University Medical School and Hospital, 20 Geonji-ro, Deokjin-gu, Jeonju 54907, Republic of Korea*

<sup>h</sup>*Research Institute of Clinical Medicine of Jeonbuk National University-Biomedical Research Institute of Jeonbuk National University Hospital, 20 Geonji-ro, Deokjin-gu, Jeonju 54907, Republic of Korea*

<sup>i</sup>*Department of Chemistry, Hanseo University, Seosan 31962, Republic of Korea*

\* Corresponding author: Kyung-Tae Lee (klee@khu.ac.kr), Chang-Hyun Oh (choh@kist.re.kr)

## Abstract

P38 $\alpha$ / MAPK14 is intracellular signalling regulator involved in biosynthesis of inflammatory mediator cytokines (TNF- $\alpha$ , IL-1, IL-6, and IL-1b), which induce the production of inflammatory proteins (iNOS, NF-kB, and COX-2). In this study, drug repurposing strategies were followed to repositioning of a series of B-RAF<sup>V600E</sup> imidazol-5-yl pyridine inhibitors to inhibit P38 $\alpha$  kinase. A group 25 reported P38 $\alpha$  kinase inhibitors were used to build a pharmacophore model for mapping the target compounds and proving their affinity for binding in P38 $\alpha$  active site. Target compounds were evaluated for their potency against P38 $\alpha$  kinase, compounds **11a** and **11d** were the most potent inhibitors (IC<sub>50</sub> = 47 nM and 45 nM, respectively). In addition, compound **11d** effectively inhibited the production of proinflammatory cytokines TNF- $\alpha$ , 1L-6, and 1L-1 $\beta$  in LPS-induced RAW 264.7 macrophages with IC<sub>50</sub> values of 78.03 nM, 17.6  $\mu$ M and 82.15 nM, respectively.

The target compounds were tested for their anti-inflammatory activity by detecting the reduction of Nitric oxide (NO) and prostaglandin (PGE2) production in LPS-stimulated RAW 264.7 macrophages. Compound **11d** exhibited satisfied inhibitory activity of the production of PGE2 and NO with IC<sub>50</sub> values of 0.29  $\mu$ M and 0.61  $\mu$ M, respectively. Molecular dynamics simulations of the most potent inhibitor **11d** were carried out to illustrate its conformational stability in the binding site of P38 $\alpha$  kinase.

## Keywords

P38 $\alpha$ , Anti- inflammatory, Pharmacophore, TNF- $\alpha$ , 1L-6, 1L-1 $\beta$  Nitric Oxide, PGE2

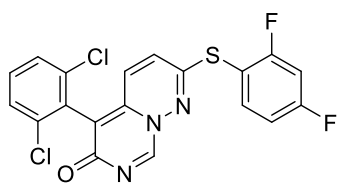
## 1. Introduction

Mitogen-activated protein kinases (MAPKs) are crucial signalling components that become activated in response to extracellular stimuli such as growth factors and regulate a wide range of cellular processes such as proliferation, stress responses, apoptosis and immune defence [1, 2]. Deregulations of MAP kinases expression are associated with numerous diseases including neurodegenerative impairment such as Alzheimer's disease, autoimmune diseases such as rheumatoid arthritis (RA), inflammatory disorders, and sometimes cancer [3-6]. P38 MAPK pathway is one of the major MAPK pathways, which is also called stress-activated protein kinase

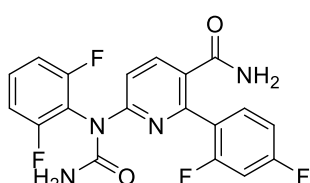
pathway as it is activated by environmental stress such as UV radiation, osmotic shock, and mechanic stress) and genotoxic stresses [7]. P38 MAPKs have four isoforms: p38 $\alpha$  (MAPK14), p38 $\beta$  (MAPK11), p38 $\gamma$  (MAPK12), and p38 $\delta$  (MAPK13) [8]. P38 $\alpha$  (MAPK14) is highest expressed isoform in most cell types and so p38 $\alpha$  is the most frequent drug target reported in the published literature [9, 10].

Chronic inflammation progression is compelled by incessant activation of inflammatory mediators cytokines like tumor necrosis factor- $\alpha$  (TNF- $\alpha$ ), interleukin-1 (IL-1), interleukin-6 (IL-6), and interleukin-1 $\beta$  (IL-1 $\beta$ ), whose biosynthesis and release is regulated by the activity of p38 $\alpha$  kinase [11-13]. Activation of TNF- $\alpha$  and IL-1 $\beta$  induces the production of other inflammatory proteins such as inducible nitric oxide synthase (iNOS), prostaglandins (PGs), receptor activator of nuclear factor NF- $\kappa$ B ligand (RANKL), and cyclooxygenase 2 (COX-2 [14]. In addition to its role in production of proinflammatory cytokines, p38 $\alpha$  kinase regulates cytosolic phospholipase phosphorylation and promotes its synthesis at transcriptional and translational level [15]. Therefore, p38 $\alpha$  kinase activation state is linked to stimulation-induced PGE2/NO production.

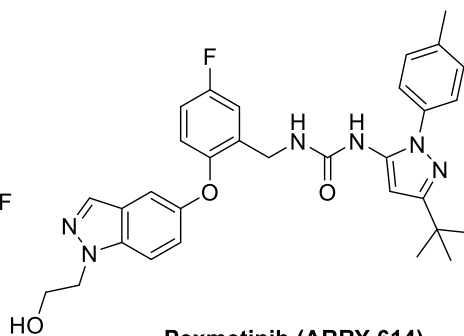
Several small molecules have been reported in the literature as p38 $\alpha$  kinase inhibitors [16-29] ([Figure 1](#)).



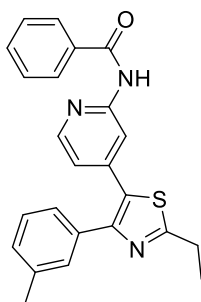
**VX-745**



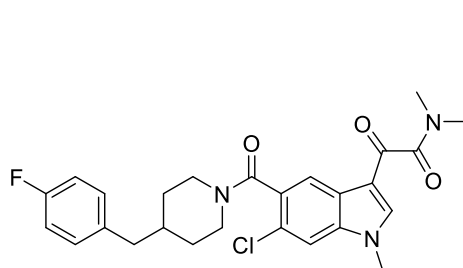
**VX-702**



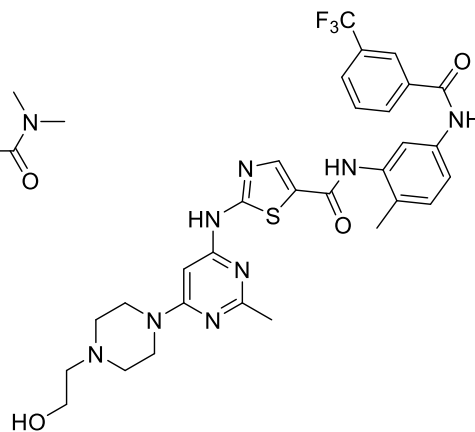
**Pexmetinib (ARRY-614)**



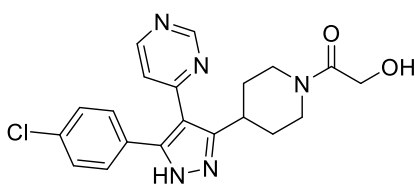
**TAK-715**



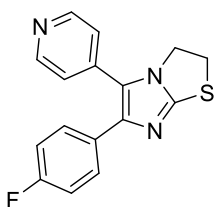
**SX011**



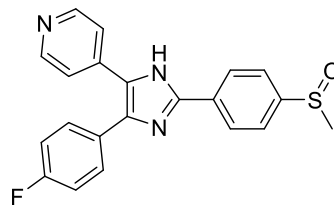
**UM-164**



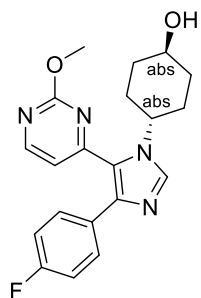
**SD 0006**



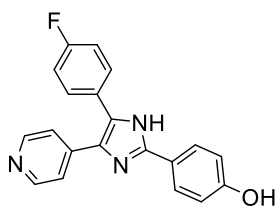
**SKF 86002**



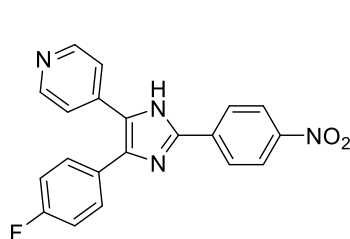
**SB203580**



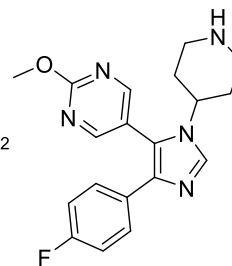
**SB239063**



**SB202190 (FHPI)**



**PD 169316**



**SB242235**

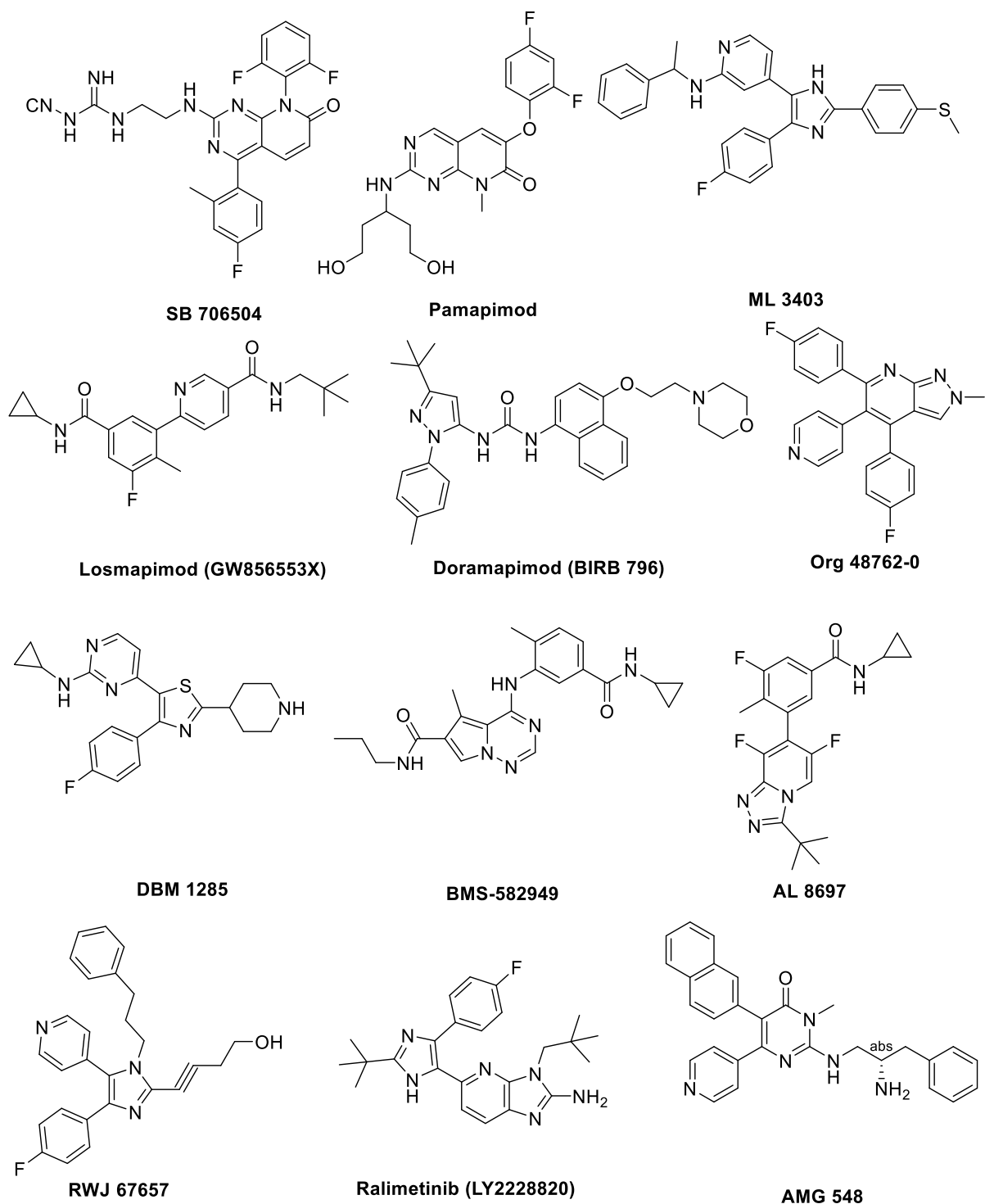


**Figure 1.** Structures of 25 reported P38 $\alpha$ /MAPK14 inhibitors (pharmacophore training set)

In a previous work, we reported a series of imidazol-5-yl pyridine derivatives as potential B-RAF<sup>V600E</sup> inhibitors [30]. Both p38 $\alpha$  kinase and B-RAF kinase are key components in MAPK pathway; B-RAF kinase binds with RAS as the upstream

activator, and mediate the MAPK signaling transduction to the MEK resulted to the activation of downstream MEK1/2 and ERK1/2 which is the upstream regulator of stress-activated protein kinase MsK1/2 [31], whereas, p38 $\alpha$  kinase is activated by the upstream MKK3/6, and sometimes by MKK4, p38 $\alpha$  kinase regulates protein kinases, including MAPK-activated kinase 2 MK2, mitogen- and stress-activated protein kinase 1 MsK1, and MAP kinase-interacting serine/threonine MNK1/2 [9, 32, 33]. In the current work, the synthesized compounds were evaluated for its P38 $\alpha$  inhibitory activity, compound **11d** was the most potent inhibitor with IC<sub>50</sub> value of 45 nM.

Further anti-inflammatory assays were conducted to the target compounds, compound **11d** exhibited satisfied inhibitory activity of the production of PGE2 and NO with IC<sub>50</sub> values of 3.8  $\mu$ M and 8.4  $\mu$ M, respectively. Also, compound **11d** effectively inhibited the production of TNF- $\alpha$ , 1L-6, and 1L-1 $\beta$  inflammatory cytokines in LPS-induced RAW 264.7 macrophages with IC<sub>50</sub> values of 78.03 nM, 17.6  $\mu$ M and 82.15 nM, respectively.

Molecular modelling studies included molecular docking for the target compounds, and molecular dynamics simulation for the most active hit **11d** were conducted in attempt to emphasis the relation between the mentioned kinase inhibitory activity for each derivative and their molecular interaction and stability in the active site of P38 $\alpha$  kinase.

## **2. Results and discussion**

### **2.1. Rational and design**

In the current work, off-target based drug repurposing strategies were followed in order to reposition B-RAF targeted inhibitors to inhibit p38 $\alpha$  kinase.

#### **2.1.1. Protein alignment**

In this study, Molecular Operating Environment (MOE, 2014) software was used to operate ligand binding site alignment protocol of the two corresponding protein kinases p38 $\alpha$  (PDB: 3GCP) and B-RAF (PDB: 4XV2).

The two crystal structures were downloaded from PDB, their energies were minimized, and were subjected to flexible alignment, where the initial pairwise

similarity matrix was build first using either a progressive or a tree-based method. Then a round-robin realignment is performed, followed by a randomized iterative refinement. The structure based realignment is performed using the existing secondary element information. After this, 3D superposition has been done on the best aligned model [34].

This direct comparison of the two enzymes binding sites describes the ligand molecular binding to provide useful insights into the compound molecular interaction mode. The result of the two pockets superposition approved the alignment of the essential interacted amino acids in the two kinases active site. As illustrated in [Figure 2](#), the two enzymes superposition showed high alignment in the adenine hinge area, ribose pocket, and hydrophobic back pocket. The two native ligands (**Dabrafenib** (P06) and **SB203580** (SB2)) of the corresponding kinases bind in the hinge region via interaction with Cys532 and Met109 amino acids, the central 5-membered ring native ligands is buried in the deep ribose pocket through interactions with Val471 and Val38 in BRAF and P38 $\alpha$  respectively.



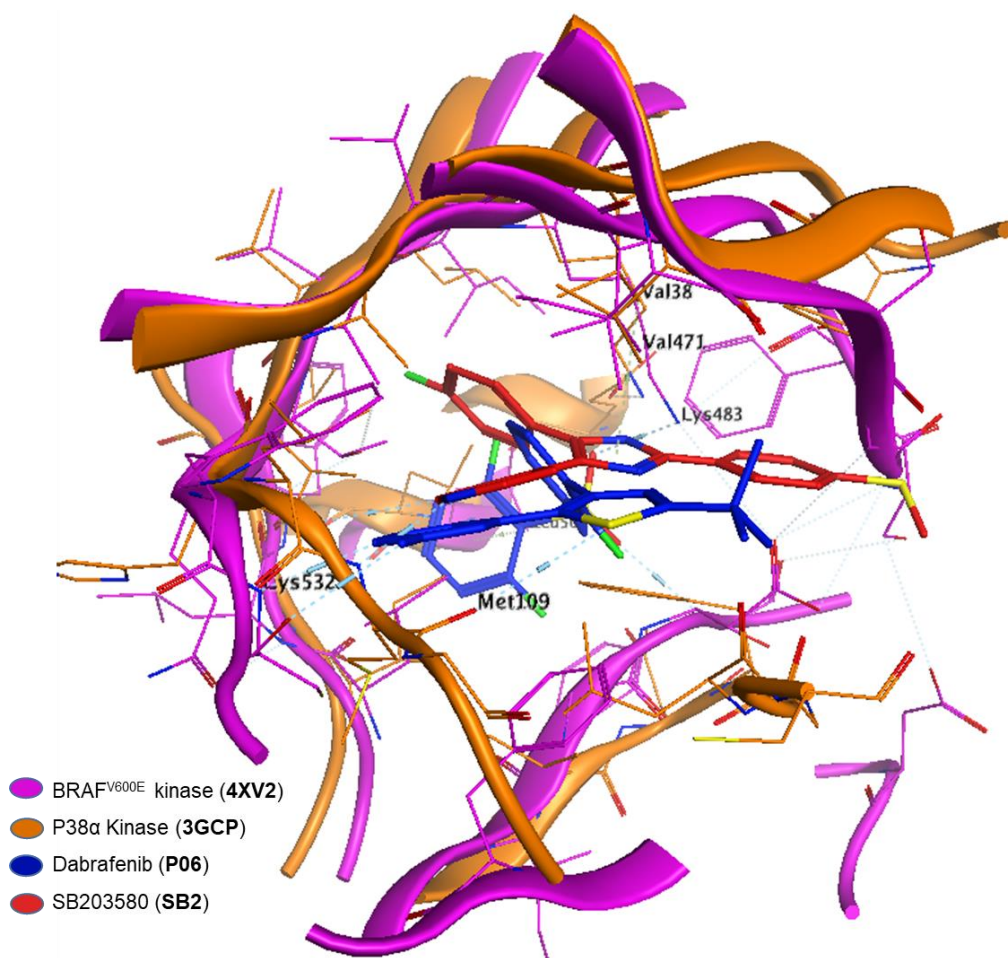


**Figure 2.** Superposition of B-RAF<sup>V600E</sup> kinase (PDB: 4XV2) and p38 $\alpha$  kinase (PDB: 3GCP) binding pockets showing the alignment between their ligands **Dabrafenib** (P06) and **SB203580** (SB2).

### 2.1.2. The SAR of the reported P38 $\alpha$ inhibitors

Many studies have reported imidazole-based derivatives acting as a potent p38 $\alpha$  kinase inhibitors where **SB203580** the pyridin-4-ylimidazole derivative was used as a lead compound to prepare imidazole-based derivatives act as ATP mimetic for inhibition of p38 $\alpha$  kinase as a target in inflammation therapy [16, 35-38]. In this regard, the structural modifications of the lead compound **SB203580** led to improving the p38 $\alpha$  kinase inhibitory activity, which in turn get insight into the structural activity relationship of the designed inhibitors. Such modifications were illustrated in replacing the central imidazole ring by bicyclic benzopyrazines and pyrazolo pyrimidines or by triazole ring resulted in more potent P38 $\alpha$  kinase inhibitors with

good anti-inflammatory activity [39-42]. Furthermore, replacement of the pyridinyl moiety in the hinge binding area by hetero bicyclic ring boosted the molecular interactions in P38 $\alpha$  kinase binding site through the additional H-bond and afforded new candidates with potent enzyme inhibitory activity [41, 43].

The essential interactions of **SB203580** inhibitor with the ATP-binding cleft are briefly illustrated in (Figure 3, a), where the 2-aminopyridyl residues bonds to the adenine hinge binding region by hydrogen bond acceptor, while, the para fluoro phenyl moiety occupies the hydrophobic back pocket. The central imidazole ring embeds into the ribose pocket and possesses H-bond interaction with the NH of Lys53. In addition, the phosphate phosphate binding region is occupied with 4-(methylsulfinyl)phenyl at position 2 of the imidazole ring [1]. The structural similarity between our Imidazolyl pyridine series and both **SB203580** and other reported imidazole-based inhibitors brought our attention to predict their binding mode and their biological activity, as well. In this work, Imidazolyl pyridine derivatives were proposed to conserve the molecular interaction behavior of **SB203580** alongside additional interactions to bring the target compounds higher binding affinity. In designing of our compounds we also guided by the reported SAR studies of tri substitution on the central imidazole scaffold, which resulted in the production of pyridinylimidazole derivatives possessing different substitution at C2-pyridine that rendered the produced candidates higher affinity into the enzyme binding site and better inhibitory activity [44]. As a result, in addition to the essential binding mode of **SB203580**, the target derivatives were expected to bind strongly in the hinge adenine region through an additional H-bond between the NH at position 2 of the pyridine and the carbonyl oxygen of Met109, the terminal sulphonamide moiety with ethyl or propyl spacer was to orient the sulphonamide aromatic moiety towards the hydrophobic front pocket (Figure 3, b).

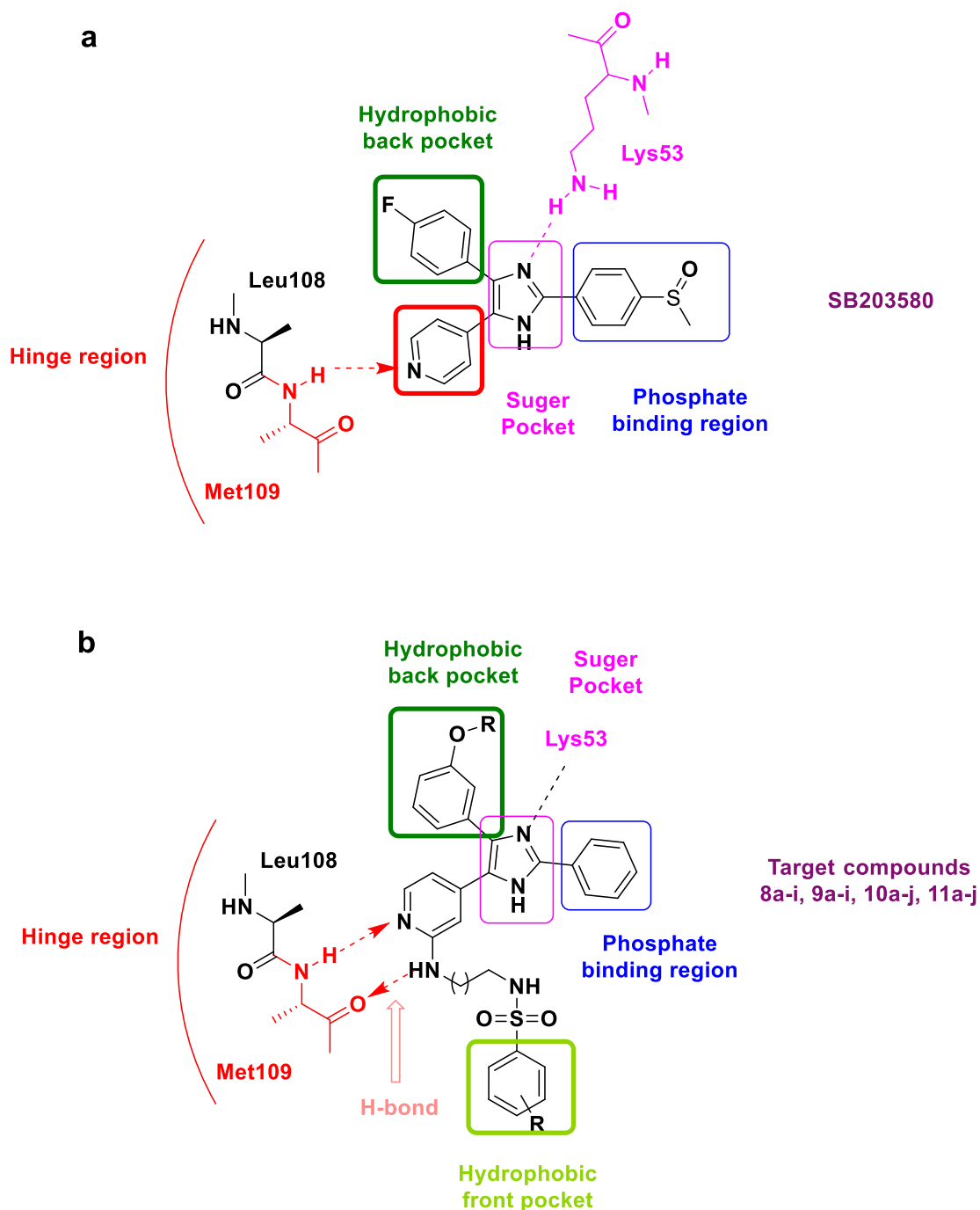


**Figure 3. a)** Binding mode of **SB203580** into ATP binding site (PDB: 3GCP), **b)** proposed binding mode of the target inhibitors into the ATP-binding.

### 2.1.3. Pharmacophore model development

Pharmacophore model were developed using MOE software. The 3D pharmacophore model was built using reported p38 $\alpha$  kinase which can properly

detect SAR of the existing p38 $\alpha$  kinase inhibitors. Then, the model was used as 3D search query for predicting the structural requirements of each compound to identify p38 $\alpha$  kinase new inhibitors. In this study, a training set of 25 p38 $\alpha$  kinase inhibitors with structural diversity and wide range of inhibitory activity were collected from different research papers (Figure 1). All compounds were built in 2D structure using ChemDraw software, MOE software was used for the molecular 3D visualization and minimization to the closest local minimum using the CHARMM-like force field. The pharmacophore query was generated using hydrogen bond acceptor (HBA), hydrogen bond donor (HBD), hydrophobic (H) and ring aromatic (RA) chemical features. A group fifteen energetically reasonable conformational models were generated. The selected pharmacophore model represented by two hydrophobic centers (F1: Hyd/Aro and F2: Hyd/Aro), one aromatic center (F3: Aro), and one center (F4: ML/Acc/Don) including H-bond donor (Don), the H-bond acceptor (Acc), and metal ligator (ML) (Figure 4).

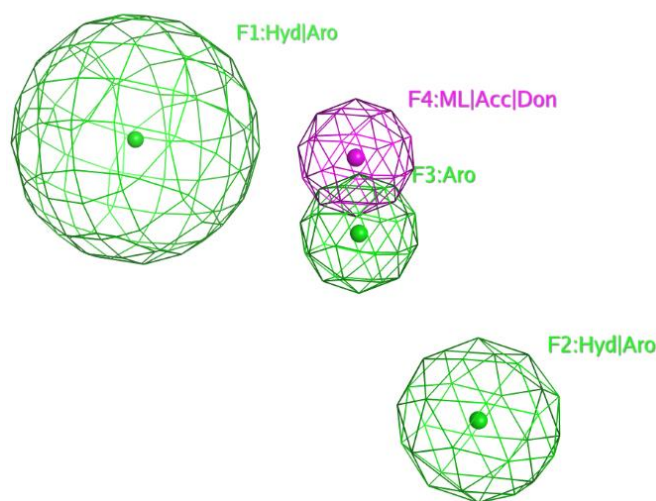


**Figure 4.** The common features pharmacophore model generated from training set alignment.

The produced pharmacophore model was used for mapping the imidazolyl pyridine target compounds and the RMSD values were determined less than 1. The target compounds showed typical fitting in the pharmacophore model. As shown in Figure 5, the first hydrophobic centre F1 was represented by the terminal aromatic sulphonamide group, the phenyl moiety at C2 of the imidazole signified the second hydrophobic centre F2, while the lateral pyridine ring represented aromatic centre F3,

the nitrogen atom of pyridine represented the H-bond acceptor (Acc) part in (F4: ML/Acc/Don) centre.

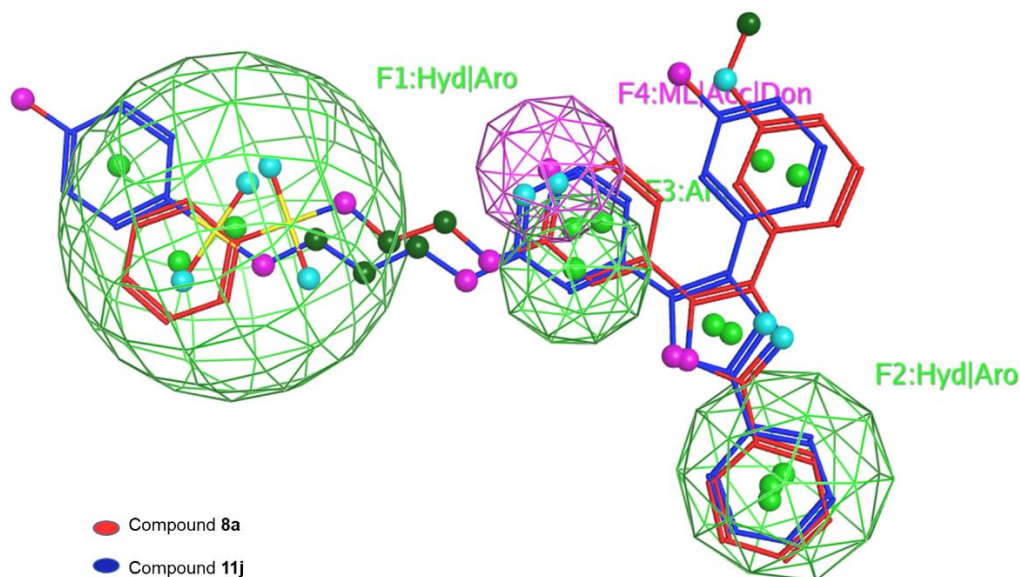
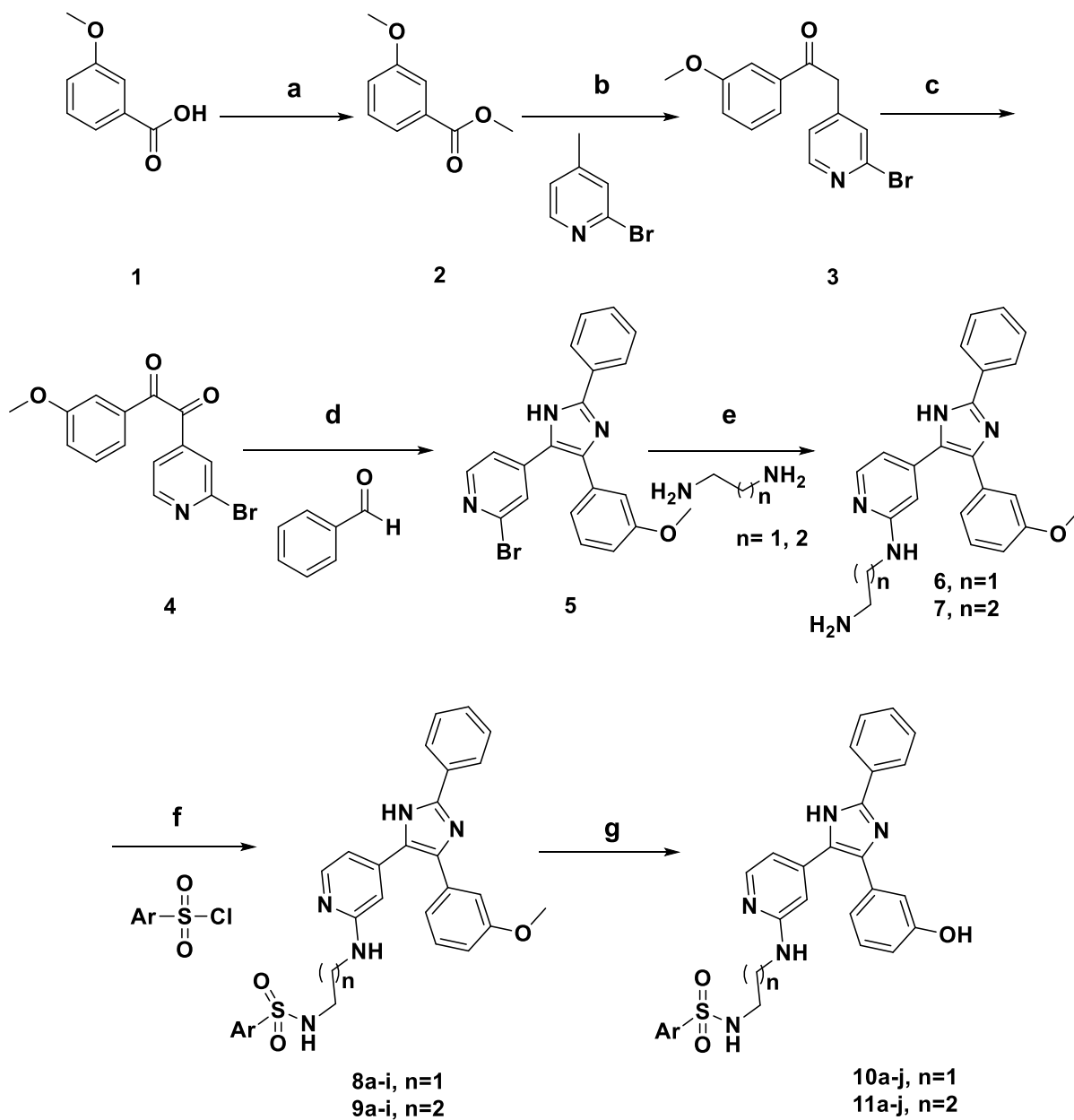


**Figure 5.** Mapping of compounds **8a** (red) and **11j** (blue) on the generated pharmacophore model.

## 2.2. Chemistry

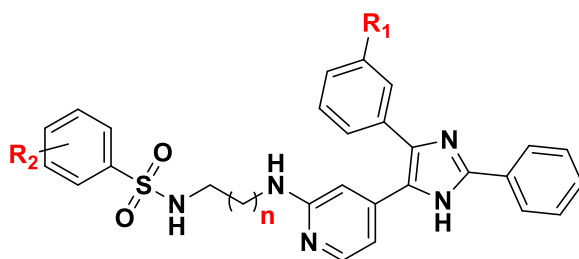
Synthesis of the target compounds **8a-i**, **9a-i**, **10a-j**, and **11a-j** was fulfilled according to **Scheme 1**. Esterification of the 3-methoxy-4-chlorobenzoic acid **1** to its corresponding methyl ester **2** was carried out by reaction with methanol in the presence of sulphuric acid. In basic media of lithium bis(trimethylsilyl)amide (LiHMDS), the methyl ester **2** reacted with 2-bromo-4-methylpyridine to afford 2-(2-bromopyridin-4-yl)-1-(3-methoxyphenyl)ethan-1-one **3**. Imidazole intermediate **5** was prepared by oxidation of **3** by hydrobromic acid in DMSO into 1-(2-bromopyridin-4-yl)-2-(3-methoxyphenyl)ethane-1,2-dione **4**, followed by cyclisation through the reaction with benzaldehyde in presence of ammonium acetate and acetic acid. Reaction of compound **5** with ethylene diamine or propylene diamine afforded compounds **6** and **7**, respectively. Subsequent reaction of **6** or **7** with different aromatic sulfonyl chlorides produced the final target compounds **8a-i** and **9a-i**. The demethylated derivatives **10a-j** and **11a-j** were obtained by demethylation of **8a-i** or **9a-i** by boron tribromide at -70 °C in presence of catalytic amount of

tetrabutylammonium iodide under N<sub>2</sub> atmosphere. The key structure of the target compounds is illustrated in [Table 1](#).



**Scheme 1. Reagents and conditions:** **a)** MeOH, c.H<sub>2</sub>SO<sub>4</sub>, 80 °C, 12 h.; **b)** LiHMDS, THF, -70 °C, 18 h.; **c)** HBr, DMSO, 55 °C, 2 h.; **d)** NH<sub>4</sub>OAc, CH<sub>3</sub>COOH, 100 °C, 4 h.; **e)** 100 °C, 12 h.; **f)** DCM, DIPEA, rt, 12 h.; **g)** BBr<sub>3</sub>, TBAI, -70 °C, 6 h.

**Table 1:** Structure of the target compounds **8a-i**, **9a-i**, **10a-j**, and **11a-j**.



Cpd.	R <sub>1</sub>	R <sub>2</sub>	n	Cpd.	R <sub>1</sub>	R <sub>2</sub>	n
<b>8a</b>	OCH <sub>3</sub>	H	1	<b>10b</b>	OH	p-Cl	1
<b>8b</b>	OCH <sub>3</sub>	p-Cl	1	<b>10c</b>	OH	p-Br	1
<b>8c</b>	OCH <sub>3</sub>	p-Br	1	<b>10d</b>	OH	p-F	1
<b>8d</b>	OCH <sub>3</sub>	p-F	1	<b>10e</b>	OH	m-Cl	1
<b>8e</b>	OCH <sub>3</sub>	m-Cl	1	<b>10f</b>	OH	2,6-Cl	1
<b>8f</b>	OCH <sub>3</sub>	2,6-Cl	1	<b>10g</b>	OH	m-F	1
<b>8g</b>	OCH <sub>3</sub>	m-F	1	<b>10h</b>	OH	p-CF <sub>3</sub>	1
<b>8h</b>	OCH <sub>3</sub>	p-CF <sub>3</sub>	1	<b>10i</b>	OH	p-OCH <sub>3</sub>	1
<b>8i</b>	OCH <sub>3</sub>	p-OCH <sub>3</sub>	1	<b>10j</b>	OH	p-OH	1
<b>9a</b>	OCH <sub>3</sub>	H	2	<b>11a</b>	OH	H	2
<b>9b</b>	OCH <sub>3</sub>	p-Cl	2	<b>11b</b>	OH	p-Cl	2
<b>9c</b>	OCH <sub>3</sub>	p-Br	2	<b>11c</b>	OH	p-Br	2
<b>9d</b>	OCH <sub>3</sub>	p-F	2	<b>11d</b>	OH	p-F	2
<b>9e</b>	OCH <sub>3</sub>	m-Cl	2	<b>11e</b>	OH	m-Cl	2
<b>9f</b>	OCH <sub>3</sub>	2,6-Cl	2	<b>11f</b>	OH	2,6-Cl	2
<b>9g</b>	OCH <sub>3</sub>	m-F	2	<b>11g</b>	OH	m-F	2
<b>9h</b>	OCH <sub>3</sub>	p-CF <sub>3</sub>	2	<b>11h</b>	OH	p-CF <sub>3</sub>	2
<b>9i</b>	OCH <sub>3</sub>	p-OCH <sub>3</sub>	2	<b>11i</b>	OH	p-OCH <sub>3</sub>	2
<b>10a</b>	OH	H	1	<b>11j</b>	OH	p-OH	2



## 2.3. Biological evaluation

### 2.3.1. *In vitro* p38a kinase inhibitory activity

The synthesized target compounds were evaluated for their *In vitro* p38a kinase inhibitory activity using ELISA technique (enzyme-linked immunosorbent assay). The inhibition activities for each derivative are illustrated in **Table 2**. The preliminary data revealed that the tested compounds exhibited a wide range of inhibitory activity against p38a/MAPK14 Kinase. Over all, compounds **10a-j** and **11a-j** with 3-hydroxy phenyl moiety at position 4 of the imidazole ring exhibited a slight higher inhibitory activity than the 3-methoxy phenyl containing derivatives **8a-i** and **9a-i**, in addition, derivatives **9a-i** and **11a-j** possessing propyl linker on the pyridine ring showed higher inhibitory activity compared to their ethyl linker possessing counterpart **8a-i** and **10a-j**.

In regard to the terminal sulfonamide moiety of methoxy bearing derivatives **8a-i** and **9a-i**, substitution with electron withdrawing groups on compounds **8a** or **9a** had diverse impact on the activity; para-substitution with bulky groups such as Br or CF<sub>3</sub> in compounds **8c**, **8h**, **9c**, and **9h** reasonably enhanced the inhibitory, whereas, para or meta substitution with small groups like Cl or F in compounds **8b**, **8d**, **8e**, **8g**, **9b**, **9d**, **9e**, and **9g** dramatically reduced the activity nearly to its half, para OMe substitution in compounds **8i** and **9i** showed no remarkable change in the activity.

However, the hydroxyl owing compounds **10a-j** and **11a-j** responded in a different manner upon substitution on the terminal sulfonamide moiety; in comparison with the unsubstituted derivatives **10a** and **11a**, para-substitution with small electron withdrawing group like F or electron donating group OH in compounds **10d**, **10j**, **11d**, and **11j** retain similar inhibitory activity, fierce activity falling was observed by substitution with electron withdrawing groups such as Cl, Br, CF<sub>3</sub>, OMe in compounds **10b**, **10c**, **10e**, **10f**, **10g**, **10h**, and **10i**, while compounds **11b**, **11c**, **11e**, **11f**, **11g**, **11h**, **11i** showed moderate activity reduction ([Table 2](#), [Figure 6](#)).



**Table 2.** *In vitro* p38a kinase % Inhibition data of target compounds **8a-i**, **9a-i**, **10a-j**, and **11a-j**.

<b>Cpd.</b>	<b>% Inhibition of p38<math>\alpha</math> kinase at (10 <math>\mu</math>M)</b>	<b>Cpd.</b>	<b>% Inhibition of p38<math>\alpha</math> kinase at (10 <math>\mu</math>M)</b>
<b>8a</b>	74.42	<b>10b</b>	46.60
<b>8b</b>	35.27	<b>10c</b>	46.78
<b>8c</b>	90.00	<b>10d</b>	97.10
<b>8d</b>	50.01	<b>10e</b>	47.86
<b>8e</b>	36.31	<b>10f</b>	38.34
<b>8f</b>	34.72	<b>10g</b>	59.63
<b>8g</b>	48.61	<b>10h</b>	36.50
<b>8h</b>	90.11	<b>10i</b>	75.05
<b>8i</b>	61.08	<b>10j</b>	99.01
<b>9a</b>	88.61	<b>11a</b>	99.80
<b>9b</b>	67.72	<b>11b</b>	87.98
<b>9c</b>	94.01	<b>11c</b>	87.31
<b>9d</b>	78.95	<b>11d</b>	99.70
<b>9e</b>	62.45	<b>11e</b>	86.83
<b>9f</b>	65.36	<b>11f</b>	81.00
<b>9g</b>	76.42	<b>11g</b>	91.00
<b>9h</b>	96.00	<b>11h</b>	75.28
<b>9i</b>	89.04	<b>11i</b>	92.02
<b>10a</b>	99.70	<b>11j</b>	98.01

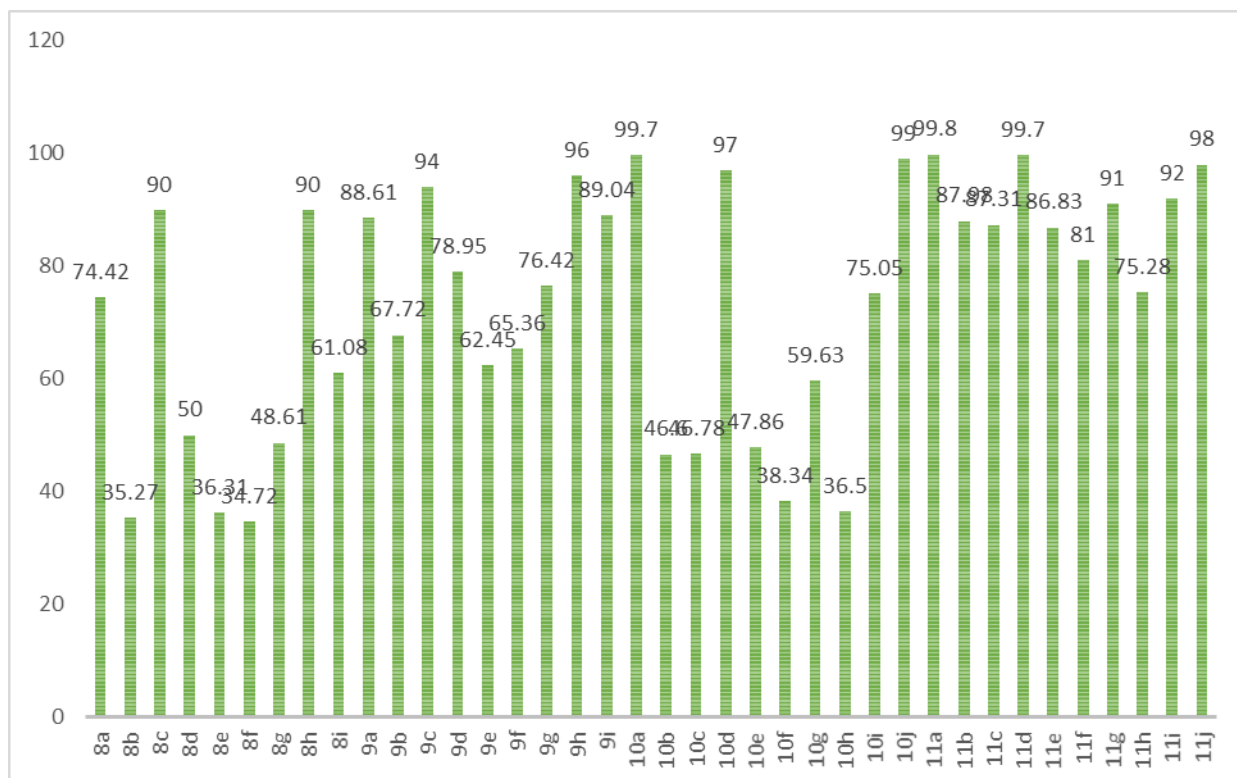


**Figure 6.** Inhibitory activities of the target compounds (**8a-i**, **9a-i**, **10a-j**, and **11a-j**) against P38 $\alpha$  kinase in terms of percent inhibition.

In order to determine the accurate potency of the final target compounds, IC<sub>50</sub> determination was performed. The test was carried out at 10 doses of tested compounds with serial dilution (3-fold) at 1  $\mu$ M. An IC<sub>50</sub> value higher than 1  $\mu$ M was estimated based on the best curve fitting available. The IC<sub>50</sub> values were illustrated in [Table 3](#).

Generally, compounds **10a-j** and **11a-j** with *meta* hydroxyl group showed higher potency compared to their methoxy analogue **8a-i** and **9a-i**. In addition, derivatives with propylene spacer between pyridine ring and terminal sulfonamide moieties **11a-j** had higher potency related to compounds having ethylene spacer **10a-j**.

Regarding the first set of compounds **8a-i**, compound **8h** which carries *para* trifluoromethyl benzene sulfonamide had the strongest potency with IC<sub>50</sub> 1.75  $\mu$ M followed by *meta* fluoro benzene sulfonamide derivative **8g** with IC<sub>50</sub> 2.54  $\mu$ M and *para* bromo benzene sulfonamide derivative **8c** with IC<sub>50</sub> 3.25  $\mu$ M. Disubstituted derivative **8f** was more active compared to monosubstituted analogue **8b** with IC<sub>50s</sub>

8.25  $\mu$ M and 16  $\mu$ M, respectively and this different in potency may be related to non-planer effect of disubstituted derivative.

For propylene spacer carrying compounds **9a-i**, slight increase in potency appeared. Compound **9h** with para trifluoromethyl benzene sulfonamide had the highest activity with  $IC_{50}$  0.98  $\mu$ M followed by **9g** with  $IC_{50}$  1.15  $\mu$ M. Compounds **9c** and **9d** showed similar potencies with  $IC_{50}$  3.52 and 3.91  $\mu$ M, respectively. *Meta* chloro (6.91  $\mu$ M) and dichloro substituted (6.75  $\mu$ M) derivatives had higher activity compared to pare substituted analogue.

Dramatic increase in potency occurred when *meta* methoxy phenyl was replaced with *meta* hydroxyl group **10a-j** and **11a-j**. In addition, unsubstituted derivatives and compounds having small size *para* substitution such as fluoro and hydroxyl group had the highest activity among these derivatives. Compounds **11a** (un substituted with propylene spacer) and **11d** (*para* fluoro with propylene spacer) were emerged to be the most potent inhibitors with  $IC_{50}$  values of 47 nm and 45 nm, respectively followed by **10a** (unsubstituted with ethylene spacer) with  $IC_{50}$  95 nM.

**Table 3.**  $IC_{50}$  values of final target compounds over p38 $\alpha$ /MAPK14 kinase.

Cpd.	P38 $\alpha$ kinase $IC_{50}$ (nM)	Cpd.	P38 $\alpha$ kinase $IC_{50}$ (nM)
<b>8a</b>	7100 $\pm$ 74.00	<b>10b</b>	11900 $\pm$ 460.00
<b>8b</b>	16000 $\pm$ 122.00	<b>10c</b>	12100 $\pm$ 395.00
<b>8c</b>	3250 $\pm$ 125.00	<b>10d</b>	<b>150 <math>\pm</math> 23.20</b>
<b>8d</b>	10000 $\pm$ 255.00	<b>10e</b>	10200 $\pm$ 246.00
<b>8e</b>	14500 $\pm$ 350.00	<b>10f</b>	14300 $\pm$ 742.00
<b>8f</b>	8250 $\pm$ 210.00	<b>10g</b>	8950 $\pm$ 460.00
<b>8g</b>	2540 $\pm$ 360.00	<b>10h</b>	13210 $\pm$ 578.00
<b>8h</b>	1750 $\pm$ 150.00	<b>10i</b>	2160 $\pm$ 199.00
<b>8i</b>	8720 $\pm$ 348.00	<b>10j</b>	510 $\pm$ 5.21

<b>9a</b>	4980 ± 416.00	<b>11a</b>	<b>47 ± 1.16</b>
<b>9b</b>	7850 ± 201.00	<b>11b</b>	<b>120 ± 6.51</b>
<b>9c</b>	3520 ± 310.00	<b>11c</b>	<b>99 ± 2.36</b>
<b>9d</b>	3910 ± 275.00	<b>11d</b>	<b>45 ± 0.98</b>
<b>9e</b>	6910 ± 175.00	<b>11e</b>	101 ± 2.22
<b>9f</b>	6750 ± 190.00	<b>11f</b>	8250 ± 35.5
<b>9g</b>	1150 ± 285.00	<b>11g</b>	321 ± 3.14
<b>9h</b>	980 ± 25.00	<b>11h</b>	961 ± 65.00
<b>9i</b>	4120 ± 142.00	<b>11i</b>	130 ± 4.56
<b>10a</b>	<b>95 ± 4.21</b>	<b>11j</b>	124 ± 5.44

### 2.3.2. In vitro anti-inflammatory activity

The anti-inflammatory activity of the active derivatives was detected by their ability to inhibit nitric oxide (NO) and prostaglandin-E2 (PGE2) production by suppression of inducible nitric oxide synthase (iNOS) and cyclooxygenase-2 (COX-2) expression in LPS-stimulated RAW264.7 cells[45]. In addition, the most active inhibitors were evaluated for their effect on inhibiting the production of pro-inflammatory cytokines (TNF- $\alpha$ , 1L-6, and 1L-1 $\beta$ )

#### 2.3.2.1. Nitric Oxide (NO) assay

RAW264.7 macrophages were pre-incubated with different concentrations of the tested compounds for 2 h, and then stimulated by LPS (1 $\mu$ g/mL) for 24 h. After incubation, the nitrite concentrations of supernatants were determined using Griess reagent [46]. In this study, **L-NIL** (L-N6-(1-iminoethyl) lysine) was used as a reference compound at concentration of 40  $\mu$ M, L-NIL is a potent and selective inhibitor of inducible nitric oxide synthase (**iNOS**) over other nitric oxide synthase isoforms[47].

The nitric oxide inhibitory activity at fixed concentration (1  $\mu$ M) and IC<sub>50</sub> for the final target compounds were represented in Table 4. Compounds **9c**, **9d**, **9h**, **10a**, **11a**, **11b**, **11c**, **11i** and **11j** exhibited the highest activity with percent inhibition 72 %, 69%, 70%, 71% 72%, 74%, 73%, 71% and 72%, and IC<sub>50</sub>s 0.62  $\mu$ M, 0.94  $\mu$ M, 0.71  $\mu$ M, 0.62  $\mu$ M, 0.58  $\mu$ M, 0.51  $\mu$ M, 0.50  $\mu$ M, 0.68  $\mu$ M and 0.66  $\mu$ M, respectively.

The data in Figure 7 reveals that a significant raise in nitric oxide concentration was noticed after stimulation of the cell lines with LPS in comparison with the LPS non-stimulated blank cells, the concentration of NO was reduced to its half in the cells which previously incubated with L-NIL. While, the most potent P38 $\alpha$  inhibitors **9c**, **10a**, **11b**, **11d**, and **11j** showed a slight reduction in NO production at concentration of 10 nm, a significant fall in NO concentration was observed in cells incubated with 100 nm and 1000 nm of compound **11j**.

**Table 4.** Nitric oxide percent inhibition at 1  $\mu$ M for final target compounds and their IC<sub>50</sub> in LPS-stimulated RAW264.7 cells

Cpd.	NO % inhibition	IC <sub>50</sub> ( $\mu$ M)	Cpd.	NO % inhibition	IC <sub>50</sub> ( $\mu$ M)
<b>8a</b>	17.81% $\pm$ 1.21	10.21 $\pm$ 1.20	<b>10b</b>	38.26 % $\pm$ 1.33	2.98 $\pm$ 0.09
<b>8b</b>	9.61% $\pm$ 1.02	20.35 $\pm$ 2.48	<b>10c</b>	28.37% $\pm$ 0.99	6.35 $\pm$ 0.06
<b>8c</b>	37.65 % $\pm$ 2.10	6.35 $\pm$ 0.98	<b>10d</b>	60.21% $\pm$ 1.61	0.71 $\pm$ 0.002
<b>8d</b>	21.56 % $\pm$ 0.99	9.84 $\pm$ 0.62	<b>10e</b>	21.96 % $\pm$ 0.74	5.32 $\pm$ 0.08
<b>8e</b>	12.65 % $\pm$ 0.88	19.81 $\pm$ 1.06	<b>10f</b>	29.11% $\pm$ 2.11	4.55 $\pm$ 0.03
<b>8f</b>	25.36% $\pm$ 1.18	9.67 $\pm$ 0.87	<b>10g</b>	37.34% $\pm$ 0.85	3.92 $\pm$ 0.09
<b>8g</b>	40.55 % $\pm$ 1.45	4.89 $\pm$ 0.71	<b>10h</b>	40.32% $\pm$ 1.46	3.99 $\pm$ 0.07
<b>8h</b>	45.32 % $\pm$ 1.68	3.12 $\pm$ 0.45	<b>10i</b>	51.25% $\pm$ 0.97	0.99 $\pm$ 0.01
<b>8i</b>	13.64% $\pm$ 0.96	9.96 $\pm$ 0.74	<b>10j</b>	62.33% $\pm$ 1.08	0.68 $\pm$ 0.01
<b>9a</b>	26.53 % $\pm$ 2.22	6.35 $\pm$ 0.61	<b>11a</b>	72.56 % $\pm$ 0.87	0.58 $\pm$ 0.01

<b>9b</b>	60.21% ± 1.77	0.85 ± 0.01	<b>11b</b>	74.29 % ± 0.82	0.51 ± 0.01
<b>9c</b>	72.18 % ± 1.35	0.62 ± 0.03	<b>11c</b>	75.25% ± 0.88	0.50 ± 0.02
<b>9d</b>	69.52 % ± 0.85	0.94 ± 0.06	<b>11d</b>	69.28 % ± 1.31	0.61 ± 0.02
<b>9e</b>	48.56 % ± 0.96	1.01± 0.02	<b>11e</b>	65.32 % ±1.35	0.67 ± 0.02
<b>9f</b>	56.54% ± 1.31	0.92 ± 0.01	<b>11f</b>	42.25% ±1.42	1.17 ± 0.06
<b>9g</b>	61.35% ± 2.14	0.88 ± 0.01	<b>11g</b>	54.27% ± 0.52	0.86 ± 0.03
<b>9h</b>	70.02% ± 0.77	0.71 ± 0.01	<b>11h</b>	44.31% ± 0.67	2.64 ± 0.07
<b>9i</b>	63.54% ± 0.81	0.83 ± 0.004	<b>11i</b>	71.28 % ± 0.89	0.68 ± 0.01
<b>10a</b>	71.55% ± 1.47	0.62 ± 0.003	<b>11j</b>	72.42 % ± 1.00	0.66 ± 0.01

### 2.3.2.2. PGE<sub>2</sub> enzyme-linked immunosorbent assay

RAW264.7 cells were incubated with LPS (1µg/mL) for 24 h. PGE<sub>2</sub> levels were analyzed using the prostaglandin E<sub>2</sub> BiotrackELISA system [48]. In this test, **NS-398** was used as a reference compound, NS-398 is a novel anti-inflammatory and analgesic agent that inhibits prostaglandin production through the inhibition of cyclooxygenase-2 (COX-2) activity [49].

Compounds **8g** and **8h** were the most potent compounds among the first series **8a-i** with percent inhibition 78.22% and 78.25% and IC<sub>50s</sub> 0.630 uM and 0.634 uM. On the other hand, compounds **9c**, **9d** and **9h** were the most potent compounds in the second series with percent inhibition 97 %, 92% and 95% and IC<sub>50s</sub> 0.551 uM, 0.541 uM, and 0.523 uM, respectively. Regarding the third series **10a-j**, compounds **10a** and **10d** showed the highest activities with percent inhibition 96% and 95% and IC<sub>50s</sub> 0.520 and 0.310 uM. Compounds **11a**, **11b**, **11c**, **11d**, **11e** and **11j** showed over 90% inhibition at 1 uM and IC<sub>50s</sub> 0.312, 0.589, 0.601, 0.290, 0.581 and 0.546 uM (Table 5).

The data in Figure 7 illustrates that remarkable jump in PGE<sub>2</sub> production was observed upon treatment with LPS, the concentration of PGE<sub>2</sub> was dramatically declined to its fifth by incubation with NS-398. At concentration 10 nm, the most

potent compounds **9c**, **10a**, **11a**, **11d**, and **11j** were obviously ineffective in reducing PGE2 production. However, by raising the concentration of the tested compounds to 100 and 1000 nM dramatic decrease in PGE2 was observed.

**Table 5.** Percent inhibition of PGE2 at 1  $\mu$ M for final target compounds and their IC<sub>50</sub> in LPS-stimulated RAW264.7 cells

Cpd.	%Inhibition of PGE <sub>2</sub>	IC <sub>50</sub> (nM)	Cpd.	%Inhibition of PGE <sub>2</sub>	IC <sub>50</sub> (nM)
<b>8a</b>	77.23% $\pm$ 1.32	643.21 $\pm$ 5.17	<b>10b</b>	81.89 % $\pm$ 0.95	612.25 $\pm$ 6.33
<b>8b</b>	69.31 % $\pm$ 2.11	716.54 $\pm$ 4.72	<b>10c</b>	58.41% $\pm$ 0.86	920.67 $\pm$ 15.21
<b>8c</b>	61.36 % $\pm$ 3.15	810.36 $\pm$ 8.31	<b>10d</b>	<b>95.68 % <math>\pm</math> 1.05</b>	310.11 $\pm$ 9.35
<b>8d</b>	62.12 % $\pm$ 3.51	797.71 $\pm$ 7.38	<b>10e</b>	60.21% $\pm$ 0.98	756.38 $\pm$ 13.61
<b>8e</b>	59.66% $\pm$ 2.84	838.86 $\pm$ 5.89	<b>10f</b>	59.25% $\pm$ 1.18	795.32 $\pm$ 9.15
<b>8f</b>	66.61 % $\pm$ 2.98	742.38 $\pm$ 4.68	<b>10g</b>	69.78% $\pm$ 0.88	698.58 $\pm$ 11.23
<b>8g</b>	78.22 % $\pm$ 1.33	634.37 $\pm$ 6.35	<b>10h</b>	71.27% $\pm$ 0.94	670.54 $\pm$ 10.27
<b>8h</b>	78.52 % $\pm$ 2.37	630.65 $\pm$ 7.61	<b>10i</b>	87.69 % $\pm$ 0.71	565.89 $\pm$ 5.66
<b>8i</b>	55.25 % $\pm$ 1.87	901.11 $\pm$ 11.25	<b>10j</b>	89.65% $\pm$ 0.84	530.24 $\pm$ 8.99
<b>9a</b>	79.21% $\pm$ 2.42	625.16 $\pm$ 9.57	<b>11a</b>	<b>96.43 % <math>\pm</math> 1.41</b>	312.39 $\pm$ 4.32
<b>9b</b>	88.36 % $\pm$ 3.21	561.21 $\pm$ 4.95	<b>11b</b>	<b>91.26% <math>\pm</math> 1.27</b>	589.28 $\pm$ 6.54
<b>9c</b>	<b>97.14 % <math>\pm</math> 1.60</b>	511.35 $\pm$ 4.21	<b>11c</b>	<b>90.99% <math>\pm</math> 1.01</b>	601.21 $\pm$ 7.89
<b>9d</b>	<b>92.35% <math>\pm</math> 1.99</b>	541.76 $\pm$ 8.64	<b>11d</b>	<b>96.93 % <math>\pm</math> 1.11</b>	290.42 $\pm$ 5.14
<b>9e</b>	85.32% $\pm$ 1.54	581.68 $\pm$ 7.89	<b>11e</b>	<b>92.35% <math>\pm</math> 0.84</b>	581.56 $\pm$ 4.98

<b>9f</b>	86.65% ± 1.16	577.71 ± 6.25	<b>11f</b>	74.65%± 0.71	797.58 ±8.74
<b>9g</b>	89.35% ± 1.56	556.52 ± 5.35	<b>11g</b>	86.88% ± 0.93	625.54 ± 7.11
<b>9h</b>	<b>95.41% ± 2.01</b>	523.35 ± 4.58	<b>11h</b>	87.58%±0.61	618.21 ± 8.16
<b>9i</b>	71.59 % ±1.97	690.49 ± 9.12	<b>11i</b>	89.47%± 0.86	601.54 ± 7.17
<b>10a</b>	<b>96.28% ± 0.05</b>	520.94 ± 4.57	<b>11j</b>	<b>92.57 % ± 0.80</b>	546 ± 3.75

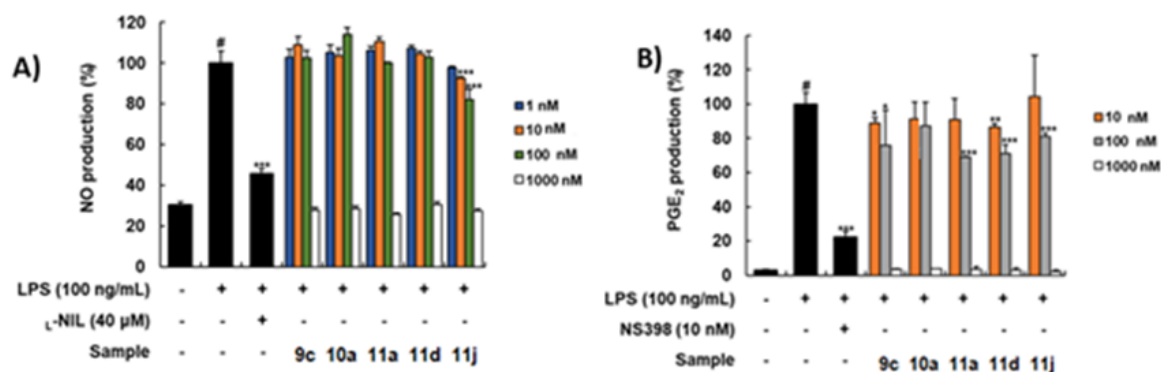


**Figure 7. A)** Nitric oxide production inhibition activity of compounds **9c**, **10a**, **11a**, **11d**, and **11j** on LPS stimulated RAW 264.7 macrophage **B)** PGE<sub>2</sub> production inhibition activity of compounds **9c**, **10a**, **11a**, **11d**, and **11j** on LPS stimulated RAW 264.7 macrophage.

### 2.3.2.3. Inflammatory cytokines production assay

Further investigation was conducted to the most potent P38α inhibitor compounds **11d** and **11a** were further evaluated for inhibitory effect on the proinflammatory cytokines TNF-α, 1L-6, and 1L-1β production in lipopolysaccharide-stimulated THP-1 human cells ([Figure 8](#)). Compound **11d** showed high potency against the production of TNF-α and 1L-1β with IC<sub>50</sub> values of 78 nM and 82 nM, respectively. While the production of 1L-6 was moderately inhibited by higher concentration of compound **11d** (IC<sub>50</sub> = 17.6 μM). Compound **11a** showed good activity against TNF-α production (IC<sub>50</sub> =



98.02 nM), but showed no remarkable activity against the production of 1L-6 and 1L-1 $\beta$ .

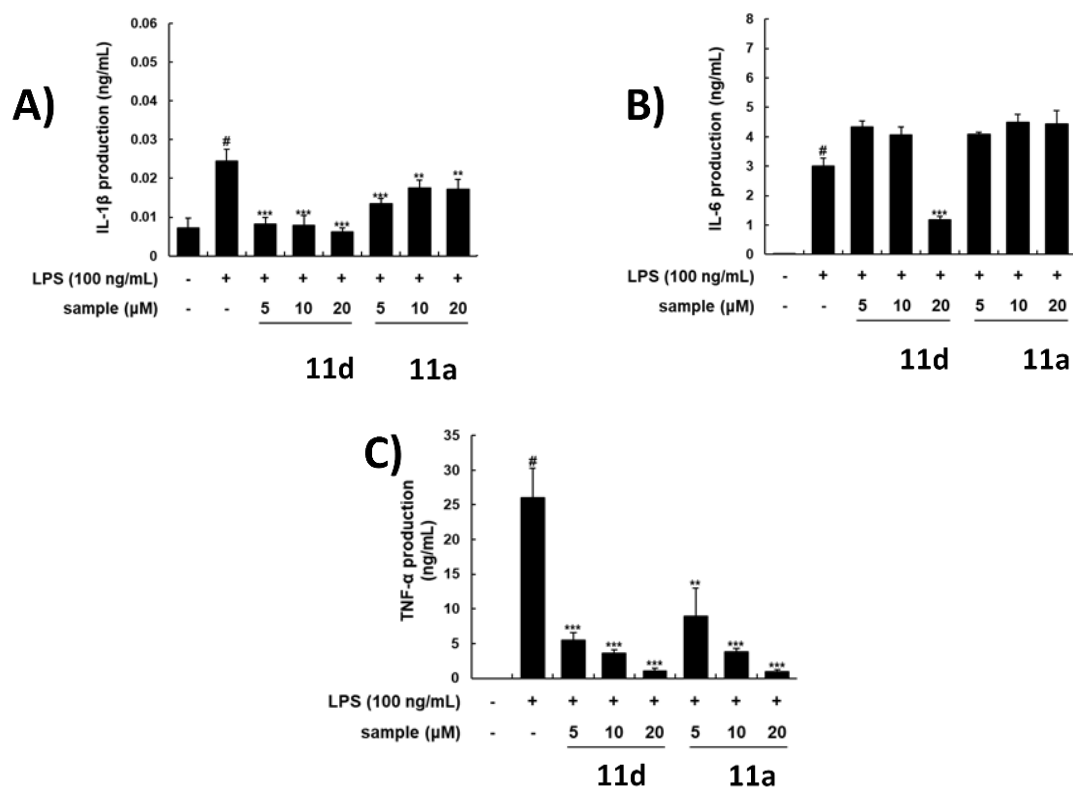


**Figure 8.** Effect of **11d** and **11a** on cytokine production in LPS-stimulated Raw 264.7 macrophage at different concentration. **A)** 1L-1 $\beta$  (ng/mL) **B)** 1L-6 (ng/mL). **C)** TNF- $\alpha$  (ng/mL).

## 2.4. Molecular Modelling Studies

### 2.4.1. Molecular docking study

In attempt to correlate the diversity in p38 $\alpha$ /MAPK14 kinase inhibitory activities and the Imidazolyl pyridine compounds structural features, Molecular docking was performed using (MOE) software. Target compounds **8a-i**, **9a-i**, **10a-j**, and **11a-j** were docked inside the active site of p38 $\alpha$ /MAPK14 kinase in complex with **SB203580** (PDB ID: 3GCP) [35] in order to define their binding pattern (**Table S1**). The obtained docking results show that the SB203580-p38 $\alpha$ /MAPK14 kinase domain

complex has a low root mean square deviation, RMSD (1.0579) that proves valid docking protocol with dock score (-12.16 kcal/mol, [Table 3](#)). The native ligand (**SB203580**) binds in the ATP pocket through H-bond formation between the Nitrogen of pyridine ring at position 5 of the imidazole ring and Met109 amino acid in the adenine hinge region, while, the hydrophobic back pocket is occupied by the 4-fluoro phenyl moiety at position 5 of the imidazole ring, the central imidazole ring embeds in the ribose pocket via arene-H-bond interaction with Val38, the oxygen of the terminal methylsulfinyl phenyl at position 2 of the imidazole ring binds in the phosphate area by forming H-bond with Tyr35 residue.

Accordingly, the target compounds were proposed to conserve the essential binding behavior of SB203580. Analysis of the docking results in [Table 6](#) revealed that most of the target compounds bind in the hinge region by the same manner of SB203580 when NH of Met109 binds to the nitrogen of the pyridine via a H-bond, besides, well alignment is observed between Imidazole scaffold of the target compounds and SB203580 imidazole where the N-3 of imidazole form H-bond with Lys53 in the sugar binding area ([Figure 9](#)). Interestingly, imidazole ring in some derivatives with a high binding score exhibit different binding mode through arene-arene interaction with Phe169 in compounds **8h**, **10d**, **11a**, **11f**, and **11i**. Additional molecular interactions are noticed in compounds **8a**, **8b**, **8c**, **8e**, **8i**, **9c**, **10b**, **10e**, **10i**, **10j**, **11c**, and **11e** because of the terminal sulfonamide moiety with ethyl or propyl linker, the oxygen of sulfonamides shares by H-bond with Cys172 which results in orientation of the aromatic groups towards the hydrophobic front pocket. Moreover, Arene-H interactions are formed between the terminal aromatic moiety of sulfonamides and amino acids Cys172, Thr185, and Gly110 in compounds **8f**, **8h**, and **9b**, respectively ([Figure 9](#)).

**Table 6:** Docking results of target compounds **8a-i**, **9a-i**, **10a-j**, and **11a-j** in p38 $\alpha$ /MAPK14 kinase (PDB ID: 3GCP).

Comp.	Energy score (Kcal/mol)	Amino acid	Binding group	Interaction	H-bond length (Å)
<b>SB203580</b>	-12.16	Met109 Tyr35 Val38	Pyridine ring (N) SOCH3 (O) Imidazole ring	H-bond H-bond	2.73 2.51

				Arene-H	
<b>8a</b>	-13.87	Lys53 Met109 Cys172	Imidazole ring (N) Pyridine ring (N) SO2	H-bond H-bond H-bond	3.47 3.47 3.95
<b>8b</b>	-12.52	Lys53 Met109 Cys172	Imidazole ring (N) Pyridine ring (N) SO2	H-bond H-bond H-bond	3.32 3.57 3.96
<b>8c</b>	-12.19	Lys53 Met109 Cys172	Imidazole ring (N) Pyridine ring (N) SO2	H-bond H-bond H-bond	3.32 3.58 3.93
<b>8d</b>	-13.42	Met109	Pyridine ring (N)	H-bond	3.39
<b>8e</b>	-12.07	Cys172	SO2	H-bond	3.95
<b>8f</b>	-11.49	Lys53 Met109 Cys172	Imidazole ring (N) Pyridine ring (N) 2,6-Cl-Phenyl ring	H-bond H-bond Arene-H	3.52 3.41
<b>8g</b>	-12.87	Lys53	HN-SO2 (NH)	H-bond	2.98
<b>8h</b>	-13.05	Lys152 Phe169 Thr185	SO2 Imidazole ring 4-CF3-Phenyl ring	H-bond Arene-Arene H-bond	3.63 2.98
<b>8i</b>	-11.84	Lys53 Cys172 Phe169 Val38	Imidazole ring (N) SO2 Imidazole ring Pyridine ring	H-bond H-bond Arene-Arene Arene-H	2.85 3.44
<b>9a</b>	-15.52	Lys53 Gly110 Val38	SO2 Phenyl ring Pyridine ring	H-bond Arene-H Arene-H	3.45
<b>9b</b>	-13.15	Gly110 Met109	4-Cl-Phenyl ring Pyridine ring (N)	Arene-H H-bond	3.41
<b>9c</b>	-13.19	Cys172 Met109	HN-SO2 (NH) Pyridine ring (N)	H-bond H-bond	4.29 3.34
<b>9d</b>	-13.74	Met109	Pyridine ring (N)	H-bond	3.3
<b>9e</b>	-12.20	Val38	Imidazole ring	Arene-H	
<b>9f</b>	-12.81	Phe169	Imidazole ring	Arene-Arene	
<b>9g</b>	-14.42	Met109	Pyridine ring (N)	H-bond	3.49
<b>9h</b>	-13.19	Phe169	Imidazole ring	Arene-Arene	
<b>9i</b>	-12.23	Lys53	Imidazole ring (N)	H-bond	3.42

<b>10a</b>	-14.09	Lys53 Met109 Cys172	Imidazole ring (N) Pyridine ring (N) SO2	H-bond H-bond H-bond	3.3 3.48 3.89
<b>10b</b>	-13.23	Met109 Cys172	Pyridine ring (N) SO2	H-bond H-bond	3.58 3.39
<b>10c</b>	-12.52	Met109	Pyridine ring (N)	H-bond	3.47
<b>10d</b>	-13.78	Lys53 Phe169	Imidazole ring (N) Imidazole ring	H-bond Arene-Arene	2.89
<b>10e</b>	-13.60	Cys172 Lys53 Phe169	SO2 HN-SO2 (NH) Imidazole ring (N) Imidazole ring	H-bond H-bond H-bond Arene-Arene	3.9 4.12 3.02
<b>10f</b>	-13.54	Met109	Pyridine ring (N)	H-bond	3.44
<b>10g</b>	-13.96	Met109	Pyridine ring (N)	H-bond	3.44
<b>10h</b>	-12.80	Met109	Pyridine ring (N)	H-bond	3.39
<b>10i</b>	-14.86	Lys53 Met109 Cys172	Imidazole ring (N) Pyridine ring (N) SO2	H-bond H-bond H-bond	3.26 3.51 4.15
<b>10j</b>	-13.09	Met109 Cys172	Pyridine ring (N) SO2	H-bond H-bond	3.32 3.95
<b>11a</b>	-12.64	Lys53 Leu171 Phe169	Imidazole ring (N) HN-SO2 (NH) Imidazole ring	H-bond H-bond Arene-Arene	3.31 3.47
<b>11b</b>	-12.31	Lys53 Phe169	Imidazole ring (N) Imidazole ring	H-bond Arene-Arene	2.85
<b>11c</b>	-14.55	Met109 Cys172	Pyridine ring (N) SO2	H-bond H-bond	3.56 3.48
<b>11d</b>	-12.79	His107 Lys53 Tyr35 Val38	3-OH phenyl (OH) SO2 NH Phenyl ring Imidazole ring	H-bond H-bond H-bond Arene-H Arene-H	2.51 2.53 2.92
<b>11e</b>	-13.45	Met109 Cys172	Pyridine ring (N) SO2	H-bond H-bond H-bond	2.91 3.49 3.54
<b>11f</b>	-12.56	Lys53 Phe169 Val38	Imidazole ring (N) Imidazole ring Pyridine ring	H-bond Arene-Arene Arene-H	2.78
<b>11g</b>	-13.45	Leu171 Met109	HN-SO2 (NH) Pyridine ring (N)	H-bond H-bond	3.16 4.2
<b>11h</b>	-12.47	Lys53 Met109	Imidazole ring (N) Pyridine ring (N)	H-bond H-bond	3.45 3.44

<b>11i</b>	-12.50	Lys53 Met109 Phe169	Imidazole ring (N) Pyridine ring (N) Imidazole ring	H-bond H-bond Arene-Arene	3.41 3.54
<b>11j</b>	-14.02	Met109	Pyridine ring (N)	H-bond	3.27

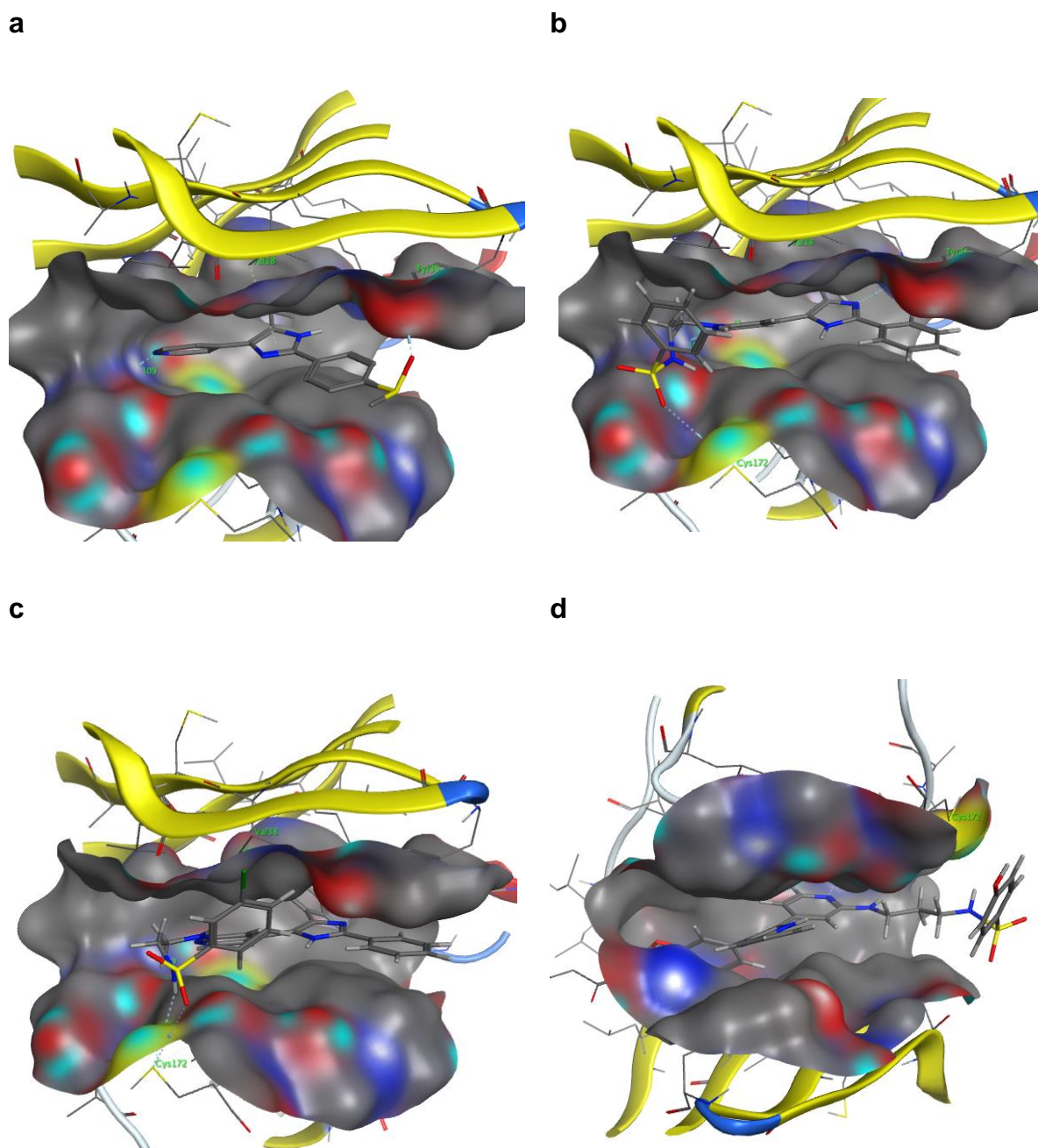


**Figure 9.** 3D representation of docking study output (PDB ID: 3GCP). **a)** 3D interaction of **SB203580** (native ligand) with p38 $\alpha$ /MAPK14 kinase enzyme domain;

**b)** 3D interaction of **8a** with p38 $\alpha$ /MAPK14 kinase enzyme domain; **c)** 3D interaction of **10e** with p38 $\alpha$ /MAPK14 kinase enzyme domain; **d)** 3D interaction of **11j** with p38 $\alpha$ /MAPK14 kinase enzyme domain.

### 2.4.1. Molecular dynamics simulations

From the previous docking findings, the most potent inhibitor compound **11d** showed high fitting affinity in the active site of P38 $\alpha$  kinase with energy score of -12.79 Kcal/mole, while the native ligand energy was -12.19 Kcal/mole (**Figure 10**). Compound **11d** binds into the kinase active site by two H-bonds with Lys53 backbone, one additional H-bond was formed between the terminals 3-hydroxy phenyl moiety and His107 residue. In addition, the central imidazole ring embedded in the ribose pocket via Arene-H interaction with Val38, the phenyl group at the imidazole position 2 participated in Arene-H interaction with Tyr35. Finally, water molecules formed a bridge of interaction between NH of Imidazole ring and Leu171, and 4-fluoro phenyl moiety and Arg67.

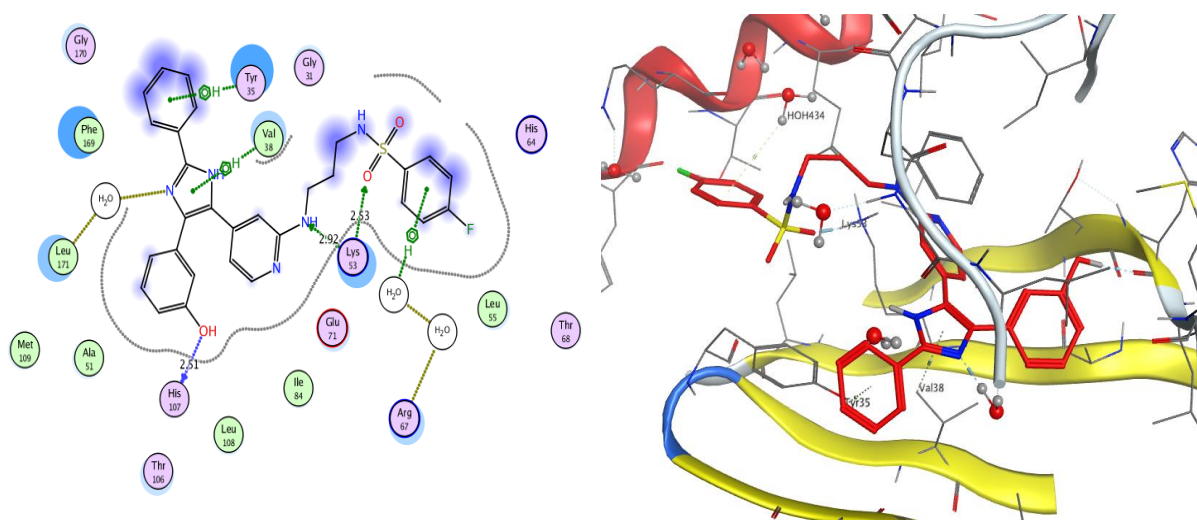


**Figure 10.** 2D and 3D interaction diagram of compound **11d** in the active site of P38 $\alpha$  kinase (PDB ID: 3GCP).

Accordingly, molecular dynamics (MD) simulations analysis was conducted for compound **11d** in a bid to study the conformational stability of its docked inhibitor-protein complex and to attain dependable drug-receptor-binding affinities.

MD simulations study was performed for 600 ns for inhibitor **11d** in comparison to the native ligand **SB203580** in the active site of the corresponding kinase (PDB ID: 3GCP). The MD simulations protocol was run at 300 K temperature, and the atomic potential energy was recorded in a time interval of 0.5 ns.

To explore the dynamic stability of both 3GCP-**11d** and 3GCP-**SB203580** complexes, the time-dependent atomic potential energy of each complex was calculated during MD trajectories. As illustrated in **Figure 11**, the ligand-protein complex (3GCP/**SB203580**) attained the equilibrium around 250 ns. While, the inhibitor-protein complex (3GCP/**11d**) achieved equilibrium around 300 ns.

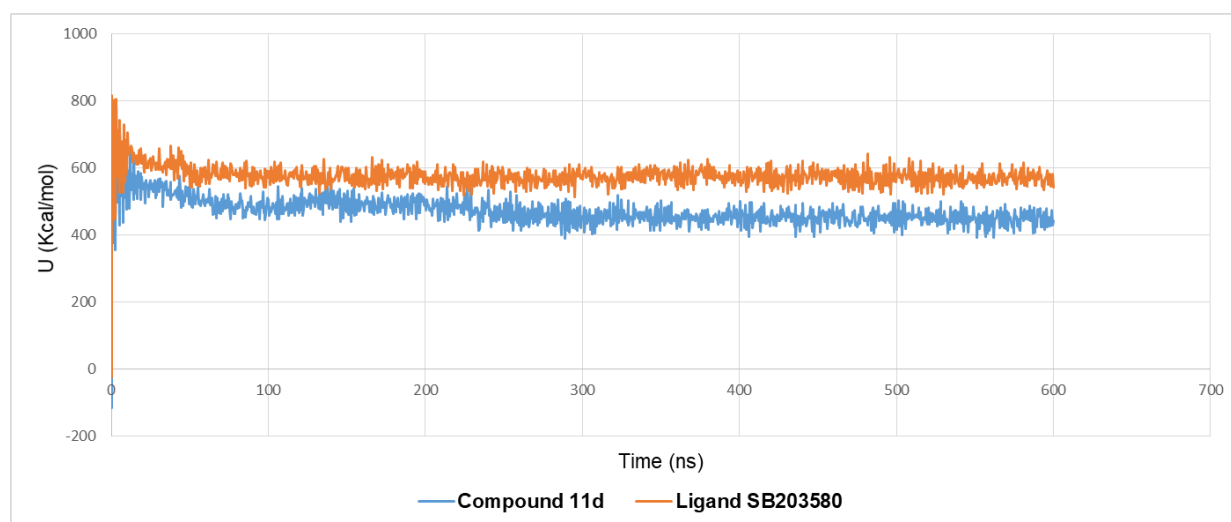


**Figure 11.** Potential energy evaluation of complex of compound **11d** and native ligand **SB203580** with P38 $\alpha$  kinase (PDB ID: 3GCP) binding site as function of time (ns).

In addition, the root mean square deviation (RMSD) values were observed during the simulation process to predict the stability of the ligand-protein complex. The recorded RMSD values were also represented as a function of time in **Figure 12**. The obtained results indicate that the native ligand and the tested inhibitor **11d** have retained their binding affinity and kept firmly bound to their respective kinase binding site. As shown in **Figure 12**, the inhibitor-protein and ligand-protein complexes



exhibited interaction stability during the first 300 ns of simulations. Then, RMSD curves of the tested ligands fluctuated for around 100 ns of simulation before its quite stability at the end of simulation time 600 ns.

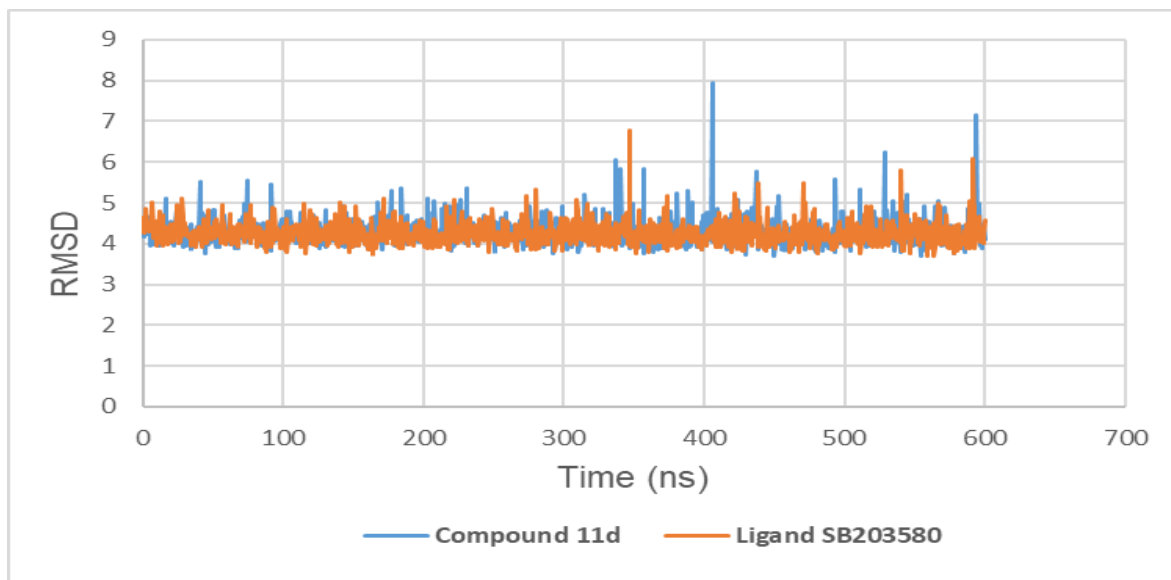


**Figure 12.** The RMSD curve from the molecular dynamics simulation of compound **11d** and native ligand **SB203580** complexes with P38 $\alpha$  kinase. The x-axis represents the simulation time (ns), while the y-axis represents the RMSD value (nm).

### 3. Structure activity relationship

The final target compounds exhibited structural diversity included different substitutions and different spacer length, which in turn bring each derivative a different structural features. As a result, broad range of the inhibitory activity was obtained over treating the enzyme with a dose of corresponding compound. Such a variability in compounds activities is illustrated in (Figure 13) as following; 1) An elevation of P38 $\alpha$  kinase inhibitory activity was observed upon demethylation of compounds **8a-i** and **9a-i** to their corresponding meta hydroxyl derivatives **10a-j** and **11a-j**, the produced hydroxyl moiety might improve the solubilisation of the compounds and increase their affinity in the enzyme binding pocket by providing additional H-bond. 2) Additionally, the propylene linker in compounds **9a-i** and **11a-j** allows the extension of the terminal aromatic sulphonamide moiety into the front hydrophobic pocket of P38 $\alpha$  kinase, and resulting in higher potency comparing to the



ethylene linker owing derivatives **8a-i** and **10a-j**. 3) Regarding to the terminal aromatic sulphonamides, substitution on the phenyl group didn't show significant impact on the activity except for the para-fluoro substituted derivatives with the propylene linker (**9d** and **11d**), while, bulky group substitution dramatically declined the activity.

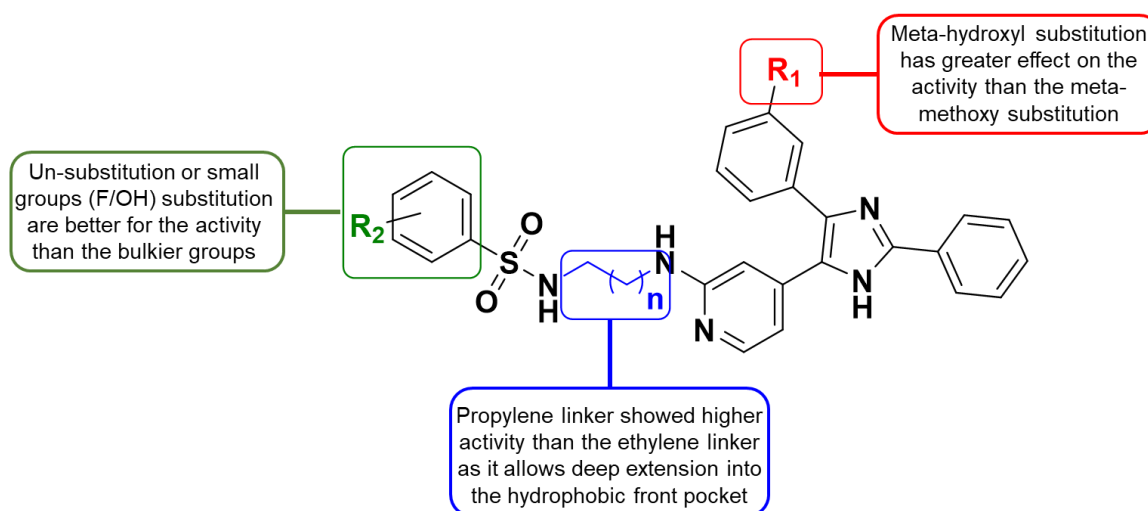


**Figure 13.** Structural activity relationship of the target compounds illustrating the effect of their structural features and the enzyme inhibitory activity.

#### 4. Conclusion

A group of off-target based drug repurposing strategies were followed to repositioning of a series of 38 imidazoly pyridine B-RAF<sup>V600E</sup> kinase inhibitors to work as p38 $\alpha$  kinase inhibitors. Protein alignment protocol was applied to superpose the crystal structures of p38 $\alpha$  kinase (PDB: 3GCP) and B-RAF<sup>V600E</sup> kinase (PDB: 4XV2), and the ligand binding site of both enzymes showed high sequence similarities. Therefore, SB203580 the native ligand of p38 $\alpha$  kinase (PDB: 3GCP) was used as a lead compound to predict the binding mode of the target compound and their expected activity, as well. Furthermore, pharmacophore model was built using a group of 25 p38 $\alpha$  kinase inhibitors with a wide range of inhibitory activity, the produced model was used for mapping the target derivatives in order to prove their fitting affinity, the tested compounds exhibited typical fitting in the model. The target compounds were evaluated for their potency to inhibit p38 $\alpha$  kinase, compounds **11a**

and **11d** emerged to be the most potent inhibitors ( $IC_{50} = 47$  nm and 45 nm, respectively). Compound **11d** was subjected to further investigation in order to determine its prolonged effect on the production of pro-inflammatory cytokines (TNF- $\alpha$ , 1L-6, and 1L-1 $\beta$ ) in LPS-stimulated RAW264.7 macrophages. Compound **11d** showed high potency against the production of TNF- $\alpha$ , 1L-6, and 1L-1 $\beta$  with  $IC_{50}$  values of 78 nM, 17.6  $\mu$ M, and 82 nM, respectively.

Moreover, the anti-inflammatory activity of was detected by determining the ability of the target compounds to inhibit nitric oxide (NO) and prostaglandin-E2 (PGE2) in LPS-stimulated RAW264.7, compound **11d** exhibited satisfied inhibitory activity of the production of PGE2 and NO with  $IC_{50}$  values of 3.8  $\mu$ M and 8.4  $\mu$ M, respectively.

To correlate the enzyme activity of the target compounds with their structure, the compounds were docked into the p38 $\alpha$  kinase crystal structure (PDB: 3GCP), most of the derivatives conserved the same binding behavior of the native ligand SB203580. In addition, the conformational stabilities of the protein–ligand complexes obtained via docking of the potent inhibitor **11d** and the native ligand were studied by applying MD simulations protocol, the potential energy was calculated during the stimulation process in a time interval of 0.5 ns for 600 ns.

The currently investigated imidazoly pyridine series is considered a starting point for further structural modification in developing potent p38 $\alpha$  kinase inhibitors with promising anti-inflammatory activity.

## 5. Experimental

### 5.1. Chemistry

The intermediate compounds as well as the target compounds were purified by flash column chromatography using silica gel 60 (0.040-0.063 mm, 230-400 mesh ASTM) and technical grade solvents.  $^1H$  NMR and  $^{13}C$  NMR analyses were carried out on a Bruker Avance 400 spectrometer using tetramethylsilane (TMS) as an internal standard. Melting points were measured on a Walden Precision Apparatus Electrothermal 9300 apparatus and were uncorrected. LC-MS analysis was conducted using the following system: Waters 2998 photodiode array detector,

Waters 3100 mass detector, Waters SFO system fluidics organizer, Waters 2545 binary gradient module, Waters reagent manager, Waters 2767 sample manager, Sunfire™ C<sup>18</sup> column (4.6 × 50 mm, 5 μm particle size); Solvent gradient = 95% A at 0 min, 1% A at 5 min; solvent A: 0.035% trifluoroacetic acid (TFA) in water; solvent B: 0.035% TFA in MeOH; flow rate = 3.0 mL/min; the AUC was calculated using Waters MassLynx 4.1 software. The solvents and liquid reagents were transferred using hypodermic syringes. All the solvents and reagents were purchased from commercial companies, and used as such.

#### 5.1.1. Methyl 3-methoxybenzoate (**2**)

A mixture of 3-methoxybenzoic (**1**, 4.24 g, 0.002 mol) and methanol (40 mL) were heated under reflux until the benzoic acid was dissolved in methanol then few drops of concentrated sulphuric acid was added to the mixture and refluxed for 8 h. The resulting mixture was cooled to room temperature, diluted with water and a saturated solution of sodium bicarbonate was added to the mixture to neutralize the benzoic acid, extracted with ethyl acetate, dried and evaporated to get the required ester compound **2**.

Yield: 90%. m.p.: 110-112 °C. <sup>1</sup>H NMR (400 MHz, CDCl<sub>3</sub>) δ 7.61 (m, 1H, Ar-H), 7.54 (m, 1H, Ar-H), 7.31 (t, *J* = 8 Hz, 1H, Ar-H), 7.07 (m, 1H, Ar-H), 3.89 (s, 1H, OCH<sub>3</sub>), 3.81 (s, 1H, OCH<sub>3</sub>). <sup>13</sup>C NMR (100 MHz, CDCl<sub>3</sub>) δ 166.85 (Ar-C), 159.86 (Ar-C), 131.41 (Ar-C), 129.6 (Ar-C), 122.16 (Ar-C), 119.36 (Ar-C), 114.22 (Ar-C), 55.29 (OOCH<sub>3</sub>), 52.04 (OCH<sub>3</sub>).

#### 5.1.2. 2-(2-Bromopyridin-4-yl)-1-(3-methoxyphenyl)ethan-1-one (**3**)

A solution of compound **2** (1.0 g, 5.0 mmol) and 2-bromo-4-picoline (0.5 mL, 5.6 mmol) in THF (5 mL) was cooled to -25 °C, and LiHMDS (3.7 mL, 1.0 M solution in THF, 19.9 mmol) was slowly added at -25 °C to the reaction mixture maintaining the temperature at -25 °C. The resulting mixture was stirred overnight at room temperature. The mixture was quenched with saturated aqueous NH<sub>4</sub>Cl (15 mL), and ethyl acetate (20 mL) was added. The organic layer was separated, and the aqueous layer was extracted with ethyl acetate (3 -10 mL). The combined organic layer was

washed with saline and dried over anhydrous sodium sulfate. The organic solvent was evaporated under vacuum and the residue was purified by flash column chromatography (silica gel, hexane ethyl acetate 1:1 v/v then switching to hexane-ethyl acetate 1:5 v/v) to yield the title compound **4**, which was subjected to the next step without further purification.

#### 5.1.3. 1-(2-Bromopyridin-4-yl)-2-(3-methoxyphenyl)ethane-1,2-dione (**4**)

A solution of compound **4** (2.0 g, 6.8 mmol) in DMSO (10 mL) was heated to 55 °C. Hydrobromic acid (2.5 ml, 20.4 mmol, 3 eq.) was added dropwise to the reaction mixture. The reaction was stirred at 55 °C for 2 hours. The reaction mixture was poured carefully to a saturated solution of sodium bicarbonate, extracted with ethyl acetate, dried and evaporated to get the required compound **4**.

Yield: 80%. m.p.: 115-117 °C. <sup>1</sup>H NMR (400 MHz, CDCl<sub>3</sub>) δ 8.63 (d, *J* = 5.2 Hz, 1H, Ar-H), 7.97 (s, 1H, Ar-H), 7.75 (d, *J* = 1.2 Hz, 1H, Ar-H), 7.74 (d, *J* = 1.2 Hz, 1H, Ar-H), 7.48 (m, 2H, Ar-H), 7.26 (m, 1H, Ar-H), 3.9 (s, 3H, OCH<sub>3</sub>). <sup>13</sup>C NMR (100 MHz, CDCl<sub>3</sub>) δ 191.71 (Ar-C), 191.01 (Ar-C), 160.26 (Ar-C), 151.57 (Ar-C), 143.47 (Ar-C), 141.19 (Ar-C), 133.25 (Ar-C), 130.3 (Ar-C), 127.24 (Ar-C), 123.39 (Ar-C), 122.65 (Ar-C), 121.26 (Ar-C), 113.08 (Ar-C), 55.61 (OCH<sub>3</sub>).

#### 5.1.4. 2-Bromo-4-(4-(3-methoxyphenyl)-2-phenyl-1H-imidazol-5-yl)pyridine (**5**)

To a solution of compound **4** (1.23 g, 4 mmol) and Benzaldehyde (0.4 ml, 4 mmol) in acetic acid (10 ml), ammonium acetate (3.1 g, 40 mmol, 10 eq.) was added. The reaction mixture was heated to 100 °C for 4 hours. The reaction mixture was poured in Ammonia solution with crushed ice. The resulted precipitate was filtered, washed with water three times, and dried under vacuum to get the titled compound **5**.

Yield: 75%. m.p.: 125-127 °C. <sup>1</sup>H NMR (400 MHz, CDCl<sub>3</sub>) δ 10.45 (s, 1H, Ar-H), 8.15 (d, *J* = 5.2 Hz, 1H, Ar-H), 7.94 (d, *J* = 7.2 Hz, 2H, Ar-H), 7.45 (m, 4H, Ar-H), 7.36 (t, *J* = 8 Hz, 1H, Ar-H), 7.04 (d, *J* = 7.6 Hz, 1H, Ar-H), 6.98 (d, *J* = 8.8 Hz, 2H, Ar-H), 3.08 (s, 3H, OCH<sub>3</sub>). <sup>13</sup>C NMR (100 MHz, CDCl<sub>3</sub>) δ 160.03 (Ar-C), 149.7 (Ar-C), 142.49 (Ar-C), 130.3 (Ar-C), 129.42 (Ar-C), 129.22 (Ar-C), 129.01 (Ar-C), 125.53 (Ar-C),

125.32 (Ar-C), 120.32 (Ar-C), 120.24 (Ar-C), 114.83 (Ar-C), 113.83 (Ar-C), 55.41 (OCH<sub>3</sub>).

#### 5.1.5. N1-(4-(4-(3-methoxyphenyl)-2-phenyl-1H-imidazol-5-yl)pyridin-2-yl)ethane(propan)- diamine (**6-7**)

A solution of compound **5** (2.0 g, 5 mmol) in ethylenediamine (3 ml, 50 mmol, 10 eq.) or propylenediamine (3.7 ml, 50 mmol, 10 eq.) was heated under reflux for 12 hours. The reaction mixture was evaporated under vacuum producing the title compounds **6** and **7**, respectively. The produced compounds were subjected to the next step reaction without further purification.

#### 5.1.6. N-(2-((4-(4-(3-methoxyphenyl)-2-phenyl-1H-imidazol-5-yl)pyridin-2-yl)amino)ethyl(propyl))substituted benzenesulfonamide (**8-9**)

To a solution of compound **6** or **7** (0.3 mmol) in anhydrous dichloromethane (6 mL), DIPEA (0.6 mmol, 2 eq.) was added at 0 °C, stirred for 15 min, then Benzenesulfonyl chlorides (0.36 mmol, 1.2 eq.) was added drop wise. The reaction mixture was stirred at room temperature for 24 h. When the reaction completed, the solvent was removed and the residue was partitioned between ethyl acetate and water. The organic layer was separated and the aqueous layer was extracted with ethyl acetate (3 -10 mL). The combined organic layer was washed with brine two times and the organic solvent was evaporated under reduced pressure. The residue was purified by column chromatography (silica gel, hexane-ethyl acetate 2:1 v/v) to give the required products **8** and **9** as solid.

##### 5.1.6.1. N-(2-((4-(4-(3-methoxyphenyl)-2-phenyl-1H-imidazol-5-yl)pyridin-2-yl)amino)ethyl)benzenesulfonamide (**8a**):

Yield: 65%. m.p.: 139-141 °C. HPLC purity 94.8%, <sup>1</sup>H NMR (400 MHz, CDCl<sub>3</sub>) δ 7.92 (d, *J* = 4.8 Hz, 2H, Ar-H), 7.73 (d, *J* = 5.16 Hz, 1H, Ar-H), 7.66 (d, *J* = 8.16 Hz, 2H, Ar-H), 7.33 (q, *J* = 8.75 Hz, 5H, Ar-H), 7.19 (t, *J* = 7.52 Hz, 1H, Ar-H), 7 (s, 2H, Ar-H), 6.83 (d, *J* = 7.4 Hz, 1H, Ar-H), 6.66 (s, 1H, Ar-H), 6.6 (d, *J* = 3.48 Hz, 1H, Ar-H), 4.96 (s, 1H, NH), 3.69 (s, 3H, OCH<sub>3</sub>), 3.3 (s, 2H, CH<sub>2</sub>CH<sub>2</sub>NHSO<sub>2</sub>), 3.02 (s, 2H,

CH<sub>2</sub>CH<sub>2</sub>NHSO<sub>2</sub>). <sup>13</sup>C NMR (100 MHz, CDCl<sub>3</sub>) δ 159.62 (Ar-C), 158.48 (Ar-C), 147.05 (Ar-C), 146.59 (Ar-C), 138.85 (Ar-C), 138.43 (Ar-C), 129.66 (Ar-C), 129.55 (Ar-C), 129.27 (Ar-C), 129.03 (Ar-C), 128.79 (Ar-C), 125.73 (Ar-C), 120.99 (Ar-C), 113.95 (Ar-C), 113.85 (Ar-C), 112.24 (Ar-C), 105.92 (Ar-C), 55.25 (OCH<sub>3</sub>), 44.01 (CH<sub>2</sub>CH<sub>2</sub>NHSO<sub>2</sub>), 41.63 (CH<sub>2</sub>CH<sub>2</sub>NHSO<sub>2</sub>). LC/MS (ESI) 526 (M +1) <sup>+</sup>.

5.1.6.2. 4-Chloro-N-(2-((4-(4-(3-methoxyphenyl)-2-phenyl-1H-imidazol-5-yl)pyridin-2-yl)amino)ethyl)benzenesulfonamide (**8b**):

Yield: 60%. m.p.: 130-132 °C. <sup>1</sup>H NMR (400 MHz, CDCl<sub>3</sub>) δ 7.95 (d, *J* = 6.6 Hz, 2H, Ar-H), 7.79 (d, *J* = 5.52 Hz, 1H, Ar-H), 7.64 (s, 1H, Ar-H), 7.61 (s, 1H, Ar-H), 7.57 (s, 1H, Ar-H), 7.55 (d, *J* = 1.72 Hz, 2H, Ar-H), 7.38 (m, 3H, Ar-H), 7.25 (d, *J* = 8 Hz, 1H, Ar-H), 7.05 (d, *J* = 5.92 Hz, 2H, Ar-H), 6.88 (dd, *J* = 1.75 Hz, 1H, Ar-H), 6.71 (s, 1H, Ar-H), 6.67 (d, *J* = 4 Hz, 1H, Ar-H), 4.94 (s, 1H, NH), 3.75 (s, 3H, OCH<sub>3</sub>), 3.38 (t, *J* = 4.84 Hz, 2H, CH<sub>2</sub>CH<sub>2</sub>NHSO<sub>2</sub>), 3.08 (t, *J* = 5.32 Hz, 2H, CH<sub>2</sub>CH<sub>2</sub>NHSO<sub>2</sub>). <sup>13</sup>C NMR (100 MHz, CDCl<sub>3</sub>) δ 159.73 (Ar-C), 158.41 (Ar-C), 146.89 (Ar-C), 146.43 (Ar-C), 139.03 (Ar-C), 132.25 (Ar-C), 129.79 (Ar-C), 129.51 (Ar-C), 129.12 (Ar-C), 128.87 (Ar-C), 127.34 (Ar-C), 125.63 (Ar-C), 120.93 (Ar-C), 113.93 (Ar-C), 112.26 (Ar-C), 105.95 (Ar-C), 55.32 (OCH<sub>3</sub>), 44.31 (CH<sub>2</sub>CH<sub>2</sub>NHSO<sub>2</sub>), 41.68 (CH<sub>2</sub>CH<sub>2</sub>NHSO<sub>2</sub>). LC/MS (ESI) 560.4 (M<sup>+</sup>).

5.1.6.3. 4-Bromo-N-(2-((4-(4-(3-methoxyphenyl)-2-phenyl-1H-imidazol-5-yl)pyridin-2-yl)amino)ethyl)benzenesulfonamide (**8c**):

Yield: 71%. m.p.: 127-129 °C. HPLC purity 95.4%, <sup>1</sup>H NMR (400 MHz, CDCl<sub>3</sub>) δ 7.96 (d, *J* = 6.8 Hz, 2H, Ar-H), 7.79 (m, 3H, Ar-H), 7.39 (m, 3H, Ar-H), 7.25 (d, *J* = 8.12 Hz, 1H, Ar-H), 7.11 (t, *J* = 8.48 Hz, 2H, Ar-H), 7.06 (d, *J* = 4 Hz, 2H, Ar-H), 6.88 (dd, *J* = 1.72 Hz, 1H, Ar-H), 6.73 (s, 1H, Ar-H), 6.66 (d, *J* = 4.88 Hz, 1H, Ar-H), 4.98 (s, 1H, NH), 3.76 (s, 3H, OCH<sub>3</sub>), 3.39 (d, *J* = 4.64 Hz, 2H, CH<sub>2</sub>CH<sub>2</sub>NHSO<sub>2</sub>), 3.09 (t, *J* = 5.28 Hz, 2H, CH<sub>2</sub>CH<sub>2</sub>NHSO<sub>2</sub>). <sup>13</sup>C NMR (100 MHz, CDCl<sub>3</sub>) δ 166.16 (Ar-C), 163.64 (Ar-C), 159.74 (Ar-C), 158.4 (Ar-C), 146.38 (Ar-C), 136.03 (Ar-C), 129.79 (Ar-C), 129.65 (Ar-C), 129.52 (Ar-C), 128.87 (Ar-C), 125.62 (Ar-C), 120.92 (Ar-C), 116.31

(Ar-C), 116.09 (Ar-C), 113.92 (Ar-C), 112.23 (Ar-C), 105.92 (Ar-C), 55.31 (OCH<sub>3</sub>), 44.21 (CH<sub>2</sub>CH<sub>2</sub>NHSO<sub>2</sub>), 41.68 (CH<sub>2</sub>CH<sub>2</sub>NHSO<sub>2</sub>). LC/MS (ESI) 605.8 (M+1)<sup>+</sup>.

5.1.6.4. 4-fluoro-N-(2-((4-(4-(3-methoxyphenyl)-2-phenyl-1H-imidazol-5-yl)pyridin-2-yl)amino)ethyl)benzenesulfonamide (**8d**):

Yield: 65%. m.p.: 133-135 °C. <sup>1</sup>H NMR (400 MHz, CDCl<sub>3</sub>) δ 7.94 (d, *J* = 6.76 Hz, 2H, Ar-H), 7.79 (t, *J* = 1.84 Hz, 2H, Ar-H), 7.65 (d, *J* = 7.84 Hz, 1H, Ar-H), 7.48 (dd, *J* = 0.92 Hz, 1H, Ar-H), 7.38 (m, 4H, Ar-H), 7.25 (t, *J* = 8.12 Hz, 1H, Ar-H), 7.05 (d, *J* = 5.8 Hz, 2H, Ar-H), 6.87 (dd, *J* = 1.76 Hz, 1H, Ar-H), 6.71 (s, 1H, Ar-H), 6.66 (d, *J* = 4.64 Hz, 1H, Ar-H), 4.93 (s, 1H, NH), 3.74 (s, 3H, OCH<sub>3</sub>), 3.38 (d, *J* = 4.68 Hz, 2H, CH<sub>2</sub>CH<sub>2</sub>NHSO<sub>2</sub>), 3.09 (t, *J* = 4.96 Hz, 2H, CH<sub>2</sub>CH<sub>2</sub>NHSO<sub>2</sub>). <sup>13</sup>C NMR (100 MHz, CDCl<sub>3</sub>) δ 159.71 (Ar-C), 158.44 (Ar-C), 146.45 (Ar-C), 141.76 (Ar-C), 135.11 (Ar-C), 132.54 (Ar-C), 130.35 (Ar-C), 129.76 (Ar-C), 129.51 (Ar-C), 128.86 (Ar-C), 127 (Ar-C), 125.63 (Ar-C), 124.96 (Ar-C), 120.94 (Ar-C), 113.97 (Ar-C), 112.28 (Ar-C), 105.97 (Ar-C), 55.31 (OCH<sub>3</sub>), 44.4 (CH<sub>2</sub>CH<sub>2</sub>NHSO<sub>2</sub>), 41.72 (CH<sub>2</sub>CH<sub>2</sub>NHSO<sub>2</sub>). LC/MS (ESI) 544.2 (M+1)<sup>+</sup>.

5.1.6.5. 3-Chloro-N-(2-((4-(4-(3-methoxyphenyl)-2-phenyl-1H-imidazol-5-yl)pyridin-2-yl)amino)ethyl)benzenesulfonamide (**8e**):

Yield: 74%. m.p.: 120-122 °C. HPLC purity 95.8%, <sup>1</sup>H NMR (400 MHz, CDCl<sub>3</sub>) δ 7.97 (d, *J* = 7.28 Hz, 2H, Ar-H), 7.82 (d, *J* = 5.48 Hz, 1H, Ar-H), 7.42 (m, 5H, Ar-H), 7.28 (q, *J* = 3.2 Hz, 2H, Ar-H), 7.08 (d, *J* = 6.96 Hz, 2H, Ar-H), 6.9 (t, *J* = 1.72 Hz, 1H, Ar-H), 6.76 (s, 1H, Ar-H), 6.69 (s, 1H, Ar-H), 4.95 (s, 1H, NH), 3.77 (s, 3H, OCH<sub>3</sub>), 3.47 (q, *J* = 5.24 Hz, 2H, CH<sub>2</sub>CH<sub>2</sub>NHSO<sub>2</sub>), 3.22 (q, *J* = 5.48 Hz, 2H, CH<sub>2</sub>CH<sub>2</sub>NHSO<sub>2</sub>). <sup>13</sup>C NMR (100 MHz, CDCl<sub>3</sub>) δ 159.74 (Ar-C), 158.37 (Ar-C), 146.53 (Ar-C), 135.45 (Ar-C), 134.91 (Ar-C), 132.27 (Ar-C), 131.55 (Ar-C), 131.37 (Ar-C), 129.8 (Ar-C), 129.53 (Ar-C), 128.87 (Ar-C), 125.61 (Ar-C), 120.93 (Ar-C), 114.03 (Ar-C), 113.86 (Ar-C), 112.28 (Ar-C), 105.78 (Ar-C), 55.34 (OCH<sub>3</sub>), 44.3 (CH<sub>2</sub>CH<sub>2</sub>NHSO<sub>2</sub>), 41.72 (CH<sub>2</sub>CH<sub>2</sub>NHSO<sub>2</sub>). LC/MS (ESI) 560.1 (M<sup>+</sup>).

5.1.6.6. 2,6-Dichloro-N-(2-((4-(4-(3-methoxyphenyl)-2-phenyl-1H-imidazol-5-yl)pyridin-2-yl)amino)ethyl)benzenesulfonamide (**8f**):

Yield: 75%. m.p.: 109-111 °C. <sup>1</sup>H NMR (400 MHz, CDCl<sub>3</sub>) δ 7.92 (d, *J* = 6.24 Hz, 2H, Ar-H), 7.75 (d, *J* = 5.52 Hz, 1H, Ar-H), 7.55 (d, *J* = 7.88 Hz, 1H, Ar-H), 7.47 (dd, *J* = 2.04 Hz, 1H, Ar-H), 7.38 (m, 4H, Ar-H), 7.2 (m, 2H, Ar-H), 7.01 (d, *J* = 7.08 Hz, 2H, Ar-H), 6.84 (t, *J* = 1.92 Hz, 1H, Ar-H), 6.66 (s, 1H, Ar-H), 6.61 (d, *J* = 5.08 Hz, 1H, Ar-H), 4.94 (s, 1H, NH), 3.71 (s, 3H, OCH<sub>3</sub>), 3.33 (d, *J* = 4.48 Hz, 2H, CH<sub>2</sub>CH<sub>2</sub>NHSO<sub>2</sub>), 3.06 (t, *J* = 5.12 Hz, 2H, CH<sub>2</sub>CH<sub>2</sub>NHSO<sub>2</sub>). <sup>13</sup>C NMR (100 MHz, CDCl<sub>3</sub>) δ 163.57 (Ar-C), 161.08 (Ar-C), 159.64 (Ar-C), 158.49 (Ar-C), 146.99 (Ar-C), 142 (Ar-C), 130.88 (Ar-C), 129.69 (Ar-C), 129.06 (Ar-C), 128.82 (Ar-C), 125.68 (Ar-C), 120.96 (Ar-C), 119.53 (Ar-C), 114.36 (Ar-C), 113.9 (Ar-C), 112.26 (Ar-C), 105.96 (Ar-C), 55.26 (OCH<sub>3</sub>), 44.22 (CH<sub>2</sub>CH<sub>2</sub>NHSO<sub>2</sub>), 41.67 (CH<sub>2</sub>CH<sub>2</sub>NHSO<sub>2</sub>). LC/MS (ESI) 593.9 (M<sup>+</sup>).

5.1.6.7. 3-Fluoro-N-(2-((4-(4-(3-methoxyphenyl)-2-phenyl-1H-imidazol-5-yl)pyridin-2-yl)amino)ethyl)benzenesulfonamide (**8g**):

Yield: 70%. m.p.: 112-114 °C. HPLC purity : 96.3%, <sup>1</sup>H NMR (400 MHz, CDCl<sub>3</sub>) δ 7.92 (d, *J* = 4.8 Hz, 2H, Ar-H), 7.73 (d, *J* = 5.16 Hz, 1H, Ar-H), 7.66 (d, *J* = 8.16 Hz, 2H, Ar-H), 7.33 (q, *J* = 8.75 Hz, 5H, Ar-H), 7.19 (t, *J* = 7.52 Hz, 1H, Ar-H), 7 (s, 2H, Ar-H), 6.83 (d, *J* = 7.4 Hz, 1H, Ar-H), 6.66 (s, 1H, Ar-H), 6.6 (d, *J* = 3.48 Hz, 1H, Ar-H), 4.96 (s, 1H, NH), 3.69 (s, 3H, OCH<sub>3</sub>), 3.3 (s, 2H, CH<sub>2</sub>CH<sub>2</sub>NHSO<sub>2</sub>), 3.02 (s, 2H, CH<sub>2</sub>CH<sub>2</sub>NHSO<sub>2</sub>). <sup>13</sup>C NMR (100 MHz, CDCl<sub>3</sub>) δ 159.62 (Ar-C), 158.48 (Ar-C), 147.05 (Ar-C), 146.59 (Ar-C), 138.85 (Ar-C), 138.43 (Ar-C), 129.66 (Ar-C), 129.55 (Ar-C), 129.27 (Ar-C), 129.03 (Ar-C), 128.79 (Ar-C), 125.73 (Ar-C), 120.99 (Ar-C), 113.95 (Ar-C), 113.85 (Ar-C), 112.24 (Ar-C), 105.92 (Ar-C), 55.25 (OCH<sub>3</sub>), 44.01 (CH<sub>2</sub>CH<sub>2</sub>NHSO<sub>2</sub>), 41.63 (CH<sub>2</sub>CH<sub>2</sub>NHSO<sub>2</sub>). LC/MS (ESI) 544.3 (M + 1)<sup>+</sup>. HRMS calculated for C<sub>29</sub>H<sub>26</sub>FN<sub>5</sub>O<sub>3</sub>S is 543.1740 found : 544.1804 (M+H).

5.1.6.8. N-(2-((4-(4-(3-methoxyphenyl)-2-phenyl-1H-imidazol-5-yl)pyridin-2-yl)amino)ethyl)-4-(trifluoromethyl)benzenesulfonamide (**8h**):

Yield: 60%. m.p.: 110-112 °C. <sup>1</sup>H NMR (400 MHz, CDCl<sub>3</sub>) δ 7.95 (d, *J* = 6.6 Hz, 2H, Ar-H), 7.79 (d, *J* = 5.52 Hz, 1H, Ar-H), 7.64 (s, 1H, Ar-H), 7.61 (s, 1H, Ar-H), 7.57 (s,



1H, Ar-H), 7.55 (d,  $J = 1.72$  Hz, 2H, Ar-H), 7.38 (m, 3H, Ar-H), 7.25 (d,  $J = 8$  Hz, 1H, Ar-H), 7.05 (d,  $J = 5.92$  Hz, 2H, Ar-H), 6.88 (dd,  $J = 1.75$  Hz, 1H, Ar-H), 6.71 (s, 1H, Ar-H), 6.67 (d,  $J = 4$  Hz, 1H, Ar-H), 4.94 (s, 1H, NH), 3.75 (s, 3H, OCH<sub>3</sub>), 3.38 (t,  $J = 4.84$  Hz, 2H, CH<sub>2</sub>CH<sub>2</sub>NHSO<sub>2</sub>), 3.08 (t,  $J = 5.32$  Hz, 2H, CH<sub>2</sub>CH<sub>2</sub>NHSO<sub>2</sub>). <sup>13</sup>C NMR (100 MHz, CDCl<sub>3</sub>) δ 159.73 (Ar-C), 158.41 (Ar-C), 146.89 (Ar-C), 146.43 (Ar-C), 139.03 (Ar-C), 132.25 (Ar-C), 129.79 (Ar-C), 129.51 (Ar-C), 129.12 (Ar-C), 128.87 (Ar-C), 127.34 (Ar-C), 125.63 (Ar-C), 120.93 (Ar-C), 113.93 (Ar-C), 112.26 (Ar-C), 105.95 (Ar-C), 55.32 (OCH<sub>3</sub>), 44.31 (CH<sub>2</sub>CH<sub>2</sub>NHSO<sub>2</sub>), 41.68 (CH<sub>2</sub>CH<sub>2</sub>NHSO<sub>2</sub>). LC/MS (ESI) 594.2 (M+1)<sup>+</sup>.

5.1.6.9. 4-Methoxy-N-(2-((4-(4-(3-methoxyphenyl)-2-phenyl-1H-imidazol-5-yl)pyridin-2-yl)amino)ethyl)benzenesulfonamide (**8i**):

Yield: 64%. m.p.: 101-103 °C. <sup>1</sup>H NMR (400 MHz, CDCl<sub>3</sub>) δ 7.97 (d,  $J = 6.8$  Hz, 2H, Ar-H), 7.74 (d,  $J = 5.6$  Hz, 1H, Ar-H), 7.69 (d,  $J = 8.84$  Hz, 2H, Ar-H), 7.33 (m, 3H, Ar-H), 7.2 (t,  $J = 7.8$  Hz, 1H, Ar-H), 7.03 (d,  $J = 7.88$  Hz, 2H, Ar-H), 6.87 (d,  $J = 8.88$  Hz, 2H, Ar-H), 6.83 (dd,  $J = 1.16$  Hz, 1H, Ar-H), 6.68 (s, 1H, Ar-H), 6.59 (d,  $J = 8$  Hz, 1H, Ar-H), 5.04 (s, 1H, NH), 3.78 (s, 3H, OCH<sub>3</sub>), 3.71 (s, 3H, OCH<sub>3</sub>), 3.33 (d,  $J = 4.48$  Hz, 2H, CH<sub>2</sub>CH<sub>2</sub>NHSO<sub>2</sub>), 3.03 (t,  $J = 5.08$  Hz, 2H, CH<sub>2</sub>CH<sub>2</sub>NHSO<sub>2</sub>). <sup>13</sup>C NMR (100 MHz, CDCl<sub>3</sub>) δ 162.75 (Ar-C), 159.59 (Ar-C), 158.52 (Ar-C), 147.04 (Ar-C), 146.65 (Ar-C), 131.32 (Ar-C), 129.63 (Ar-C), 129.01 (Ar-C), 128.94 (Ar-C), 128.77 (Ar-C), 125.74 (Ar-C), 121 (Ar-C), 114.22 (Ar-C), 113.82 (Ar-C), 112.13 (Ar-C), 105.83 (Ar-C), 55.55 (OCH<sub>3</sub>), 55.25 (OCH<sub>3</sub>), 43.7 (CH<sub>2</sub>CH<sub>2</sub>NHSO<sub>2</sub>), 41.55 (CH<sub>2</sub>CH<sub>2</sub>NHSO<sub>2</sub>). LC/MS (ESI) 556.3 (M<sup>+</sup>).

5.1.6.10. N-(3-((4-(4-(3-methoxyphenyl)-2-phenyl-1H-imidazol-5-yl)pyridin-2-yl)amino)propyl)benzenesulfonamide (**9a**):

Yield: 65%. m.p.: 105 °C. HPLC purity 96.4%, <sup>1</sup>H NMR (400 MHz, CDCl<sub>3</sub>) δ 7.96 (d,  $J = 6.76$  Hz, 2H, Ar-H), 7.8 (m, 3H, Ar-H), 7.51 (t,  $J = 4.8$  Hz, 1H, Ar-H), 7.43 (t,  $J = 7.76$  Hz, 2H, Ar-H), 7.36 (m,  $J = 6.8$  Hz, 3H, Ar-H), 7.24 (t,  $J = 8.04$  Hz, 1H, Ar-H), 7.05 (d,  $J = 5.75$  Hz, 2H, Ar-H), 6.87 (t,  $J = 4$  Hz, 1H, Ar-H), 6.68 (s, 1H, Ar-H), 6.62 (d,  $J = 3.72$  Hz, 1H, Ar-H), 4.74 (s, 1H, NH), 3.73 (s, 3H, OCH<sub>3</sub>), 3.28 (t,  $J = 5.92$  Hz, 2H, CH<sub>2</sub>CH<sub>2</sub>CH<sub>2</sub>NHSO<sub>2</sub>), 2.92 (t,  $J = 5.76$  Hz, 2H, CH<sub>2</sub>CH<sub>2</sub>CH<sub>2</sub>NHSO<sub>2</sub>), 1.6 (t,  $J = 5.8$  Hz, 2H, CH<sub>2</sub>CH<sub>2</sub>CH<sub>2</sub>NHSO<sub>2</sub>). <sup>13</sup>C NMR (100 MHz, CDCl<sub>3</sub>) δ 159.66 (Ar-C),

158.77 (Ar-C), 146.9 (Ar-C), 146.69 (Ar-C), 140.08 (Ar-C), 132.41 (Ar-C), 129.59 (Ar-C), 129.03 (Ar-C), 128.83 (Ar-C), 126.86 (Ar-C), 125.68 (Ar-C), 120.95 (Ar-C), 113.96 (Ar-C), 113.82 (Ar-C), 111.73 (Ar-C), 55.29 (OCH<sub>3</sub>), 40.17 (CH<sub>2</sub>CH<sub>2</sub>CH<sub>2</sub>NHSO<sub>2</sub>), 38.37 (CH<sub>2</sub>CH<sub>2</sub>CH<sub>2</sub>NHSO<sub>2</sub>), 29.91 (CH<sub>2</sub>CH<sub>2</sub>CH<sub>2</sub>NHSO<sub>2</sub>). LC/MS (ESI) 540.1 (M<sup>+</sup>).

5.1.6.11. 4-Chloro-N-(3-((4-(4-(3-methoxyphenyl)-2-phenyl-1H-imidazol-5-yl)pyridin-2-yl)amino)propyl)benzenesulfonamide (**9b**):

Yield: 65%. m.p.: 108-110 °C. HPLC purity 97.1% <sup>1</sup>H NMR (400 MHz, CDCl<sub>3</sub>) δ 7.95 (d, *J* = 6.52 Hz, 2H, Ar-H), 7.82 (d, *J* = 5.52 Hz, 1H, Ar-H), 7.7 (d, *J* = 8.64 Hz, 2H, Ar-H), 7.39 (q, *J* = 6.72 Hz, 4H, Ar-H), 7.29 (d, *J* = 2.36 Hz, 1H, Ar-H), 7.25 (d, *J* = 8.04 Hz, 1H, Ar-H), 7.05 (d, *J* = 6.8 Hz, 2H, Ar-H), 6.89 (t, *J* = 1.76 Hz, 1H, Ar-H), 6.71 (s, 1H, Ar-H), 6.63 (d, *J* = 4.76 Hz, 1H, Ar-H), 4.73 (s, 1H, NH), 3.75 (s, 3H, OCH<sub>3</sub>), 3.31 (q, *J* = 5.64 Hz, 2H, CH<sub>2</sub>CH<sub>2</sub>CH<sub>2</sub>NHSO<sub>2</sub>), 2.91 (t, *J* = 5.68 Hz, 2H, CH<sub>2</sub>CH<sub>2</sub>CH<sub>2</sub>NHSO<sub>2</sub>), 1.62 (t, *J* = 5.8 Hz, 2H, CH<sub>2</sub>CH<sub>2</sub>CH<sub>2</sub>NHSO<sub>2</sub>). <sup>13</sup>C NMR (100 MHz, CDCl<sub>3</sub>) δ 159.7 (Ar-C), 158.71 (Ar-C), 146.87 (Ar-C), 138.73 (Ar-C), 129.77 (Ar-C), 129.54 (Ar-C), 129.26 (Ar-C), 129.08 (Ar-C), 128.85 (Ar-C), 128.36 (Ar-C), 125.65 (Ar-C), 120.93 (Ar-C), 113.92 (Ar-C), 111.74 (Ar-C), 105.81 (Ar-C), 55.3 (OCH<sub>3</sub>), 40.1 (CH<sub>2</sub>CH<sub>2</sub>CH<sub>2</sub>NHSO<sub>2</sub>), 38.34 (CH<sub>2</sub>CH<sub>2</sub>CH<sub>2</sub>NHSO<sub>2</sub>), 29.93 (CH<sub>2</sub>CH<sub>2</sub>CH<sub>2</sub>NHSO<sub>2</sub>). LC/MS (ESI) 574.1 (M<sup>+</sup>).

5.1.6.12. 4-Bromo-N-(3-((4-(4-(3-methoxyphenyl)-2-phenyl-1H-imidazol-5-yl)pyridin-2-yl)amino)propyl)benzenesulfonamide (**9c**):

Yield: 70%. m.p.: 120-122 °C. HPLC purity 96.8% <sup>1</sup>H NMR (400 MHz, CDCl<sub>3</sub>) δ 7.96 (d, *J* = 6.72 Hz, 2H, Ar-H), 7.82 (d, *J* = 5.56 Hz, 1H, Ar-H), 7.64 (d, *J* = 8.6 Hz, 2H, Ar-H), 7.57 (d, *J* = 8.6 Hz, 2H, Ar-H), 7.4 (d, *J* = 7.4 Hz, 2H, Ar-H), 7.29 (q, *J* = 5.16 Hz, 2H, Ar-H), 7.06 (d, *J* = 7.24 Hz, 2H, Ar-H), 6.91 (t, *J* = 1.76 Hz, 1H, Ar-H), 6.74 (s, 1H, Ar-H), 6.66 (d, *J* = 4.96 Hz, 1H, Ar-H), 4.84 (s, 1H, NH), 3.76 (s, 3H, OCH<sub>3</sub>), 3.33 (q, *J* = 5.8 Hz, 2H, CH<sub>2</sub>CH<sub>2</sub>CH<sub>2</sub>NHSO<sub>2</sub>), 2.93 (t, *J* = 5.6 Hz, 2H, CH<sub>2</sub>CH<sub>2</sub>CH<sub>2</sub>NHSO<sub>2</sub>), 1.64 (m, 2H, CH<sub>2</sub>CH<sub>2</sub>CH<sub>2</sub>NHSO<sub>2</sub>). <sup>13</sup>C NMR (100 MHz, CDCl<sub>3</sub>) δ 159.74 (Ar-C), 158.57 (Ar-C), 139.31 (Ar-C), 132.24 (Ar-C), 129.83 (Ar-C), 129.51 (Ar-C), 129.12 (Ar-C), 128.88 (Ar-C), 128.48 (Ar-C), 127.2 (Ar-C), 125.63 (Ar-C), 120.92 (Ar-C),

114.03 (Ar-C), 113.93 (Ar-C), 111.71 (Ar-C), 55.33 (OCH<sub>3</sub>), 40.09 (CH<sub>2</sub>CH<sub>2</sub>CH<sub>2</sub>NHSO<sub>2</sub>), 38.35 (CH<sub>2</sub>CH<sub>2</sub>CH<sub>2</sub>NHSO<sub>2</sub>), 29.93 (CH<sub>2</sub>CH<sub>2</sub>CH<sub>2</sub>NHSO<sub>2</sub>).  
LC/MS (ESI) 618.1 (M<sup>+</sup>).

5.1.6.13. 4-Fluoro-N-(3-((4-(4-(3-methoxyphenyl)-2-phenyl-1H-imidazol-5-yl)pyridin-2-yl)amino)propyl)benzenesulfonamide (**9d**):

Yield: 72%. m.p.: 112-114 °C. HPLC purity 97.4%, <sup>1</sup>H NMR (400 MHz, CDCl<sub>3</sub>) δ 7.94 (t, *J* = 1.8 Hz, 2H, Ar-H), 7.77 (m, 3H, Ar-H), 7.35 (d, *J* = 6.76 Hz, 3H, Ar-H), 7.22 (t, *J* = 8.04 Hz, 1H, Ar-H), 7.08 (t, *J* = 8.56 Hz, 1H, Ar-H), 7.02 (d, *J* = 5.68 Hz, 2H, Ar-H), 6.86 (t, *J* = 1.84 Hz, 1H, Ar-H), 6.67 (s, 1H, Ar-H), 6.59 (d, *J* = 5.04 Hz, 1H, Ar-H), 4.7 (s, 1H, NH), 3.71 (s, 3H, OCH<sub>3</sub>), 3.25 (d, *J* = 8 Hz, 2H, CH<sub>2</sub>CH<sub>2</sub>CH<sub>2</sub>NHSO<sub>2</sub>), 2.88 (t, *J* = 5.64 Hz, 2H, CH<sub>2</sub>CH<sub>2</sub>CH<sub>2</sub>NHSO<sub>2</sub>), 1.58 (t, *J* = 8 Hz, 2H, CH<sub>2</sub>CH<sub>2</sub>CH<sub>2</sub>NHSO<sub>2</sub>).  
<sup>13</sup>C NMR (100 MHz, CDCl<sub>3</sub>) δ 166.08 (Ar-C), 163.55 (Ar-C), 159.63 (Ar-C), 158.84 (Ar-C), 146.96 (Ar-C), 146.72 (Ar-C), 136.2 (Ar-C), 129.69 (Ar-C), 129.03 (Ar-C), 128.81 (Ar-C), 125.71 (Ar-C), 120.96 (Ar-C), 116.07 (Ar-C), 113.91 (Ar-C), 111.77 (Ar-C), 105.75 (Ar-C), 55.25 (OCH<sub>3</sub>), 40.12 (CH<sub>2</sub>CH<sub>2</sub>CH<sub>2</sub>NHSO<sub>2</sub>), 38.33 (CH<sub>2</sub>CH<sub>2</sub>CH<sub>2</sub>NHSO<sub>2</sub>), 29.86 (CH<sub>2</sub>CH<sub>2</sub>CH<sub>2</sub>NHSO<sub>2</sub>). <sup>19</sup>F NMR (400 MHz, DMSO-*d*<sub>6</sub>) -107.17 (d, 1F, *J* = 8.00 Hz). LC/MS (ESI) 558.1 (M<sup>+</sup>).

5.1.6.14. 3-Chloro-N-(3-((4-(4-(3-methoxyphenyl)-2-phenyl-1H-imidazol-5-yl)pyridin-2-yl)amino)propyl)benzenesulfonamide (**9e**):

Yield: 71%. m.p.: 113-115 °C. HPLC 97.3%, <sup>1</sup>H NMR (400 MHz, CDCl<sub>3</sub>) δ 7.94 (t, *J* = 1.36 Hz, 2H, Ar-H), 7.78 (m, 2H, Ar-H), 7.64 (d, *J* = 7.8 Hz, 1H, Ar-H), 7.47 (q, *J* = 0.8 Hz, 1H, Ar-H), 7.35 (m, 4H, Ar-H), 7.22 (t, *J* = 8.04 Hz, 1H, Ar-H), 7.02 (d, *J* = 6.12 Hz, 2H, Ar-H), 6.86 (t, *J* = 1.8 Hz, 1H, Ar-H), 6.67 (s, 1H, Ar-H), 6.61 (d, *J* = 5.04 Hz, 1H, Ar-H), 4.71 (s, 1H, NH), 3.71 (s, 3H, OCH<sub>3</sub>), 3.27 (d, *J* = 5.76 Hz, 2H, CH<sub>2</sub>CH<sub>2</sub>CH<sub>2</sub>NHSO<sub>2</sub>), 2.9 (t, *J* = 5.6 Hz, 2H, CH<sub>2</sub>CH<sub>2</sub>CH<sub>2</sub>NHSO<sub>2</sub>), 1.59 (t, *J* = 5.72 Hz, 2H, CH<sub>2</sub>CH<sub>2</sub>CH<sub>2</sub>NHSO<sub>2</sub>). <sup>13</sup>C NMR (100 MHz, CDCl<sub>3</sub>) δ 159.63 (Ar-C), 158.81 (Ar-C), 146.67 (Ar-C), 141.98 (Ar-C), 135.1 (Ar-C), 132.46 (Ar-C), 130.36 (Ar-C), 129.55 (Ar-C), 128.83 (Ar-C), 126.95 (Ar-C), 125.69 (Ar-C), 124.93 (Ar-C), 120.97 (Ar-C), 113.89 (Ar-C), 111.77 (Ar-C), 105.79 (Ar-C), 55.27 (OCH<sub>3</sub>), 40.14

(CH<sub>2</sub>CH<sub>2</sub>CH<sub>2</sub>NHSO<sub>2</sub>), 38.32 (CH<sub>2</sub>CH<sub>2</sub>CH<sub>2</sub>NHSO<sub>2</sub>), 29.94 (CH<sub>2</sub>CH<sub>2</sub>CH<sub>2</sub>NHSO<sub>2</sub>).  
LC/MS (ESI) 574.1 (M+1)<sup>+</sup>. HRMS calculated for C<sub>30</sub>H<sub>28</sub>ClN<sub>5</sub>O<sub>3</sub>S is 573.1601  
found : 574.1689 (M+H).

5.1.6.15. 2,6-dichloro-N-(3-((4-(4-(3-methoxyphenyl)-2-phenyl-1H-imidazol-5-yl)pyridin-2-yl)amino)propyl)benzenesulfonamide (**9f**):

Yield: 63%. m.p.: 117-119 °C. HPLC purity 95.8%, <sup>1</sup>H NMR (400 MHz, CDCl<sub>3</sub>) δ 7.94 (d, *J* = 6.84 Hz, 2H, Ar-H), 7.82 (d, *J* = 5.36 Hz, 1H, Ar-H), 7.41 (d, *J* = 7.88 Hz, 2H, Ar-H), 7.35 (d, *J* = 7.52 Hz, 2H, Ar-H), 7.26 (m, 3H, Ar-H), 7.02 (s, 2H, Ar-H), 6.84 (d, *J* = 7.56 Hz, 1H, Ar-H), 6.63 (d, *J* = 15.2 Hz, 2H, Ar-H), 4.66 (s, 1H, NH), 3.71 (s, 3H, OCH<sub>3</sub>), 3.3 (d, *J* = 5.44 Hz, 2H, CH<sub>2</sub>CH<sub>2</sub>CH<sub>2</sub>NHSO<sub>2</sub>), 3.04 (d, *J* = 4.6 Hz, 2H, CH<sub>2</sub>CH<sub>2</sub>CH<sub>2</sub>NHSO<sub>2</sub>), 1.59 (d, *J* = 5.04 Hz, 2H, CH<sub>2</sub>CH<sub>2</sub>CH<sub>2</sub>NHSO<sub>2</sub>). <sup>13</sup>C NMR (100 MHz, CDCl<sub>3</sub>) δ 159.6 (Ar-C), 158.92 (Ar-C), 147.05 (Ar-C), 144.68 (Ar-C), 135.97 (Ar-C), 134.76 (Ar-C), 132.23 (Ar-C), 131.39 (Ar-C), 129.63 (Ar-C), 128.79 (Ar-C), 125.71 (Ar-C), 120.98 (Ar-C), 117.23 (Ar-C), 113.96 (Ar-C), 111.81 (Ar-C), 105.69 (Ar-C), 55.27 (OCH<sub>3</sub>), 40.22 (CH<sub>2</sub>CH<sub>2</sub>CH<sub>2</sub>NHSO<sub>2</sub>), 38.31 (CH<sub>2</sub>CH<sub>2</sub>CH<sub>2</sub>NHSO<sub>2</sub>), 30.29 (CH<sub>2</sub>CH<sub>2</sub>CH<sub>2</sub>NHSO<sub>2</sub>). LC/MS (ESI) 608.54 (M<sup>+</sup>).

5.1.6.16. 3-fluoro-N-(3-((4-(4-(3-methoxyphenyl)-2-phenyl-1H-imidazol-5-yl)pyridin-2-yl)amino)propyl)benzenesulfonamide (**9g**):

Yield: 72%. m.p.: 101-103 °C. <sup>1</sup>H NMR (400 MHz, CDCl<sub>3</sub>) δ 7.94 (d, *J* = 6.56 Hz, 2H, Ar-H), 7.82 (d, *J* = 5.52 Hz, 1H, Ar-H), 7.57 (d, *J* = 7.88 Hz, 1H, Ar-H), 7.5 (m, 1H, Ar-H), 7.4 (m, 4H, Ar-H), 7.23 (t, *J* = 8.28 Hz, 1H, Ar-H), 7.2 (dd, *J* = 1.92 Hz, 1H, Ar-H), 7.04 (d, *J* = 6.84 Hz, 2H, Ar-H), 6.88 (t, *J* = 1.96 Hz, 1H, Ar-H), 6.71 (s, 1H, Ar-H), 6.63 (d, *J* = 5.2 Hz, 1H, Ar-H), 4.72 (s, 1H, NH), 3.74 (s, 3H, OCH<sub>3</sub>), 3.3 (q, *J* = 5.88 Hz, 2H, CH<sub>2</sub>CH<sub>2</sub>CH<sub>2</sub>NHSO<sub>2</sub>), 2.93 (t, *J* = 5.88 Hz, 2H, CH<sub>2</sub>CH<sub>2</sub>CH<sub>2</sub>NHSO<sub>2</sub>), 1.62 (t, *J* = 5.92 Hz, 2H, CH<sub>2</sub>CH<sub>2</sub>CH<sub>2</sub>NHSO<sub>2</sub>). <sup>13</sup>C NMR (100 MHz, CDCl<sub>3</sub>) δ 161.1 (Ar-C), 159.68 (Ar-C), 158.74 (Ar-C), 146.87 (Ar-C), 142.33 (Ar-C), 130.86 (Ar-C), 130.79 (Ar-C), 129.53 (Ar-C), 128.85 (Ar-C), 125.64 (Ar-C), 122.62 (Ar-C), 120.94 (Ar-C), 119.4 (Ar-C), 114.36 (Ar-C), 113.87 (Ar-C), 111.75 (Ar-C), 55.29 (OCH<sub>3</sub>), 40.13 (CH<sub>2</sub>CH<sub>2</sub>CH<sub>2</sub>NHSO<sub>2</sub>), 38.31 (CH<sub>2</sub>CH<sub>2</sub>CH<sub>2</sub>NHSO<sub>2</sub>), 29.98 (CH<sub>2</sub>CH<sub>2</sub>CH<sub>2</sub>NHSO<sub>2</sub>). LC/MS (ESI) 557.64 (M<sup>+</sup>).

5.1.6.17. N-(3-((4-(4-(3-methoxyphenyl)-2-phenyl-1H-imidazol-5-yl)pyridin-2-yl)amino)propyl)-4-(trifluoromethyl)benzenesulfonamide (**9h**):

Yield: 65%. m.p.: 110-112 °C. HPLC purity 96.2%, <sup>1</sup>H NMR (400 MHz, CDCl<sub>3</sub>) δ 7.92 (t, *J* = 2.16 Hz, 2H, Ar-H), 7.88 (d, *J* = 8 Hz, 2H, Ar-H), 7.68 (d, *J* = 8.32 Hz, 2H, Ar-H), 7.34 (t, *J* = 1.36 Hz, 3H, Ar-H), 7.23 (t, *J* = 8.08 Hz, 1H, Ar-H), 7.01 (d, *J* = 6.08 Hz, 2H, Ar-H), 6.86 (t, *J* = 4 Hz, 1H, Ar-H), 6.7 (s, 1H, Ar-H), 6.6 (d, *J* = 5.16 Hz, 1H, Ar-H), 4.68 (s, 1H, NH), 3.71 (s, 3H, OCH<sub>3</sub>), 3.27 (d, *J* = 4 Hz, 2H, CH<sub>2</sub>CH<sub>2</sub>CH<sub>2</sub>NHSO<sub>2</sub>), 2.92 (t, *J* = 4.08 Hz, 2H, CH<sub>2</sub>CH<sub>2</sub>CH<sub>2</sub>NHSO<sub>2</sub>), 1.59 (t, *J* = 5.08 Hz, 2H, CH<sub>2</sub>CH<sub>2</sub>CH<sub>2</sub>NHSO<sub>2</sub>). <sup>13</sup>C NMR (100 MHz, CDCl<sub>3</sub>) δ 159.66 (Ar-C), 158.85 (Ar-C), 146.94 (Ar-C), 143.95 (Ar-C), 134.1 (Ar-C), 129.72 (Ar-C), 128.82 (Ar-C), 127.35 (Ar-C), 126.16 (Ar-C), 125.69 (Ar-C), 124.61 (Ar-C), 121.9 (Ar-C), 120.95 (Ar-C), 113.97 (Ar-C), 111.81 (Ar-C), 105.88 (Ar-C), 55.24 (OCH<sub>3</sub>), 40.12 (CH<sub>2</sub>CH<sub>2</sub>CH<sub>2</sub>NHSO<sub>2</sub>), 38.31 (CH<sub>2</sub>CH<sub>2</sub>CH<sub>2</sub>NHSO<sub>2</sub>), 29.98 (CH<sub>2</sub>CH<sub>2</sub>CH<sub>2</sub>NHSO<sub>2</sub>). LC/MS (ESI) 607.65 (M<sup>+</sup>).

5.1.6.18. 4-methoxy-N-(3-((4-(4-(3-methoxyphenyl)-2-phenyl-1H-imidazol-5-yl)pyridin-2-yl)amino)propyl)benzenesulfonamide (**9i**):

Yield: 60%. m.p.: 100-102 °C. HPLC purity 95.9%, <sup>1</sup>H NMR (400 MHz, CDCl<sub>3</sub>) δ 7.97 (d, *J* = 6.84 Hz, 2H, Ar-H), 7.81 (d, *J* = 5.52 Hz, 1H, Ar-H), 7.36 (q, *J* = 6.12 Hz, 3H, Ar-H), 7.23 (t, *J* = 8.08 Hz, 1H, Ar-H), 7.06 (d, *J* = 5.2 Hz, 2H, Ar-H), 6.87 (m, 3H, Ar-H), 6.67 (s, 1H, Ar-H), 6.61 (s, 1H, Ar-H), 4.76 (s, 1H, NH), 3.81 (s, 3H, OCH<sub>3</sub>), 3.72 (s, 3H, OCH<sub>3</sub>), 3.27 (q, *J* = 5.84 Hz, 2H, CH<sub>2</sub>CH<sub>2</sub>CH<sub>2</sub>NHSO<sub>2</sub>), 2.88 (t, *J* = 5.4 Hz, 2H, CH<sub>2</sub>CH<sub>2</sub>CH<sub>2</sub>NHSO<sub>2</sub>), 1.6 (t, *J* = 5.88 Hz, 2H, CH<sub>2</sub>CH<sub>2</sub>CH<sub>2</sub>NHSO<sub>2</sub>). <sup>13</sup>C NMR (100 MHz, CDCl<sub>3</sub>) δ 162.69 (Ar-C), 159.63 (Ar-C), 158.8 (Ar-C), 146.79 (Ar-C), 129.63 (Ar-C), 129.02 (Ar-C), 128.8 (Ar-C), 125.71 (Ar-C), 120.97 (Ar-C), 114.19 (Ar-C), 113.95 (Ar-C), 113.79 (Ar-C), 111.74 (Ar-C), 55.55 (OCH<sub>3</sub>), 55.27 (OCH<sub>3</sub>), 40.19 (CH<sub>2</sub>CH<sub>2</sub>CH<sub>2</sub>NHSO<sub>2</sub>), 38.45 (CH<sub>2</sub>CH<sub>2</sub>CH<sub>2</sub>NHSO<sub>2</sub>), 29.77 (CH<sub>2</sub>CH<sub>2</sub>CH<sub>2</sub>NHSO<sub>2</sub>). LC/MS (ESI) 570.3 (M<sup>+</sup>).

5.1.7. N-(2-((4-(4-(3-hydroxyphenyl)-2-phenyl-1H-imidazol-5-yl)pyridin-2-yl)amino)ethyl(propyl))substituted benzenesulfonamide (**10-11**)

To a solution of compound **8** or **9** (0.3 mmol) in methylene chloride (3 mL), BBr<sub>3</sub> (3 mL of a 1M solution in methylene chloride) was added drop wise at -78 °C under N<sub>2</sub>. The reaction mixture was stirred at the same temperature for 1 h, and then allowed to warm to room temperature and stirred for another 3 h. The mixture was quenched with saturated aqueous Na<sub>2</sub>CO<sub>3</sub>. Ethyl acetate (5 mL) was added and the organic layer was separated. The aqueous layer was extracted with ethyl acetate (X 2). The combined organic layer extracts were washed with brine, and dried over anhydrous Na<sub>2</sub>SO<sub>4</sub>. After evaporation of the organic solvent, the residue was purified by short column chromatography (silica gel, using ethyl acetate then switching to ethyl acetate-methanol 4:1 v/v) to yield the title compound.

5.1.7.1. N-(2-((4-(4-(3-hydroxyphenyl)-2-phenyl-1H-imidazol-5-yl)pyridin-2-yl)amino)ethyl)benzenesulfonamide (**10a**):

Yield: 68%. m.p.: 180-182 °C. HPLC purity 97.2% <sup>1</sup>H NMR (400 MHz, MeOH) δ 7.98 (d, *J* = 7.2 Hz, 2H, Ar-H), 7.82 (q, *J* = 1.6 Hz, 3H, Ar-H), 7.51 (m, 1H, Ar-H), 7.46 (m, 4H, Ar-H), 7.39 (t, *J* = 2.4 Hz, 1H, Ar-H), 7.23 (t, *J* = 8 Hz, 1H, Ar-H), 6.98 (t, *J* = 2.4 Hz, 1H, Ar-H), 6.83 (dd, *J* = 2.4 Hz, 1H, Ar-H), 6.7 (d, *J* = 5.2 Hz, 2H, Ar-H), 3.32 (q, *J* = 4 Hz, 2H, CH<sub>2</sub>CH<sub>2</sub>NHSO<sub>2</sub>), 3.03 (t, *J* = 6 Hz, 2H, CH<sub>2</sub>CH<sub>2</sub>NHSO<sub>2</sub>). <sup>13</sup>C NMR (100 MHz, MeOD) δ 158.69 (Ar-C), 157.37 (Ar-C), 147.18 (Ar-C), 146.43 (Ar-C), 140.25 (Ar-C), 132.28 (Ar-C), 129.63 (Ar-C), 129.58 (Ar-C), 128.86 (Ar-C), 128.58 (Ar-C), 126.57 (Ar-C), 125.7 (Ar-C), 119.8 (Ar-C), 115.43 (Ar-C), 115 (Ar-C), 111.48 (Ar-C), 106.22 (Ar-C), 42.35 (CH<sub>2</sub>CH<sub>2</sub>NHSO<sub>2</sub>), 41.06 (CH<sub>2</sub>CH<sub>2</sub>NHSO<sub>2</sub>). LC/MS (ESI) 512.0 (M<sup>+</sup>).

5.1.7.2. 4-chloro-N-(2-((4-(4-(3-hydroxyphenyl)-2-phenyl-1H-imidazol-5-yl)pyridin-2-yl)amino)ethyl)benzenesulfonamide (**10b**):

Yield: 74%. m.p.: 115-117 °C. HPLC purity 97.1% <sup>1</sup>H NMR (400 MHz, MeOD) δ 8.01 (t, *J* = 1.2 Hz, 2H, Ar-H), 7.8 (t, *J* = 6.44 Hz, 3H, Ar-H), 4.89 (m, 4H, Ar-H), 7.4 (t, *J* = 7.28 Hz, 1H, Ar-H), 7.25 (m, 1H, Ar-H), 7 (q, *J* = 1.84 Hz, 2H, Ar-H), 6.85 (dd, *J* =

1.36 Hz, 1H, Ar-H), 6.71 (t,  $J = 5.68$  Hz, 2H, Ar-H), 3.33 (t,  $J = 8$  Hz, 2H, CH<sub>2</sub>CH<sub>2</sub>NHSO<sub>2</sub>), 3.07 (t,  $J = 5.88$  Hz, 2H, CH<sub>2</sub>CH<sub>2</sub>NHSO<sub>2</sub>). <sup>13</sup>C NMR (100 MHz, MeOD)  $\delta$  158.62 (Ar-C), 157.36 (Ar-C), 147.17 (Ar-C), 146.41 (Ar-C), 139.1 (Ar-C), 138.38 (Ar-C), 129.64 (Ar-C), 129.58 (Ar-C), 129.04 (Ar-C), 128.82 (Ar-C), 128.59 (Ar-C), 128.3 (Ar-C), 125.72 (Ar-C), 119.85 (Ar-C), 115.48 (Ar-C), 115.03 (Ar-C), 111.45 (Ar-C), 106.14 (Ar-C), 42.39 (CH<sub>2</sub>CH<sub>2</sub>NHSO<sub>2</sub>), 40.98 (CH<sub>2</sub>CH<sub>2</sub>NHSO<sub>2</sub>). LC/MS (ESI) 546.3 (M<sup>+</sup>).

5.1.7.3. 4-bromo-N-(2-((4-(4-(3-hydroxyphenyl)-2-phenyl-1H-imidazol-5-yl)pyridin-2-yl)amino)ethyl)benzenesulfonamide (**10c**):

Yield: 72%. m.p.: 145-147 °C. HPLC purity 97.6%, <sup>1</sup>H NMR (400 MHz, MeOD)  $\delta$  8 (d,  $J = 1.2$  Hz, 1H, Ar-H), 7.98 (s, 1H, Ar-H), 7.82 (d,  $J = 5.52$  Hz, 1H, Ar-H), 7.71 (s, 1H, Ar-H), 7.69 (s, 1H, Ar-H), 7.64 (d,  $J = 8$  Hz, 2H, Ar-H), 7.45 (m, 3H, Ar-H), 7.25 (t,  $J = 8$  Hz, 1H, Ar-H), 6.98 (t,  $J = 1.2$  Hz, 2H, Ar-H), 6.83 (m, 1H, Ar-H), 6.72 (dd,  $J = 1.08$  Hz, 1H, Ar-H), 6.67 (s, 1H, Ar-H), 3.33 (q,  $J = 1.64$  Hz, 2H, CH<sub>2</sub>CH<sub>2</sub>NHSO<sub>2</sub>), 3.06 (t,  $J = 5.96$  Hz, 2H, CH<sub>2</sub>CH<sub>2</sub>NHSO<sub>2</sub>). <sup>13</sup>C NMR (100 MHz, MeOD)  $\delta$  158.61 (Ar-C), 157.36 (Ar-C), 147.16 (Ar-C), 146.44 (Ar-C), 139.63 (Ar-C), 132.03 (Ar-C), 129.65 (Ar-C), 129.55 (Ar-C), 128.78 (Ar-C), 128.55 (Ar-C), 128.33 (Ar-C), 126.73 (Ar-C), 125.7 (Ar-C), 119.82 (Ar-C), 115.45 (Ar-C), 114.98 (Ar-C), 111.42 (Ar-C), 106.11 (Ar-C), 42.33 (CH<sub>2</sub>CH<sub>2</sub>NHSO<sub>2</sub>), 40.94 (CH<sub>2</sub>CH<sub>2</sub>NHSO<sub>2</sub>). HRMS calculated for C<sub>28</sub>H<sub>24</sub>BrN<sub>5</sub>O<sub>3</sub>S is 590.9460 found: 591.5048 (M+H).

5.1.7.4. 4-fluoro-N-(2-((4-(4-(3-hydroxyphenyl)-2-phenyl-1H-imidazol-5-yl)pyridin-2-yl)amino)ethyl)benzenesulfonamide (**10d**):

Yield: 74%. m.p.: 143-145 °C. HPLC purity 97.8 % <sup>1</sup>H NMR (400 MHz, MeOD)  $\delta$  7.99 (d,  $J = 7.2$  Hz, 2H, Ar-H), 7.87 (m, 2H, Ar-H), 7.82 (d,  $J = 4$  Hz, 1H, Ar-H), 7.47 (t,  $J = 7.08$  Hz, 2H, Ar-H), 7.41 (t,  $J = 7.24$  Hz, 1H, Ar-H), 7.23 (m, 3H, Ar-H), 7.98 (t,  $J = 6.48$  Hz, 2H, Ar-H), 6.83 (m, 1H, Ar-H), 6.71 (t,  $J = 3.72$  Hz, 2H, Ar-H), 3.33 (t,  $J = 6$  Hz, 2H, CH<sub>2</sub>CH<sub>2</sub>NHSO<sub>2</sub>), 3.05 (t,  $J = 6$  Hz, 2H, CH<sub>2</sub>CH<sub>2</sub>NHSO<sub>2</sub>). <sup>13</sup>C NMR (100 MHz, MeOD)  $\delta$  166.16 (Ar-C), 163.65 (Ar-C), 158.66 (Ar-C), 157.35 (Ar-C), 147.17 (Ar-C), 146.42 (Ar-C), 136.56 (Ar-C), 129.63 (Ar-C), 129.45 (Ar-C), 128.78 (Ar-C), 128.55

(Ar-C), 125.69 (Ar-C), 119.81 (Ar-C), 115.92 (Ar-C), 115.43 (Ar-C), 114.98 (Ar-C), 111.45 (Ar-C), 106.15 (Ar-C), 42.31 (CH<sub>2</sub>CH<sub>2</sub>NHSO<sub>2</sub>), 41 (CH<sub>2</sub>CH<sub>2</sub>NHSO<sub>2</sub>). LC/MS 530 (M<sup>+</sup>). HRMS calculated for C<sub>28</sub>H<sub>24</sub>FN<sub>5</sub>O<sub>3</sub>S is 529.5904 found : 530.1628 (M+H).

5.1.7.5. 3-chloro-N-(2-((4-(4-(3-hydroxyphenyl)-2-phenyl-1H-imidazol-5-yl)pyridin-2-yl)amino)ethyl)benzenesulfonamide (**10e**):

Yield: 73%. m.p.: 138-140 °C. <sup>1</sup>H NMR (400 MHz, MeOD) δ 7.98 (d, *J* = 7.2 Hz, 2H, Ar-H), 7.83 (q, *J* = 2.04 Hz, 2H, Ar-H), 7.73 (d, *J* = 7.76 Hz, 1H, Ar-H), 7.53 (dd, *J* = 0.76 Hz, 1H, Ar-H), 7.46 (m, 3H, Ar-H), 7.39 (t, *J* = 7.24 Hz, 1H, Ar-H), 7.24 (m, 1H, Ar-H), 6.99 (t, *J* = 2.24 Hz, 2H, Ar-H), 6.84 (dd, *J* = 1.48 Hz, 1H, Ar-H), 6.71 (t, *J* = 5.56 Hz, 2H, Ar-H), 3.33 (t, *J* = 5.92 Hz, 2H, CH<sub>2</sub>CH<sub>2</sub>NHSO<sub>2</sub>), 3.06 (t, *J* = 5.96 Hz, 2H, CH<sub>2</sub>CH<sub>2</sub>NHSO<sub>2</sub>). <sup>13</sup>C NMR (100 MHz, MeOD) δ 158.65 (Ar-C), 157.35 (Ar-C), 147.16 (Ar-C), 146.48 (Ar-C), 142.28 (Ar-C), 134.73 (Ar-C), 132.2 (Ar-C), 130.46 (Ar-C), 129.55 (Ar-C), 128.56 (Ar-C), 126.48 (Ar-C), 125.69 (Ar-C), 124.93 (Ar-C), 119.84 (Ar-C), 115.46 (Ar-C), 115 (Ar-C), 111.48 (Ar-C), 106.13 (Ar-C), 42.37 (CH<sub>2</sub>CH<sub>2</sub>NHSO<sub>2</sub>), 41.02 (CH<sub>2</sub>CH<sub>2</sub>NHSO<sub>2</sub>). LC/MS (ESI) 545.8 (M<sup>+</sup>).

5.1.7.6. 2,6-dichloro-N-(2-((4-(4-(3-hydroxyphenyl)-2-phenyl-1H-imidazol-5-yl)pyridin-2-yl)amino)ethyl)benzenesulfonamide (**10f**):

Yield: 64%. m.p.: 141-143 °C. <sup>1</sup>H NMR (400 MHz, MeOD) δ 7.98 (d, *J* = 7.6 Hz, 2H, Ar-H), 7.78 (d, *J* = 5.6 Hz, 1H, Ar-H), 7.41 (m, 5H, Ar-H), 7.27 (m, 2H, Ar-H), 6.98 (t, *J* = 6.8 Hz, 2H, Ar-H), 6.83 (dd, *J* = 2 Hz, 1H, Ar-H), 6.7 (d, *J* = 5.6 Hz, 1H, Ar-H), 6.65 (s, 1H, Ar-H), 3.33 (q, *J* = 5.6 Hz, 2H, CH<sub>2</sub>CH<sub>2</sub>NHSO<sub>2</sub>), 3.18 (t, *J* = 6 Hz, 2H, CH<sub>2</sub>CH<sub>2</sub>NHSO<sub>2</sub>). <sup>13</sup>C NMR (100 MHz, MeOD) δ 158.58 (Ar-C), 157.37 (Ar-C), 147.16 (Ar-C), 146.44 (Ar-C), 135.55 (Ar-C), 134.45 (Ar-C), 132.47 (Ar-C), 131.28 (Ar-C), 129.63 (Ar-C), 128.81 (Ar-C), 128.59 (Ar-C), 125.7 (Ar-C), 119.85 (Ar-C), 115.47 (Ar-C), 115 (Ar-C), 111.51 (Ar-C), 106.24 (Ar-C), 42.34 (CH<sub>2</sub>CH<sub>2</sub>NHSO<sub>2</sub>), 40.9 (CH<sub>2</sub>CH<sub>2</sub>NHSO<sub>2</sub>). LC/MS (ESI) 579.9 (M<sup>+</sup>).



5.1.7.7. 3-fluoro-N-(2-((4-(4-(3-hydroxyphenyl)-2-phenyl-1H-imidazol-5-yl)pyridin-2-yl)amino)ethyl)benzenesulfonamide (**10g**):

Yield: 74%. m.p.: 118-120 °C. <sup>1</sup>H NMR (400 MHz, MeOD) δ 8 (d, *J* = 7.32 Hz, 2H, Ar-H), 7.82 (d, *J* = 6.04 Hz, 1H, Ar-H), 7.66 (d, *J* = 8 Hz, 1H, Ar-H), 7.58 (d, *J* = 8.24 Hz, 1H, Ar-H), 7.53 (t, *J* = 8.08 Hz, 1H, Ar-H), 7.46 (m, 2H, Ar-H), 7.39 (t, *J* = 7.16 Hz, 1H, Ar-H), 7.28 (m, 2H, Ar-H), 6.99 (d, *J* = 6.88 Hz, 2H, Ar-H), 6.85 (t, *J* = 1.68 Hz, 1H, Ar-H), 6.72 (d, *J* = 4.64 Hz, 2H, Ar-H), 3.35 (t, *J* = 5.92 Hz, 2H, CH<sub>2</sub>CH<sub>2</sub>NHSO<sub>2</sub>), 3.08 (t, *J* = 6 Hz, 2H, CH<sub>2</sub>CH<sub>2</sub>NHSO<sub>2</sub>). <sup>13</sup>C NMR (100 MHz, MeOD) δ 163.65 (Ar-C), 161.17 (Ar-C), 158.58 (Ar-C), 147.18 (Ar-C), 146.26 (Ar-C), 142.58 (Ar-C), 142.51 (Ar-C), 131.05 (Ar-C), 130.98 (Ar-C), 129.67 (Ar-C), 128.67 (Ar-C), 125.72 (Ar-C), 122.57 (Ar-C), 119.86 (Ar-C), 115.48 (Ar-C), 113.81 (Ar-C), 111.49 (Ar-C), 104.19 (Ar-C), 42.41 (CH<sub>2</sub>CH<sub>2</sub>NHSO<sub>2</sub>), 41.05 (CH<sub>2</sub>CH<sub>2</sub>NHSO<sub>2</sub>). LC/MS (ESI) 530.1 (M<sup>+</sup>).

5.1.7.8. N-(2-((4-(4-(3-hydroxyphenyl)-2-phenyl-1H-imidazol-5-yl)pyridin-2-yl)amino)ethyl)-4-(trifluoromethyl)benzenesulfonamide (**10h**):

Yield: 65%. m.p.: 117-119 °C. <sup>1</sup>H NMR (400 MHz, MeOD) δ 8 (q, *J* = 2.16 Hz, 4H, Ar-H), 7.81 (d, *J* = 7.92 Hz, 3H, Ar-H), 7.46 (t, *J* = 7.68 Hz, 2H, Ar-H), 7.39 (m, 1H, Ar-H), 7.24 (t, *J* = 8.08 Hz, 1H, Ar-H), 6.99 (m, *J* = 2.08 Hz, 2H, Ar-H), 6.84 (dd, *J* = 1.44 Hz, 1H, Ar-H), 6.71 (t, *J* = 4 Hz, 2H, Ar-H), 3.33 (m, 2H, CH<sub>2</sub>CH<sub>2</sub>NHSO<sub>2</sub>), 3.1 (t, *J* = 5.92 Hz, 2H, CH<sub>2</sub>CH<sub>2</sub>NHSO<sub>2</sub>). <sup>13</sup>C NMR (100 MHz, MeOD) δ 158.65 (Ar-C), 157.34 (Ar-C), 147.19 (Ar-C), 146.48 (Ar-C), 144.34 (Ar-C), 133.63 (Ar-C), 133.3 (Ar-C), 129.62 (Ar-C), 128.55 (Ar-C), 127.37 (Ar-C), 125.98 (Ar-C), 124.86 (Ar-C), 122.15 (Ar-C), 119.84 (Ar-C), 115.46 (Ar-C), 115 (Ar-C), 111.51 (Ar-C), 106.13 (Ar-C), 42.41 (CH<sub>2</sub>CH<sub>2</sub>NHSO<sub>2</sub>), 41.07 (CH<sub>2</sub>CH<sub>2</sub>NHSO<sub>2</sub>). <sup>19</sup>F NMR (400 MHz, DMSO-*d*<sub>6</sub>) -16.55 (s, 1F). LC/MS (ESI) 580.1 (M<sup>+</sup>).

5.1.7.9. N-(2-((4-(4-(3-hydroxyphenyl)-2-phenyl-1H-imidazol-5-yl)pyridin-2-yl)amino)ethyl)-4-methoxybenzenesulfonamide (**10i**):

Yield: 55%. m.p.: 120-122 °C. HPLC purity 96.4%, <sup>1</sup>H NMR (400 MHz, MeOD) δ 7.99 (d, *J* = 7.36 Hz, 2H, Ar-H), 7.82 (d, *J* = 5.48 Hz, 1H, Ar-H), 7.75 (d, *J* = 8.8 Hz, 2H, Ar-H), 7.48 (t, *J* = 8.76 Hz, 2H, Ar-H), 7.42 (t, *J* = 7.36 Hz, 1H, Ar-H), 7.25 (t, *J* = 8.16 Hz, 1H, Ar-H), 6.98 (t, *J* = 6.64 Hz, 4H, Ar-H), 6.85 (dd, *J* = 5.36 Hz, 1H, Ar-H),

6.7 (t,  $J = 5.64$  Hz, 2H, Ar-H), 3.7 (s, 3H, CH<sub>3</sub>), 3.32 (t,  $J = 6.56$  Hz, 2H, CH<sub>2</sub>CH<sub>2</sub>NHSO<sub>2</sub>), 3.02 (t,  $J = 6$  Hz, 2H, CH<sub>2</sub>CH<sub>2</sub>NHSO<sub>2</sub>). <sup>13</sup>C NMR (100 MHz, MeOD)  $\delta$  162.92 (Ar-C), 158.68 (Ar-C), 157.36 (Ar-C), 147.15 (Ar-C), 146.42 (Ar-C), 131.66 (Ar-C), 129.54 (Ar-C), 128.78 (Ar-C), 128.55 (Ar-C), 125.68 (Ar-C), 119.8 (Ar-C), 115.42 (Ar-C), 115.26 (Ar-C), 114.96 (Ar-C), 113.9 (Ar-C), 111.37 (Ar-C), 106.11 (Ar-C), 54.75 (CH<sub>3</sub>), 42.26 (CH<sub>2</sub>CH<sub>2</sub>NHSO<sub>2</sub>), 40.92 (CH<sub>2</sub>CH<sub>2</sub>NHSO<sub>2</sub>). LC/MS (ESI) 542 (M<sup>+</sup>).

5.1.7.10. 4-hydroxy-N-(2-((4-(4-(3-hydroxyphenyl)-2-phenyl-1H-imidazol-5-yl)pyridin-2-yl)amino)ethyl)benzenesulfonamide (**10j**):

Yield: 55%. m.p.: 122-124 °C. HPLC purity 95.8% <sup>1</sup>H NMR (400 MHz, MeOD)  $\delta$  8 (d,  $J = 8.4$  Hz, 1H, Ar-H), 7.69 (d,  $J = 8.8$  Hz, 1H, Ar-H), 7.48 (t,  $J = 6.8$  Hz, 1H, Ar-H), 7.42 (t,  $J = 8.4$  Hz, 1H, Ar-H), 7.25 (t,  $J = 8.4$  Hz, 1H, Ar-H), 6.99 (d,  $J = 3.2$  Hz, 1H, Ar-H), 6.88 (d,  $J = 8.8$  Hz, 1H, Ar-H), 6.84 (dd,  $J = 6$  Hz, 2H, Ar-H), 6.72 (d,  $J = 5.6$  Hz, 1H, Ar-H), 1.64 (m, 2H, CH<sub>2</sub>CH<sub>2</sub>NHSO<sub>2</sub>), 1.4 (m, 2H, CH<sub>2</sub>CH<sub>2</sub>NHSO<sub>2</sub>). <sup>13</sup>C NMR (100 MHz, MeOD)  $\delta$  161.44 (Ar-C), 158.7 (Ar-C), 157.35 (Ar-C), 147.18 (Ar-C), 146.36 (Ar-C), 130.07 (Ar-C), 129.63 (Ar-C), 128.93 (Ar-C), 128.8 (Ar-C), 128.57 (Ar-C), 125.69 (Ar-C), 119.8 (Ar-C), 115.4 (Ar-C), 115.29 (Ar-C), 114.97 (Ar-C), 111.43 (Ar-C), 106.21 (Ar-C), 42.29 (CH<sub>2</sub>CH<sub>2</sub>NHSO<sub>2</sub>), 41.06 (CH<sub>2</sub>CH<sub>2</sub>NHSO<sub>2</sub>). LC/MS (ESI) 527.9 (M<sup>+</sup>).

5.1.7.11. N-(3-((4-(4-(3-hydroxyphenyl)-2-phenyl-1H-imidazol-5-yl)pyridin-2-yl)amino)propyl)benzenesulfonamide (**11a**):

Yield: 65%. m.p.: 123-125 °C. <sup>1</sup>H NMR (400 MHz, MeOD)  $\delta$  7.98 (d,  $J = 7.32$  Hz, 2H, Ar-H), 7.83 (q,  $J = 7.12$  Hz, 3H, Ar-H), 7.53 (,  $J = 7.04$  Hz, 3H, Ar-H), 7.46 (q,  $J = 4.04$  Hz, 2H, Ar-H), 7.38 (t,  $J = 7.2$  Hz, 1H, Ar-H), 7.24 (t,  $J = 8.04$  Hz, 1H, Ar-H), 6.99 (t,  $J = 2.02$  Hz, 2H, Ar-H), 6.84 (dd,  $J = 1.28$  Hz, 1H, Ar-H), 6.72 (d,  $J = 5.52$  Hz, 1H, Ar-H), 6.68 (s, 1H, Ar-H), 3.21 (t,  $J = 6.56$  Hz, 2H, CH<sub>2</sub>CH<sub>2</sub>CH<sub>2</sub>NHSO<sub>2</sub>), 2.92 (t,  $J = 6.6$  Hz, 2H, CH<sub>2</sub>CH<sub>2</sub>CH<sub>2</sub>NHSO<sub>2</sub>), 1.66 (t,  $J = 6.6$  Hz, 2H, CH<sub>2</sub>CH<sub>2</sub>CH<sub>2</sub>NHSO<sub>2</sub>). <sup>13</sup>C NMR (100 MHz, MeOD)  $\delta$  158.78 (Ar-C), 157.35 (Ar-C), 147.19 (Ar-C), 146.28 (Ar-C), 140.26 (Ar-C), 132.26 (Ar-C), 129.6 (Ar-C), 128.88 (Ar-C), 128.58 (Ar-C), 126.58

(Ar-C), 125.71 (Ar-C), 119.85 (Ar-C), 115.47 (Ar-C), 115.04 (Ar-C), 111.11 (Ar-C), 105.96 (Ar-C), 40.3 (CH<sub>2</sub>CH<sub>2</sub>CH<sub>2</sub>NHSO<sub>2</sub>), 38.39 (CH<sub>2</sub>CH<sub>2</sub>CH<sub>2</sub>NHSO<sub>2</sub>), 28.97 (CH<sub>2</sub>CH<sub>2</sub>CH<sub>2</sub>NHSO<sub>2</sub>). LC/MS (ESI) 526.2 (M<sup>+</sup>).

5.1.7.12. 4-chloro-N-(3-((4-(4-(3-hydroxyphenyl)-2-phenyl-1H-imidazol-5-yl)pyridin-2-yl)amino)propyl)benzenesulfonamide (**11b**):

Yield: 62%. m.p.: 130-132 °C. <sup>1</sup>H NMR (400 MHz, MeOD) δ 7.99 (t, *J* = 6.92 Hz, 2H, Ar-H), 7.82 (m, 3H, Ar-H), 7.53 (t, *J* = 2.36 Hz, 1H, Ar-H), 7.51 (t, *J* = 1.8 Hz, 1H, Ar-H), 7.47 (q, *J* = 7.68 Hz, 2H, Ar-H), 7.41 (m, 1H, Ar-H), 7.25 (t, *J* = 7.88 Hz, 1H, Ar-H), 6.99 (t, *J* = 2.04 Hz, 2H, Ar-H), 6.83 (m, 1H, Ar-H), 6.73 (dd, *J* = 1.24 Hz, 1H, Ar-H), 6.69 (s, 1H, Ar-H), 3.22 (t, *J* = 6.64 Hz, 2H, CH<sub>2</sub>CH<sub>2</sub>CH<sub>2</sub>NHSO<sub>2</sub>), 2.95 (t, *J* = 6.72 Hz, 2H, CH<sub>2</sub>CH<sub>2</sub>CH<sub>2</sub>NHSO<sub>2</sub>), 1.67 (m, 2H, CH<sub>2</sub>CH<sub>2</sub>CH<sub>2</sub>NHSO<sub>2</sub>). <sup>13</sup>C NMR (100 MHz, MeOD MeOH) δ 158.81 (Ar-C), 157.37 (Ar-C), 147.17 (Ar-C), 146.31 (Ar-C), 139.17 (Ar-C), 138.35 (Ar-C), 129.63 (Ar-C), 129.04 (Ar-C), 128.78 (Ar-C), 128.55 (Ar-C), 128.29 (Ar-C), 125.69 (Ar-C), 119.82 (Ar-C), 115.45 (Ar-C), 114.99 (Ar-C), 111.06 (Ar-C), 105.94 (Ar-C), 40.28 (CH<sub>2</sub>CH<sub>2</sub>CH<sub>2</sub>NHSO<sub>2</sub>), 38.32 (CH<sub>2</sub>CH<sub>2</sub>CH<sub>2</sub>NHSO<sub>2</sub>), 28.94 (CH<sub>2</sub>CH<sub>2</sub>CH<sub>2</sub>NHSO<sub>2</sub>). LC/MS (ESI) 560.1 (M<sup>+</sup>).

5.1.7.13. 4-bromo-N-(3-((4-(4-(3-hydroxyphenyl)-2-phenyl-1H-imidazol-5-yl)pyridin-2-yl)amino)propyl)benzenesulfonamide (**11c**):

Yield: 60%. m.p.: 128-130 °C. HPLC purity 96.3%, <sup>1</sup>H NMR (400 MHz, MeOD) δ 8 (d, *J* = 7.28 Hz, 2H, Ar-H), 7.85 (d, *J* = 5.44 Hz, 1H, Ar-H), 7.72 (q, *J* = 8.66 Hz, 4H, Ar-H), 7.49 (t, *J* = 7.08 Hz, 2H, Ar-H), 7.43 (t, *J* = 6.28 Hz, 1H, Ar-H), 7.26 (t, *J* = 7.84 Hz, 1H, Ar-H), 6.99 (t, *J* = 6.4 Hz, 2H, Ar-H), 6.84 (t, *J* = 1.48 Hz, 1H, Ar-H), 6.73 (d, *J* = 5.2 Hz, 1H, Ar-H), 6.68 (s, 1H, Ar-H), 3.23 (t, *J* = 6.64 Hz, 2H, CH<sub>2</sub>CH<sub>2</sub>CH<sub>2</sub>NHSO<sub>2</sub>), 2.95 (t, *J* = 6.76 Hz, 2H, CH<sub>2</sub>CH<sub>2</sub>CH<sub>2</sub>NHSO<sub>2</sub>), 1.68 (m, 2H, CH<sub>2</sub>CH<sub>2</sub>CH<sub>2</sub>NHSO<sub>2</sub>). <sup>13</sup>C NMR (100 MHz, MeOD) δ 158.95 (Ar-C), 157.4 (Ar-C), 147.14 (Ar-C), 146.54 (Ar-C), 139.73 (Ar-C), 132.06 (Ar-C), 129.67 (Ar-C), 128.75 (Ar-C), 128.37 (Ar-C), 126.67 (Ar-C), 125.67 (Ar-C), 119.77 (Ar-C), 115.42 (Ar-C), 114.97 (Ar-C), 111.02 (Ar-C), 105.91 (Ar-C), 40.28 (CH<sub>2</sub>CH<sub>2</sub>CH<sub>2</sub>NHSO<sub>2</sub>), 38.26

(CH<sub>2</sub>CH<sub>2</sub>CH<sub>2</sub>NHSO<sub>2</sub>), 28.95 (CH<sub>2</sub>CH<sub>2</sub>CH<sub>2</sub>NHSO<sub>2</sub>). <sup>+</sup>). HRMS calculated for C<sub>29</sub>H<sub>26</sub>BrN<sub>5</sub>O<sub>3</sub>S is 604.5230 found : 605.5318 (M+H).

5.1.7.14. 4-fluoro-N-(3-((4-(4-(3-hydroxyphenyl)-2-phenyl-1H-imidazol-5-yl)pyridin-2-yl)amino)propyl)benzenesulfonamide (**11d**):

Yield: 75%. m.p.: 147-149 °C. HPLC purity 96.5%, <sup>1</sup>H NMR (400 MHz, MeOD) δ 7.98 (d, *J* = 7.2 Hz, 2H, Ar-H), 7.88 (m, 2H, Ar-H), 7.83 (d, *J* = 5.6 Hz, 1H, Ar-H), 7.46 (t, *J* = 7.2 Hz, 2H, Ar-H), 7.4 (t, *J* = 7.2 Hz, 1H, Ar-H), 7.26 (q, *J* = 2 Hz, 3H, Ar-H), 6.99 (d, *J* = 8.4 Hz, 2H, Ar-H), 6.83 (dd, *J* = 1.6 Hz, 1H, Ar-H), 6.71 (d, *J* = 5.2 Hz, 1H, Ar-H), 6.68 (s, 1H, Ar-H), 3.22 (t, *J* = 6.8 Hz, 2H, CH<sub>2</sub>CH<sub>2</sub>CH<sub>2</sub>NHSO<sub>2</sub>), 2.93 (t, *J* = 6.4 Hz, 2H, CH<sub>2</sub>CH<sub>2</sub>CH<sub>2</sub>NHSO<sub>2</sub>), 1.67 (m, 2H, CH<sub>2</sub>CH<sub>2</sub>CH<sub>2</sub>NHSO<sub>2</sub>). <sup>13</sup>C NMR (100 MHz, MeOD) δ 166.16 (Ar-C), 163.66 (Ar-C), 158.95 (Ar-C), 157.54 (Ar-C), 136.67 (Ar-C), 129.65 (Ar-C), 129.46 (Ar-C), 128.78 (Ar-C), 128.56 (Ar-C), 125.69 (Ar-C), 119.8 (Ar-C), 115.96 (Ar-C), 115.44 (Ar-C), 114.97 (Ar-C), 111.07 (Ar-C), 105.96 (Ar-C), 40.28 (CH<sub>2</sub>CH<sub>2</sub>CH<sub>2</sub>NHSO<sub>2</sub>), 38.33 (CH<sub>2</sub>CH<sub>2</sub>CH<sub>2</sub>NHSO<sub>2</sub>), 29.37 (CH<sub>2</sub>CH<sub>2</sub>CH<sub>2</sub>NHSO<sub>2</sub>). <sup>19</sup>F NMR (400 MHz, DMSO-*d*<sub>6</sub>) -107.24 (d, 1F, *J* = 56 Hz). LC/MS (ESI) 544.1 (M + 1) <sup>+</sup>.

5.1.7.15. 3-chloro-N-(3-((4-(4-(3-hydroxyphenyl)-2-phenyl-1H-imidazol-5-yl)pyridin-2-yl)amino)propyl)benzenesulfonamide (**11e**):

Yield: 70%. m.p.: 142-144 °C. <sup>1</sup>H NMR (400 MHz, MeOD) δ 7.99 (d, *J* = 1.36 Hz, 1H, Ar-H), 7.98 (s, 1H, Ar-H), 7.84 (m, 2H, Ar-H), 7.76 (dt, *J* = 1.04 Hz, 1H, Ar-H), 7.57 (m, 1H, Ar-H), 7.48 (m, 3H, Ar-H), 7.41 (m, 1H, Ar-H), 7.25 (t, *J* = 7.84 Hz, 1H, Ar-H), 6.98 (m, 2H, Ar-H), 6.84 (dd, *J* = 1.72 Hz, 1H, Ar-H), 6.72 (dd, *J* = 1.12 Hz, 1H, Ar-H), 6.68 (s, 1H, Ar-H), 3.23 (t, *J* = 6.68 Hz, 2H, CH<sub>2</sub>CH<sub>2</sub>CH<sub>2</sub>NHSO<sub>2</sub>), 2.95 (t, *J* = 6.76 Hz, 2H, CH<sub>2</sub>CH<sub>2</sub>CH<sub>2</sub>NHSO<sub>2</sub>), 1.68 (m, 2H, CH<sub>2</sub>CH<sub>2</sub>CH<sub>2</sub>NHSO<sub>2</sub>). <sup>13</sup>C NMR (100 MHz, MeOD) δ 158.85 (Ar-C), 157.36 (Ar-C), 147.16 (Ar-C), 146.36 (Ar-C), 142.35 (Ar-C), 134.77 (Ar-C), 132.17 (Ar-C), 130.5 (Ar-C), 129.56 (Ar-C), 128.55 (Ar-C), 126.46 (Ar-C), 125.68 (Ar-C), 124.95 (Ar-C), 119.81 (Ar-C), 115.44 (Ar-C), 111.07 (Ar-C), 105.96 (Ar-C), 40.3 (CH<sub>2</sub>CH<sub>2</sub>CH<sub>2</sub>NHSO<sub>2</sub>), 38.32 (CH<sub>2</sub>CH<sub>2</sub>CH<sub>2</sub>NHSO<sub>2</sub>), 28.99 (CH<sub>2</sub>CH<sub>2</sub>CH<sub>2</sub>NHSO<sub>2</sub>). LC/MS (ESI) 560.2 (M<sup>+</sup>).

5.1.7.16. 2,6-dichloro-N-(3-((4-(4-(3-hydroxyphenyl)-2-phenyl-1H-imidazol-5-yl)pyridin-2-yl)amino)propyl)benzenesulfonamide (**11f**):

Yield: 75%. m.p.: 138-140 °C. <sup>1</sup>H NMR (400 MHz, MeOD) δ 7.99 (d, *J* = 6.48 Hz, 2H, Ar-H), 7.83 (d, *J* = 4.28 Hz, 1H, Ar-H), 7.48 (d, *J* = 6.88 Hz, 4H, Ar-H), 7.39 (dd, *J* = 6.56 Hz, 2H, Ar-H), 7.24 (d, *J* = 7.2 Hz, 1H, Ar-H), 6.99 (d, *J* = 8.08 Hz, 2H, Ar-H), 6.84 (d, *J* = 6.48 Hz, 1H, Ar-H), 6.7 (m, 2H, Ar-H), 3.23 (s, 2H, CH<sub>2</sub>CH<sub>2</sub>CH<sub>2</sub>NHSO<sub>2</sub>), 3.07 (s, 2H, CH<sub>2</sub>CH<sub>2</sub>CH<sub>2</sub>NHSO<sub>2</sub>), 1.69 (s, 2H, CH<sub>2</sub>CH<sub>2</sub>CH<sub>2</sub>NHSO<sub>2</sub>). <sup>13</sup>C NMR (100 MHz, MeOD) δ 158.84 (Ar-C), 157.36 (Ar-C), 147.15 (Ar-C), 146.41 (Ar-C), 135.76 (Ar-C), 134.51 (Ar-C), 131.32 (Ar-C), 129.59 (Ar-C), 128.79 (Ar-C), 125.69 (Ar-C), 119.82 (Ar-C), 115.44 (Ar-C), 115 (Ar-C), 111.09 (Ar-C), 105.99 (Ar-C), 40.06 (CH<sub>2</sub>CH<sub>2</sub>CH<sub>2</sub>NHSO<sub>2</sub>), 38.28 (CH<sub>2</sub>CH<sub>2</sub>CH<sub>2</sub>NHSO<sub>2</sub>), 29.4 (CH<sub>2</sub>CH<sub>2</sub>CH<sub>2</sub>NHSO<sub>2</sub>). LC/MS (ESI) 594.2 (M<sup>+</sup>).

5.1.7.17. 3-fluoro-N-(3-((4-(4-(3-hydroxyphenyl)-2-phenyl-1H-imidazol-5-yl)pyridin-2-yl)amino)propyl)benzenesulfonamide (**11g**):

Yield: 60%. m.p.: 140-142 °C. <sup>1</sup>H NMR (400 MHz, MeOD) δ 7.99 (d, *J* = 6.88 Hz, 2H, Ar-H), 7.83 (d, *J* = 4.8 Hz, 1H, Ar-H), 7.67 (d, *J* = 7.24 Hz, 1H, Ar-H), 7.56 (m, 2H, Ar-H), 7.43 (m, 3H, Ar-H), 7.32 (dt, *J* = 6.96 Hz, 2H, Ar-H), 6.98 (s, 2H, Ar-H), 6.84 (d, *J* = 7.28 Hz, 1H, Ar-H), 6.7 (m, 2H, Ar-H), 3.23 (s, 2H, CH<sub>2</sub>CH<sub>2</sub>CH<sub>2</sub>NHSO<sub>2</sub>), 2.96 (s, 2H, CH<sub>2</sub>CH<sub>2</sub>CH<sub>2</sub>NHSO<sub>2</sub>), 1.68 (t, *J* = 5.68 Hz, 2H, CH<sub>2</sub>CH<sub>2</sub>CH<sub>2</sub>NHSO<sub>2</sub>). <sup>13</sup>C NMR (100 MHz, MeOD) δ 163.7 (Ar-C), 161.22 (Ar-C), 158.8 (Ar-C), 157.35 (Ar-C), 147.18 (Ar-C), 142.64 (Ar-C), 131.03 (Ar-C), 130.95 (Ar-C), 129.59 (Ar-C), 128.56 (Ar-C), 125.7 (Ar-C), 122.59 (Ar-C), 119.07 (Ar-C), 115.46 (Ar-C), 113.78 (Ar-C), 111.1 (Ar-C), 105.97 (Ar-C), 40.32 (CH<sub>2</sub>CH<sub>2</sub>CH<sub>2</sub>NHSO<sub>2</sub>), 38.35 (CH<sub>2</sub>CH<sub>2</sub>CH<sub>2</sub>NHSO<sub>2</sub>), 28.99 (CH<sub>2</sub>CH<sub>2</sub>CH<sub>2</sub>NHSO<sub>2</sub>). LC/MS (ESI) 544.2 (M + 1)<sup>+</sup>.

5.1.7.18. N-(3-((4-(4-(3-hydroxyphenyl)-2-phenyl-1H-imidazol-5-yl)pyridin-2-yl)amino)propyl)-4-(trifluoromethyl)benzenesulfonamide (**11h**):

Yield: 70%. m.p.: 118-120 °C. <sup>1</sup>H NMR (400 MHz, MeOD) δ 8.03 (d, *J* = 8.2 Hz, 2H, Ar-H), 8 (d, *J* = 7.2 Hz, 2H, Ar-H), 7.87 (s, 1H, Ar-H), 7.83 (t, *J* = 4.36 Hz, 2H, Ar-H), 7.47 (t, *J* = 8 Hz, 2H, Ar-H), 7.41 (t, *J* = 7.2 Hz, 1H, Ar-H), 7.25 (t, *J* = 7.8 Hz, 1H, Ar-H), 7 (d, *J* = 8 Hz, 2H, Ar-H), 6.84 (dd, *J* = 1.72 Hz, 1H, Ar-H), 6.72 (t, *J* = 4.2 Hz, 2H, Ar-H), 3.24 (t, *J* = 6.64 Hz, 2H, CH<sub>2</sub>CH<sub>2</sub>CH<sub>2</sub>NHSO<sub>2</sub>), 2.98 (t, *J* = 6.72 Hz, 2H,

CH<sub>2</sub>CH<sub>2</sub>CH<sub>2</sub>NHSO<sub>2</sub>), 1.69 (m, 2H, CH<sub>2</sub>CH<sub>2</sub>CH<sub>2</sub>NHSO<sub>2</sub>). <sup>13</sup>C NMR (100 MHz, MeOD) δ 158.7665 (Ar-C), 157.3769 (Ar-C), 147.1943 (Ar-C), 144.4041 (Ar-C), 133.6514 (Ar-C), 129.6259 (Ar-C), 127.3952 (Ar-C), 126.0172 (Ar-C), 125.9802 (Ar-C), 124.8846 (Ar-C), 122.1808 (Ar-C), 119.814 (Ar-C), 115.4464 (Ar-C), 111.0724 (Ar-C), 105.9958 (Ar-C), 40.3301 (CH<sub>2</sub>CH<sub>2</sub>CH<sub>2</sub>NHSO<sub>2</sub>), 38.3261 (CH<sub>2</sub>CH<sub>2</sub>CH<sub>2</sub>NHSO<sub>2</sub>), 29.0156 (CH<sub>2</sub>CH<sub>2</sub>CH<sub>2</sub>NHSO<sub>2</sub>). LC/MS (ESI) 594.1 (M +1) <sup>+</sup>.

5.1.7.19. N-(3-((4-(4-(3-hydroxyphenyl)-2-phenyl-1H-imidazol-5-yl)pyridin-2-yl)amino)propyl)-4-methoxybenzenesulfonamide (**11i**):

Yield: 70%. m.p.: 120-122 °C. <sup>1</sup>H NMR (400 MHz, MeOD) δ 8 (d, *J* = 7.24 Hz, 2H, Ar-H), 7.84 (d, *J* = 5.16 Hz, 1H, Ar-H), 7.77 (d, *J* = 8.6 Hz, 2H, Ar-H), 7.49 (t, *J* = 7.04 Hz, 2H, Ar-H), 7.43 (d, *J* = 6.92 Hz, 1H, Ar-H), 7.26 (t, *J* = 7.68 Hz, 1H, Ar-H), 7.01 (t, *J* = 8.8 Hz, 4H, Ar-H), 6.84 (d, *J* = 8.4 Hz, 1H, Ar-H), 6.73 (d, *J* = 5 Hz, 1H, Ar-H), 6.69 (s, 1H, Ar-H), 2.83 (s, 3H, OCH<sub>3</sub>), 3.23 (t, *J* = 6.04 Hz, 2H, CH<sub>2</sub>CH<sub>2</sub>CH<sub>2</sub>NHSO<sub>2</sub>), 2.91 (t, *J* = 6.4 Hz, 2H, CH<sub>2</sub>CH<sub>2</sub>CH<sub>2</sub>NHSO<sub>2</sub>), 1.67 (t, *J* = 6.4 Hz, 2H, CH<sub>2</sub>CH<sub>2</sub>CH<sub>2</sub>NHSO<sub>2</sub>). <sup>13</sup>C NMR (100 MHz, MeOD) δ 162.9251 (Ar-C), 158.8438 (Ar-C), 147.1582 (Ar-C), 131.7538 (Ar-C), 129.5501 (Ar-C), 128.904 (Ar-C), 128.5467 (Ar-C), 125.6733 (Ar-C), 119.7921 (Ar-C), 115.4281 (Ar-C), 114.9691 (Ar-C), 110.9773 (Ar-C), 105.9006 (Ar-C), 54.7721 (OCH<sub>3</sub>), 40.2178 (CH<sub>2</sub>CH<sub>2</sub>CH<sub>2</sub>NHSO<sub>2</sub>), 38.3466 (CH<sub>2</sub>CH<sub>2</sub>CH<sub>2</sub>NHSO<sub>2</sub>), 28.9007 (CH<sub>2</sub>CH<sub>2</sub>CH<sub>2</sub>NHSO<sub>2</sub>). LC/MS (ESI) 556.1 (M +1) <sup>+</sup>.

5.1.7.20. 4-hydroxy-N-(3-((4-(4-(3-hydroxyphenyl)-2-phenyl-1H-imidazol-5-yl)pyridin-2-yl)amino)propyl)benzenesulfonamide (**11j**):

Yield: 60%. m.p.: 130-132 °C. <sup>1</sup>H NMR (400 MHz, MeOD) δ 7.97 (d, *J* = 7.2 Hz, 2H, Ar-H), 7.8 (d, *J* = 5.6 Hz, 1H, Ar-H), 7.68 (d, *J* = 8.4 Hz, 2H, Ar-H), 7.44 (t, *J* = 4.6 Hz, 2H, Ar-H), 7.38 (t, *J* = 7.2 Hz, 1H, Ar-H), 7.24 (t, *J* = 8.4 Hz, 1H, Ar-H), 6.99 (d, *J* = 6.4 Hz, 2H, Ar-H), 6.89 (d, *J* = 8.8 Hz, 2H, Ar-H), 6.84 (dd, *J* = 1.2 Hz, 1H, Ar-H), 6.71 (t, *J* = 2.8 Hz, 2H, Ar-H), 3.21 (t, *J* = 6.4 Hz, 2H, CH<sub>2</sub>CH<sub>2</sub>CH<sub>2</sub>NHSO<sub>2</sub>), 2.89 (t, *J* = 6.4 Hz, 2H, CH<sub>2</sub>CH<sub>2</sub>CH<sub>2</sub>NHSO<sub>2</sub>), 1.66 (t, *J* = 6.4 Hz, 2H, CH<sub>2</sub>CH<sub>2</sub>CH<sub>2</sub>NHSO<sub>2</sub>). <sup>13</sup>C NMR (100 MHz, MeOD) δ 161.39 (Ar-C), 158.44 (Ar-C), 157.33 (Ar-C), 147.27 (Ar-

C), 145.63 (Ar-C), 130.11 (Ar-C), 129.66 (Ar-C), 128.97 (Ar-C), 128.59 (Ar-C), 125.73 (Ar-C), 119.89 (Ar-C), 115.47 (Ar-C), 115.35 (Ar-C), 111.08 (Ar-C), 106.05 (Ar-C), 40.24 (CH<sub>2</sub>CH<sub>2</sub>CH<sub>2</sub>NHSO<sub>2</sub>), 38.47 (CH<sub>2</sub>CH<sub>2</sub>CH<sub>2</sub>NHSO<sub>2</sub>), 28.84 (CH<sub>2</sub>CH<sub>2</sub>CH<sub>2</sub>NHSO<sub>2</sub>). LC/MS (ESI) 542.1 (M +1) <sup>+</sup>.

## **5.2. Pharmacological screening**

### **5.2.1. *In vitro* P38 $\alpha$ kinase assay**

Thermo Fisher Scientific, SelectScreen Kinase Profiling Services was used for screening of the target compounds in single point concentrations mode, and 5-points titration mode for IC<sub>50</sub> determination.

Assay protocol: as reported on Thermo Fisher Scientific website using 100  $\mu$ M concentration of ATP.

### **5.2.2. Inflammatory cytokines production assay**

#### **5.2.2.1. Cell Culture and Treatment**

RAW 264.7 macrophages were obtained from the Korean Cell Line Bank. Mouse peritoneal macrophage cells were obtained 4 days after the intraperitoneal injection of 2 mL of thioglycollate to the 10-week-old C57BL/6 male mice and isolated. The cells were treated with the tested compounds and then stimulated with lipopolysaccharide (LPS) (100 ng/mL) for the incubated time.

#### **5.2.2.2. PGE<sub>2</sub> and cytokine production assay**

After 24 h incubation, the supernatant was collected and PGE<sub>2</sub>, IL-1 $\beta$ , TNF- $\alpha$ , and IL-6 levels in cell culture media were quantified by PGE<sub>2</sub> (Enzo Life Sciences, Inc., Farmingdale, NY, USA), IL-1 $\beta$  (R&D Systems, MN, USA), and TNF- $\alpha$  and IL-6 (BD Bio-science, Sand Diego, CA, USA) enzyme immunoassay (EIA) kits according to the manufacturer's instructions. N-[2-(Cyclohexyloxy)-4-nitrophenyl]methanesulfonamide (NS-398), a selective cyclooxygenase-2 (COX-2)

inhibitor, was purchased from Sigma Aldrich (St. Louis, MO, USA) and used as a positive control for blocking PGE<sub>2</sub> production [50].

### 5.2.3. Nitric oxide assay

After 24 h incubation with the tested compound and LPS, the supernatant was collected and nitrite levels in culture media were detected using Griess reaction and presumed to reflect NO levels. LN6 -(1-Iminoethyl)lysine dihydrochloride (L-NIL) was used as a positive control for blocking NO production.

## 5.3. Molecular Modeling studies

### 5.3.1. Molecular Docking study

The X-ray crystal structure of P38 $\alpha$  in complex with **SB203580** (PDB ID: 3GCP) was downloaded from the protein data bank ([www.rcsb.org](http://www.rcsb.org)) in PDB format. The 2D structure of the target compounds were assembled using ChemDraw software. Molecular Operating Environment (MOE) software was used for the molecular docking operation of the target compounds **8a-i**, **9a-i**, **10a-j**, and **11a-j** with P38 $\alpha$  kinase enzyme domain (PDB ID: 3GCP). The protein structure was prepared for the molecular docking procedure by applying 3D protonation of both enzyme amino acids and the native ligand (SB203580). In addition, water of crystallization was removed from the kinase domain. The active site was isolated. The docking simulation of native ligands (SB203580) with the active site of P38 $\alpha$  kinase (PDB ID: 3GCP) was investigated in order to validate the docking protocol. Both 3D protonation and energy minimization were performed for the target compounds using MOE software.

### 5.3.2. Molecular dynamics simulations

The molecular dynamics (MD) simulations study was carried out for the obtained docked protein complex of the native ligand **SB203580** and compound **11d**, using standard default parameter setting in the MOE 2014 software in order to examine the conformational stability of their docked complexes in the active site of the corresponding kinase (PDB ID: 3GCP).



MOE implemented four algorithms, the Nos\_e-Poincar\_e-Andersen (NPA), the Nos\_e-Hoover-Andersen (NHA), Berendsen velocity/position (BER) and Nanoscale Molecular Dynamics (NAMD). In this study, MD calculations were performed by using NPA, the most precise algorithm for long-time simulations [51]. The system optimization was obtained by energy minimization, applying MMFF94x force field, water as a solvent, six margins and delete far existing solvent with distance greater than 4 Å.

The MD simulation protocol was run for 600 ns at 300 K temperature, the potential energy (kcal/mole) was recorded at intervals of 0.5 ns.

Also, the root mean square deviation (RMSD) values were observed during the whole MD simulation process in order to determine the stability of the ligand-receptor complex during the MD simulation.

### **Acknowledgements**

This work was supported by Korea Institute of Science and Technology (KIST), and KIST Project (2E29340).

### **Conflict of Interest**

The authors declare no conflict of interest.

## References

1. Tong, L., et al., *A highly specific inhibitor of human p38 MAP kinase binds in the ATP pocket*. Nature structural biology, 1997. **4**(4): p. 311-316.
2. Peti, W. and R. Page, *Molecular basis of MAP kinase regulation*. Protein science, 2013. **22**(12): p. 1698-1710.
3. Schett, G., et al., *How antirheumatic drugs protect joints from damage in rheumatoid arthritis*. Arthritis & Rheumatism: Official Journal of the American College of Rheumatology, 2008. **58**(10): p. 2936-2948.
4. Du, Y., et al., *MKP-1 reduces A $\beta$  generation and alleviates cognitive impairments in Alzheimer's disease models*. Signal transduction and targeted therapy, 2019. **4**(1): p. 1-12.
5. Laufer, S.A., et al., *Design, synthesis, and biological evaluation of novel Tri-and tetrasubstituted imidazoles as highly potent and specific ATP-mimetic inhibitors of p38 MAP kinase: Focus on optimized interactions with the enzyme's surface-exposed front region*. Journal of medicinal chemistry, 2008. **51**(14): p. 4122-4149.
6. Dhillon, A.S., et al., *MAP kinase signalling pathways in cancer*. Oncogene, 2007. **26**(22): p. 3279-3290.
7. Nebreda, A.R. and A. Porras, *p38 MAP kinases: beyond the stress response*. Trends in biochemical sciences, 2000. **25**(6): p. 257-260.
8. Enslin, H., D.M. Branch, and R.J. Davis, *Molecular determinants that mediate selective activation of p38 MAP kinase isoforms*. The EMBO journal, 2000. **19**(6): p. 1301-1311.
9. Cuenda, A. and S. Rousseau, *p38 MAP-kinases pathway regulation, function and role in human diseases*. Biochimica et Biophysica Acta (BBA)-Molecular Cell Research, 2007. **1773**(8): p. 1358-1375.
10. El-Gamal, M.I., et al., *Discovery of a potent p38 $\alpha$ /MAPK14 kinase inhibitor: Synthesis, in vitro/in vivo biological evaluation, and docking studies*. European journal of medicinal chemistry, 2019. **183**: p. 111684.
11. Schieven, G.L., *The biology of p38 kinase: a central role in inflammation*. Current topics in medicinal chemistry, 2005. **5**(10): p. 921-928.
12. Westra, J., et al., *Chemokine production and E-selectin expression in activated endothelial cells are inhibited by p38 MAPK (mitogen activated protein kinase) inhibitor RWJ 67657*. International immunopharmacology, 2005. **5**(7-8): p. 1259-1269.
13. Takami, M., et al., *Phosphodiesterase inhibitors stimulate osteoclast formation via TRANCE/RANKL expression in osteoblasts: possible involvement of ERK and p38 MAPK pathways*. FEBS letters, 2005. **579**(3): p. 832-838.
14. Berghe, W.V., et al., *Signal transduction by tumor necrosis factor and gene regulation of the inflammatory cytokine interleukin-6*. Biochemical pharmacology, 2000. **60**(8): p. 1185-1195.
15. Guijas, C., et al., *Simultaneous activation of p38 and JNK by arachidonic acid stimulates the cytosolic phospholipase A2-dependent synthesis of lipid droplets in human monocytes*. Journal of Lipid Research, 2012. **53**(11): p. 2343-2354.

16. Ayala, J.M., et al., *Serum-induced monocyte differentiation and monocyte chemotaxis are regulated by the p38 MAP kinase signal transduction pathway*. Journal of leukocyte biology, 2000. **67**(6): p. 869-875.
17. Tamhane, M., et al., *Comparative renal excretion of VX-702, a novel p38 MAPK inhibitor, and methotrexate in the perfused rat kidney model*. Drug development and industrial pharmacy, 2010. **36**(3): p. 315-322.
18. Zhu, D., et al., *Synthesis and p38 Inhibitory Activity of Some Novel Substituted N, N'-Diarylurea Derivatives*. Molecules, 2016. **21**(5): p. 677.
19. Azevedo, R., et al., *X-ray structure of p38 $\alpha$  bound to TAK-715: comparison with three classic inhibitors*. Acta Crystallographica Section D: Biological Crystallography, 2012. **68**(8): p. 1041-1050.
20. Gilani, R.A., et al., *UM-164: a potent c-Src/p38 kinase inhibitor with in vivo activity against triple-negative breast cancer*. Clinical Cancer Research, 2016. **22**(20): p. 5087-5096.
21. Burnette, B.L., et al., *SD0006: a potent, selective and orally available inhibitor of p38 kinase*. Pharmacology, 2009. **84**(1): p. 42-60.
22. Fu, Y., et al., *The p38 MAPK inhibitor, PD169316, inhibits transforming growth factor  $\beta$ -induced Smad signaling in human ovarian cancer cells*. Biochemical and biophysical research communications, 2003. **310**(2): p. 391-397.
23. Cohen, S.B., et al., *Evaluation of the efficacy and safety of pamapimod, a p38 MAP kinase inhibitor, in a double-blind, methotrexate-controlled study of patients with active rheumatoid arthritis*. Arthritis & Rheumatism: Official Journal of the American College of Rheumatology, 2009. **60**(2): p. 335-344.
24. Mihara, K., et al., *A potent and selective p38 inhibitor protects against bone damage in murine collagen-induced arthritis: a comparison with neutralization of mouse TNF $\alpha$* . British journal of pharmacology, 2008. **154**(1): p. 153-164.
25. Newby, L.K., et al., *Losmapimod, a novel p38 mitogen-activated protein kinase inhibitor, in non-ST-segment elevation myocardial infarction: a randomised phase 2 trial*. The Lancet, 2014. **384**(9949): p. 1187-1195.
26. Moon, S.-H., S.-W. Choi, and S.H. Kim, *In vitro anti-osteoclastogenic activity of p38 inhibitor doramapimod via inhibiting migration of pre-osteoclasts and NFATc1 activity*. Journal of pharmacological sciences, 2015. **129**(3): p. 135-142.
27. Kang, J.S., et al., *DMB1285 [cyclopropyl-{4-[4-(4-fluorophenyl)-2-piperidin-4-yl-thiazol-5-yl]pyrimidin-2-yl} amine] suppresses tumor necrosis factor- $\alpha$  production by blocking p38 mitogen-activated protein kinase/mitogen-activated protein kinase-activated protein kinase 2 signaling pathway*. Journal of Pharmacology and Experimental Therapeutics, 2010.
28. Liu, C., et al., *Discovery of 4-(5-(cyclopropylcarbamoyl)-2-methylphenylamino)-5-methyl-N-propylpyrrolo [1, 2-f][1, 2, 4] triazine-6-carboxamide (BMS-582949), a clinical p38 $\alpha$  MAP kinase inhibitor for the treatment of inflammatory diseases*. Journal of medicinal chemistry, 2010. **53**(18): p. 6629-6639.
29. Dominguez, C., D.A. Powers, and N. Tamayo, *p38 MAP kinase inhibitors: many are made, but few are chosen*. Current opinion in drug discovery & development, 2005. **8**(4): p. 421-430.
30. Ali, E.M., et al., *Design, synthesis, and biological evaluation of novel imidazole derivatives possessing terminal sulphonamides as potential BRAFV600E inhibitors*. Bioorganic Chemistry, 2020: p. 104508.
31. Yang, H., et al., *RG7204 (PLX4032), a selective BRAFV600E inhibitor, displays potent antitumor activity in preclinical melanoma models*. Cancer research, 2010. **70**(13): p. 5518-5527.
32. Ono, K. and J. Han, *The p38 signal transduction pathway activation and function*. Cellular signalling, 2000. **12**(1): p. 1-13.

33. Wagner, E.F. and Á.R. Nebreda, *Signal integration by JNK and p38 MAPK pathways in cancer development*. Nature Reviews Cancer, 2009. **9**(8): p. 537-549.
34. Needleman, S.B. and C.D. Wunsch, *A general method applicable to the search for similarities in the amino acid sequence of two proteins*. Journal of molecular biology, 1970. **48**(3): p. 443-453.
35. Simard, J.R., et al., *Development of a fluorescent-tagged kinase assay system for the detection and characterization of allosteric kinase inhibitors*. Journal of the American Chemical Society, 2009. **131**(37): p. 13286-13296.
36. Manthey, C.L., et al., *SB202190, a selective inhibitor of p38 mitogen-activated protein kinase, is a powerful regulator of LPS-induced mRNAs in monocytes*. Journal of leukocyte biology, 1998. **64**(3): p. 409-417.
37. Fijen, J., et al., *Suppression of the clinical and cytokine response to endotoxin by RWJ-67657, a p38 mitogen-activated protein-kinase inhibitor, in healthy human volunteers*. Clinical & Experimental Immunology, 2001. **124**(1): p. 16-20.
38. Badger, A., et al., *Differential effects of SB 242235, a selective p38 mitogen-activated protein kinase inhibitor, on IL-1 treated bovine and human cartilage/chondrocyte cultures*. Osteoarthritis and cartilage, 2000. **8**(6): p. 434-443.
39. Carta, A., et al., *Novel substituted quinoxaline 1, 4-dioxides with in vitro antimycobacterial and anticandida activity*. European journal of medicinal chemistry, 2002. **37**(5): p. 355-366.
40. McClure, K.F., et al., *Theoretical and experimental design of atypical kinase inhibitors: application to p38 MAP kinase*. Journal of medicinal chemistry, 2005. **48**(18): p. 5728-5737.
41. Tariq, S., O. Alam, and M. Amir, *Synthesis, anti-inflammatory, p38 $\alpha$  MAP kinase inhibitory activities and molecular docking studies of quinoxaline derivatives containing triazole moiety*. Bioorganic Chemistry, 2018. **76**: p. 343-358.
42. Somakala, K., S. Tariq, and M. Amir, *Synthesis, evaluation and docking of novel pyrazolo pyrimidines as potent p38 $\alpha$  MAP kinase inhibitors with improved anti-inflammatory, ulcerogenic and TNF- $\alpha$  inhibitory properties*. Bioorganic chemistry, 2019. **87**: p. 550-559.
43. Liu, C., et al., *Benzothiazole based inhibitors of p38 $\alpha$  MAP kinase*. Bioorganic & medicinal chemistry letters, 2008. **18**(6): p. 1874-1879.
44. Heider, F., et al., *Pyridinylimidazoles as dual glycogen synthase kinase 3 $\beta$ /p38 $\alpha$  mitogen-activated protein kinase inhibitors*. European journal of medicinal chemistry, 2019. **175**: p. 309-329.
45. Jacobs, A.T. and L.J. Ignarro, *Lipopolysaccharide-induced expression of interferon- $\beta$  mediates the timing of inducible nitric-oxide synthase induction in RAW 264.7 macrophages*. Journal of Biological Chemistry, 2001. **276**(51): p. 47950-47957.
46. Amano, F. and T. Noda, *Improved detection of nitric oxide radical (NO $\bullet$ ) production in an activated macrophage culture with a radical scavenger, carboxy PTIO, and Griess reagent*. FEBS letters, 1995. **368**(3): p. 425-428.
47. Moore, W.M., et al., *L-N6-(1-iminoethyl) lysine: a selective inhibitor of inducible nitric oxide synthase*. Journal of medicinal chemistry, 1994. **37**(23): p. 3886-3888.
48. Aroonrerk, N., A. Suksamrarn, and K. Kirtikara, *A sensitive direct ELISA for detection of prostaglandin E2*. Journal of immunoassay & immunochemistry, 2007. **28**(4): p. 319-330.
49. Futaki, N., et al., *NS-398, a new anti-inflammatory agent, selectively inhibits prostaglandin G/H synthase/cyclooxygenase (COX-2) activity in vitro*. Prostaglandins, 1994. **47**(1): p. 55-59.
50. Han, H.-S., et al., *Cirsimarín, a flavone glucoside from the aerial part of Cirsium japonicum var. ussuriense (Regel) Kitam. ex Ohwi, suppresses the JAK/STAT and IRF-3 signaling pathway in LPS-stimulated RAW 264.7 macrophages*. Chemico-biological interactions, 2018. **293**: p. 38-47.

51. Sturgeon, J.B. and B.B. Laird, *Symplectic algorithm for constant-pressure molecular dynamics using a Nosé–Poincaré thermostat*. *The Journal of Chemical Physics*, 2000. **112**(8): p. 3474-3482.

**Declaration of interests**

The authors declare that they have no known competing financial interests or personal relationships that could have appeared to influence the work reported in this paper.

The authors declare the following financial interests/personal relationships which may be considered as potential competing interests:



Click here to access/download  
**Supplementary Material**  
BMC-Supportive-19-12-20.doc

